VOLATILITY CHARACTERIZATION OF PARTICLE EMISSIONS FROM PREMIXED LOW TEMPERATURE COMPRESSION IGNITION COMBUSTION

A DISSERTATION

SUBMITTED TO THE FACULTY OF

UNIVERSITY OF MINNESOTA

BY

GLENN LUCACHICK

IN PARTIAL FULFILLMENT OF THE REQUIREMENTS

FOR THE DEGREE OF

DOCTOR OF PHILOSOPHY

Professor William Northrop, Adviser

July 2016

Acknowledgements

The past four years as a Ph.D. student have given me a deeper understanding of engineering that I ever imagined I would attain. This would not have been possible without my peers and the faculty that challenged me and guided me on this journey. I am grateful to have met all of the other students that worked with me and helped me along the way. I would like to thank my committee of advisors for sharing their vast knowledge with me. Special thanks to Prof. Peter McMurry, who despite not being on my committee, advised me, and supplied me with numerous aerosol processing instruments. Great thanks to General Motors, which supplied funding and the engine used for my studies. Most importantly, I thank my wife Melanie who has been ever so patient, loving, and supportive over the past few years.

Dedication

This work is dedicated to my grandfather Art Dolan, a self-taught farmer and diesel mechanic who has grown increasingly irritated with the “unnecessary” complexity of engines. It’s better that he doesn’t know the current state of affairs.

Abstract

This thesis constitutes an extensive volatility characterization of particles from engines operating in two low temperature combustion (LTC) modes, partially premixed compression ignition (PPCI), and reactivity controlled compression ignition (RCCI). Low temperature combustion is of research interest because it offers the potential to reduce soot and oxides of nitrogen (NOx) while capitalizing on the inherently high efficiency of compression ignition engines. While particle emissions from conventional diesel combustion (CDC) have been extensively studied and characterized, particle emissions from LTC modes have been shown to be distinctly different, and demand investigation. These particles have been shown to be primarily organic material with small amounts of solid soot and ash, in contrast to particles from CDC that are primarily soot with small amounts of adsorbed organic material. In this work, advanced aerosol experimental techniques have been applied to characterize the volatility of these particles. The results have shown that their composition results in formation that is especially sensitive to dilution conditions. The experimental data have been used to develop aerosol simulations that identify formation mechanisms responsible for the unique volatility characteristics of LTC particle emissions. Particle volatility characteristics shown in the experiments suggest that heavy unburned oil and fuel alkanes contribute greatly to particle growth, forming the bulk of total particle volume. Further, elevated levels of lower molecular weight, low volatility organic compounds resulting from LTC may contribute to the inception of particles due to homogeneous nucleation; however, the results show that

despite ultra-low fuel sulfur concentrations, heterogeneous nucleation of particles by sulfuric acid and water is most likely contributor to nucleation mode particle formation for LTC modes.

Table of Contents

List of Tables

List of Figures

1 Introduction

Low temperature combustion (LTC) has become an attractive research topic as it offers the potential to limit the production of emissions in-cylinder while maintaining high engine thermal efficiency. This is made possible by combining the strengths of both spark ignition and compression ignition engines in a carefully controlled combustion event. Specifically, the high compression ratio and lack of throttling common to diesel combustion contributes to high thermodynamic cycle efficiency, while the premixed nature of LTC combustion, common to spark ignition engines, results in greatly reduced emissions of soot and oxides of nitrogen (NOx). The LTC strategies investigated in this study are partially premixed compression ignition (PPCI) and reactivity controlled compression ignition (RCCI). These strategies differ from the premixed combustion type known as homogeneous charge compression ignition (HCCI) in that they are easier to control by virtue of their largely injection-dependent combustion. In the pursuit of improving engine efficiency using advanced combustion modes like LTC, characterization of their emissions, including particle emissions, must be better understood. Such emissions have serious implications on human health and the environment as well for the regulations designed to limit them.

1.1 Motivation

The internal combustion engine's high efficiency, excellent performance and the relative abundance of liquid fossil fuels have made it the primary power source for on

and off-road vehicles in industrialized societies. The EPA has projected this use to continue for decades even with volatile oil prices, and the implementation of aggressive environmental regulations (EIA 2012). Historically, the higher cost of diesel fuel and higher primary cost of diesel vehicles has inhibited their popularity in the U.S. for passenger vehicles. Recently, the greater fuel efficiency of diesel engines over spark ignition (SI) engines have led to increased sales of diesel passenger vehicles, but their popularity in the U.S is still limited. Although some economic forecasts predict diesel passenger vehicle market share to triple by 2015 in the United States, this would still only represent a market penetration of 3%. With continually tightened corporate average fuel economy (CAFE) standards as seen in Figure **1**, automakers have additional incentive to increase diesel vehicle sales, which encourages their research in advanced engine technologies (Shuldiner 2012; Sabatini 2012).

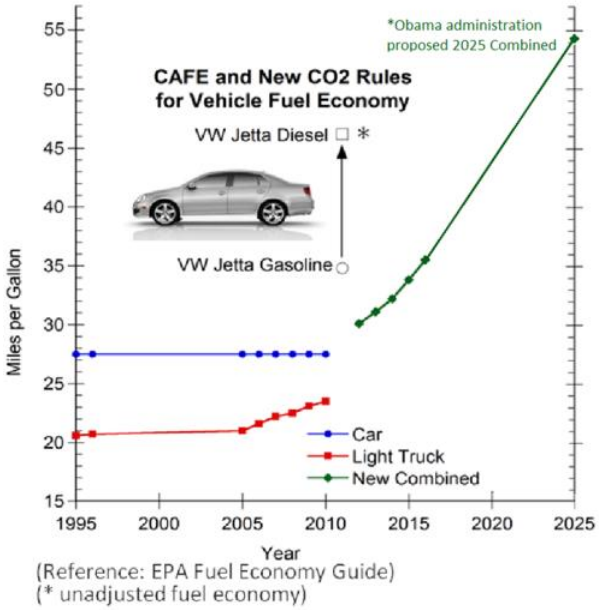

Figure 1**: Recent and proposed vehicle CAFE standards**

Along with more stringent fuel economy rules, regulations for traditional criteria pollutants have been aggressively tightened over the past two decades as reflected in Figure 2, which shows the requirement of order of magnitude reductions in vehicle PM, bus PM, and NOx emissions expressed as emission mass per engine work produced (g/bhp-hr). This march towards zero pollutant emissions has forced a progression of technology in the last 40 years that McClellan et al. 2012 described as "evolutionary", with the most recent years being "revolutionary". The most significant recent improvements have been the introduction of diesel oxidation catalyst (DOC) plus diesel particulate filter (DPF) aftertreatment systems that have reduced emissions to levels far below that set by the newest standards (McClellan et al. 2012).

Aftertreatment effectiveness has been enhanced by ever decreasing regulated fuel sulfur levels also shown in Figure 2. Currently commercially available ultra-low sulfur diesel (ULSD) now contains less than 15 ppm sulfur. McClellan et al. categorize diesel exhaust from these latest technology engines as “new technology diesel exhaust”, and diesel exhaust from pre 1988 diesel engines as “traditional diesel exhaust”, with transitional technology improvements bridging this span from 1988 to 2006. Reduced sulfur levels also have the advantage of reducing particle emissions by limiting nucleation of sulfuric acid/water upon primary dilution.

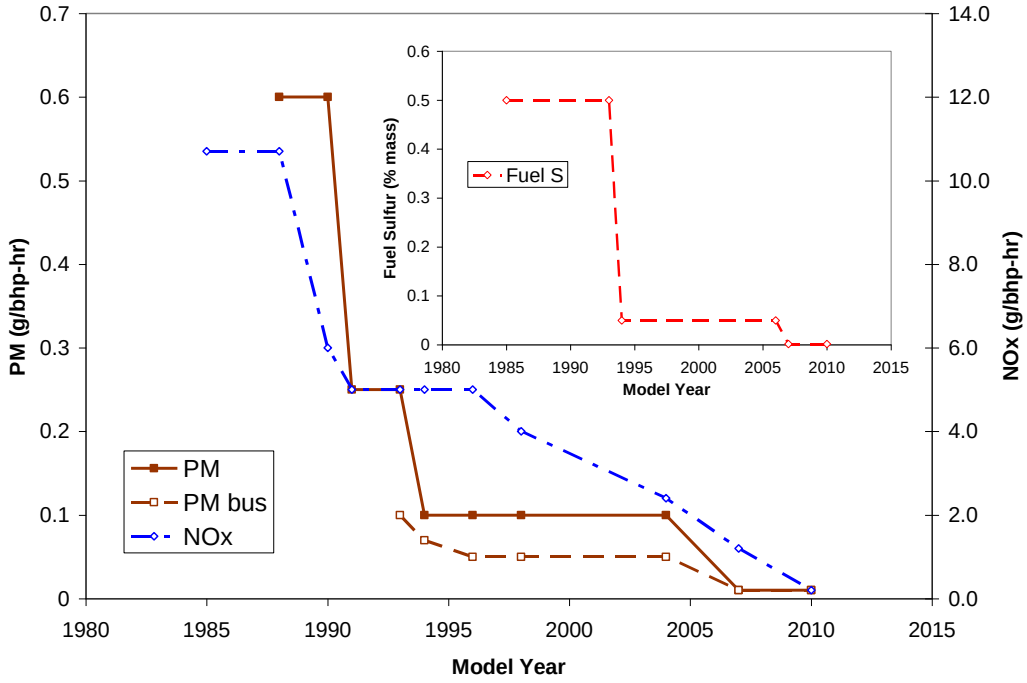

Figure 2. U.S. EPA heavy-duty on-highway regulated emissions standards for NOx, PM and fuel sulfur standard vs. time (Dieselnet, 2013). Specific emissions are calculated as mass per hp-hour produced.

Reduction of diesel emissions to current regulated levels has required technological advancements in multiple areas. Turbocharging, cooled exhaust gas recirculation (EGR), electronic controls, and higher-pressure fuel injection are among the technologies industry has used to reduce engine out emissions. Advancements in aftertreatment technology that achieve lower tailpipe emissions are enhanced by reduced catalyst-poisoning fuel sulfur levels. Lower fuel sulfur also has significantly reduced sulfate emissions from engines, traditionally a major contributor to PM emissions from diesels.

In further pursuit of further improvement in efficiency and engine-out emissions, LTC has shown potential as an alternative to CDC. Single fuel PPCI is a relatively new method for achieving simultaneously low soot and NOx emissions and has been implemented by some engine manufacturers in production vehicles at light engine loads. To achieve PPCI operation, ignition delay, the time between injection and start of combustion, is extended using extensive EGR dilution and modified injection timing. A disadvantage of PPCI is its limited operating range due to excessive in-cylinder peak pressure and insufficient time for mixing prior to combustion at long injection durations.

Extensive studies have been conducted that have shown that diesel is not the optimum fuel for PPCI, due to the high levels of EGR required to delay ignition, and cylinder wall-wetting due to longer spray penetration from low volatility and high surface tension (Kalghatgi et al. 2013). As a result, gasoline has been studied as a PPCI fuel by many researchers. Gasoline's resistance to autoignition can be exploited to achieve higher loads than diesel at lower EGR rates, but conversely the reduced auto-ignition makes it difficult to achieve combustion at low load conditions.

In an effort to capitalize on the autoignition characteristics of both gasoline and diesel, Inagaki et al. (2006) explored dual fuel premixed compression ignition. From this study it was determined that different fuel ratios could be used to cover a wide range of

different operating conditions. More recent application of similar dual-fuel strategies has been coined reactivity controlled compression ignition (RCCI). The concept is described by Kokjohn et al. (2011) as a combustion strategy that uses a premixed charge of a low reactivity fuel such as gasoline combined with direct injection of a high reactivity fuel such as diesel during the compression stroke. It has been shown to be effective over loads greater than twice that achievable with PPCI due to the ability better modulate in-cylinder fuel air mixture reactivity.

Some hurdles exist in implementing LTC in practice. In addition to the limited load range of PPCI, and the complexity of dual fuel systems for RCCI, LTC operating conditions have been shown to significantly increase hydrocarbon (HC) emissions. Jacobs et al. (2005) reported about double the total HC emissions and 20 times the amount of CO for PPCI over a CDC mode at the same engine speed and load. Prior studies have suggested that unburned HC from PPCI used in low engine load operating conditions have the potential to form nucleation mode semi-volatile particulate matter (SVPM) in higher concentrations than CDC (Northrop 2010). In addition, these studies have shown that engine-out PM from LTC has significantly higher total organic fraction (TOF). TOF is the fraction of PM comprised of partially-reacted species, unburned fuel and lubricating oil. Partially reacted species of concern for SVPM formation include those with lower volatility than the original fuel such as polycyclic aromatic hydrocarbons (PAH) or organic acids. Higher HC and CO emissions from LTC

combustion have also been shown to contribute to DOC deactivation, especially at the low exhaust temperatures resulting from low engine loads and higher charge heat capacity common to LTC. This deactivation inhibits oxidation of low volatility species that comprise SVPM (Manbae Han, Assanis, Jacobs, et al. 2008) potentially leading to higher than desirable PM emissions even downstream of aftertreatment catalysts meant to eliminate them (Northrop 2010). Further, modern engines that incorporate LTC modes will be equipped with aftertreatment systems designed for conventional combustion. The composition and growth of SVPM resulting from high engine-out HC emissions of LTC modes in diesel engines has not been well explained in the literature and its characterization forms the basis for this research.

In addition to environmental and health risks from LTC particles, challenges exist related to their measurement. The volatile nature of PM from LTC makes characterization difficult. In a recent study conducted by Kolodziej et al. (2013), three established methods, the ORNL Microwave Extraction method, the Horiba MEXA 1370 PM analyzer, and the NIOSH 5040 method (Birch & Cary 1996) were used to determine elemental versus organic carbon (EC/OC) ratios for LTC. For a 5.5 Bar IMEP PPCI mode similar to 4 Bar LLTC conducted in this study, they found the resulting EC/OC ratios as follows: 0.11 for NIOSH method 5040, 0.24 for the Oak Ridge National Laboratory developed microwave extraction technique, and 5.1 for a Horiba MEXA Analyzer. This represents a 46-fold difference in measured EC/OC ratio. Such

differences in measured EC/OC highlight the challenges facing researchers in characterizing PM from LTC. Most of the difficulty in determining the quantity and composition of semi-volatile PM in LTC exhaust relates to how extracted samples are collected, stored and pre-treated. Evaporation of semi-volatile compounds from a filter prior to analysis for example, can lead to significant errors in measured concentration. The objective of this study is to characterize semi-volatile PM from LTC operating modes using online aerosol processing techniques that give results in near real-time, thus reducing experimental errors. It compares PM from engines operating in LTC and CDC modes. Characterizing such emissions is necessary for accurately quantifying the evolution of low volatility HC emissions from LTC and predicting their behavior in the primary exhaust plume. The behavior of these particles upon atmospheric dilution has important implications on human health, the environment, and meeting current and future emissions regulations.

2 Background

2.1 Conventional Diesel Combustion

Conventional diesel combustion (CDC) has been the dominant combustion strategy in diesel engines since its invention by Rudolf Diesel in the 19th century. The ideal diesel cycle uses a constant pressure power stroke, which was intended to be achieved by introducing fuel in a controlled, diffusion-burn process. Unfortunately, fuel injection in conventional diesel combustion creates regions of temperature and fuel

concentration that promote the creation of soot and NOx. Conventional diesel combustion exhibits a tradeoff phenomenon, where efforts to reduce soot cause an increase in NOx, and vice versa. This so-called soot versus NOx tradeoff was analyzed by Chirico et al. (2010), and Dec (1997) in an experimental study of conventional diesel combustion using optical methods. They were able to identify the location of soot and NOx production in the diffusive diesel flame, as seen in Figure 3. During the premixed combustion that begins shortly after the fuel is injected, and during premixed burning that occurs during the later stages of combustion, the fuel-air mixture is very rich, and does not generate NOx. At the edge of the diffusion flame, temperatures are relatively high as the mixture approaches stoichiometric concentrations, which causes NOx formation. Soot is formed as rich combustion products downstream of the premixed flame pyrolize into carbonaceous soot precursors, and also during the diffusion controlled portion of combustion at the perimeter of the flame where high temperatures enable pyrolysis reactions.

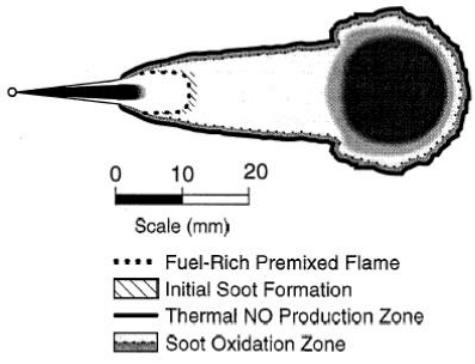

Figure 3: Illustration from Dec et al. (1997) showing regions of soot and NOx formation

The soot-NOx tradeoff can be seen practically by changing engine operating parameters. For example, increasing EGR at four different loads causes a reduction in NOx with an increase in soot as determined by optical opacity as seen in Figure 4 (Zheng et al. 2004). A similar effect is seen for advancing diesel fuel injection timing (Heywood 1988).

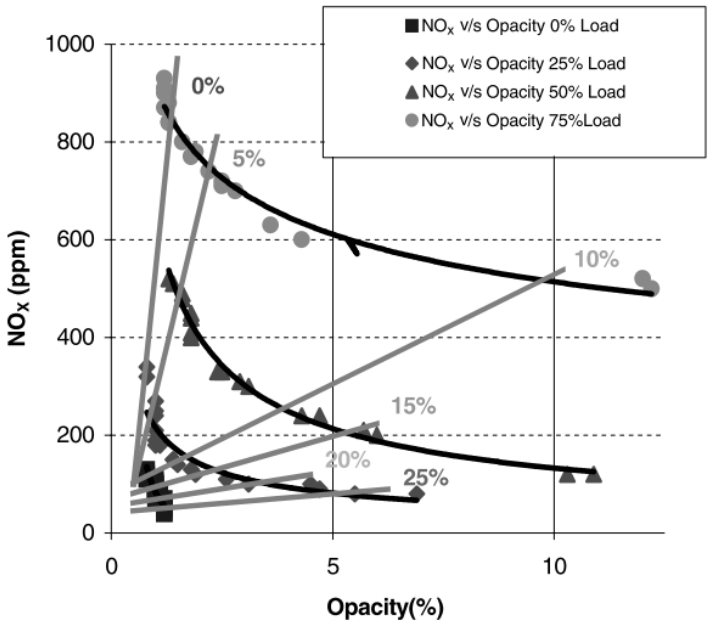

Figure 4: Trade-off between exhaust NOx and smoke vs. EGR and load (Zheng et. al 2004)

2.2 Low Temperature Combustion Background

Recent research has focused on LTC modes to defeat the soot versus NOx tradeoff in CDC. PPCI is enabled by high fuel injection pressure and increased EGR rates combined with EGR cooling to reduce the oxygen content in the mixture, and also increase its heat capacity. These factors increase ignition delay, and therefore increase

mixing in the combustion chamber mostly eliminating the diffusion burn portion of combustion. This greatly reduces both NOx and soot (Jacobs, 2007) by operating in temperature and equivalence ratio regions where little soot and NOx production occurs (Figure 5). There are different practical methods for achieving PPCI. In early PPCI, fuel injected during the compression stroke is uniformly mixed through the combustion chamber, and combustion is premixed. Late-injection PPCI occurs near TDC, with start of ignition delayed until well after TDC, encouraging premixing, and avoiding high peak temperatures.

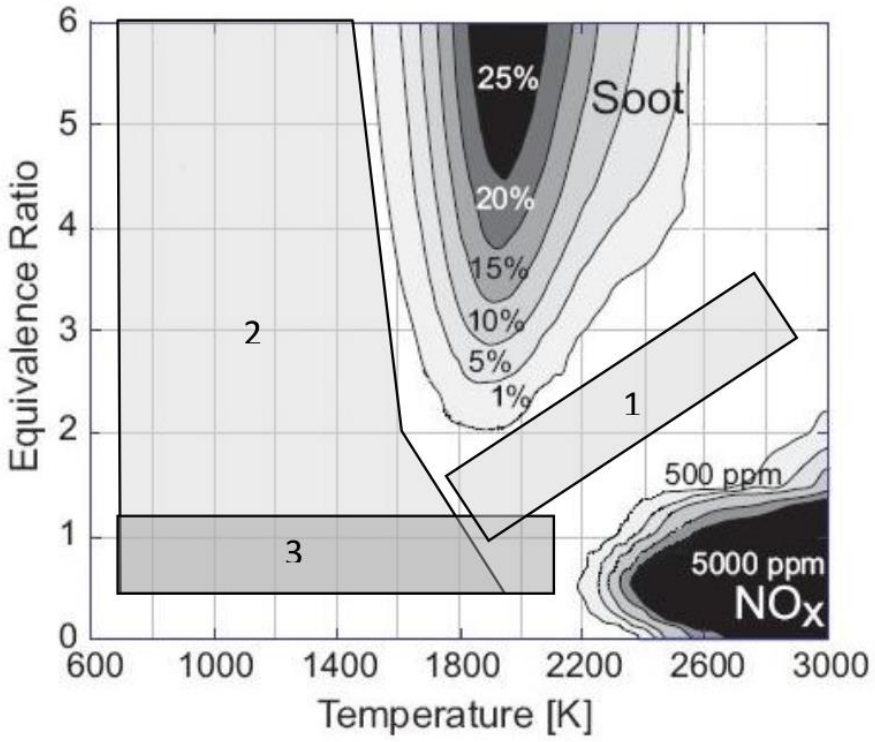

Figure 5: Local equivalence ratio versus temperature plot with soot and NOx island taken from Northrop (2009) in an adaption from (Kook et al., 2005) . Numerical values from (Kitamura et al. 2002) from numerical simulation of n-heptane and air at 6 MPa and a residence time of 2ms.

PPCI does have disadvantages despite its reduced soot and NOx emissions. First, PPCI is only possible for low loads because as the fuel mass injected into the cylinder increases, peak cylinder temperatures begin to increase near TDC, which encourages potentially destructive fuel pre-ignition. For late PPCI strategies, increasing injection duration exceeds the ignition delay leading back to conventional diffusion burning. In an exploration of the load limits of PPCI in a 4 cylinder diesel engine (Knafl et al. 2006), found that at 1500 rpm, 700 kPa BMEP was possible with acceptably low soot and NOx for a late injection strategy. This is equivalent to 17.6 kW, which is power enough to propel a small vehicle at highway speeds.

Of greatest significance to the work conducted for this thesis, PPCI has higher CO and HC emissions due to over-lean and cold areas within the combustion chamber. These emissions are generally much lower in conventional combustion because of the extended time for combustion to occur (Northrop, 2009). These increased emissions are associated with an increase in brake specific fuel consumption (BSFC) related to corresponding decreasing combustion efficiency (Jacobs et al., 2005). It is thought that such products of incomplete combustion contribute to more volatile PM content, unlike conventional combustion where the PM content is dominated by EC.

Reactivity controlled compression ignition (RCCI) is a dual fuel LTC strategy that uses a premixed charge of a low reactivity fuel such as gasoline combined with direct

injection of a high reactivity fuel such as diesel during the compression stroke (Reitz & Duraisamy 2015).

2.3 Review of Prior Exhaust Particle Characterization

2.3.1 Conventional Combustion Particle Characterization

In review of diesel combustion particulate, (Kittelson 1998) describes diesel exhaust particles as highly agglomerated solid carbonaceous material and ash, and volatile organic and sulfur compounds as seen in Figure 6. Generally, the volatile organic compounds are mostly comprised of unburned and partially combusted fuel and engine oil. For CDC, the TOF can range from 10% to 90% by mass. Recent research (Sakurai, Tobias, et al. 2003) on conventional diesel combustion has shown that most of the PM TOF is contributed by engine oil for conventional combustion. In that study, the composition experiments were conducted using TDMA, a technique that was used heavily in this research.

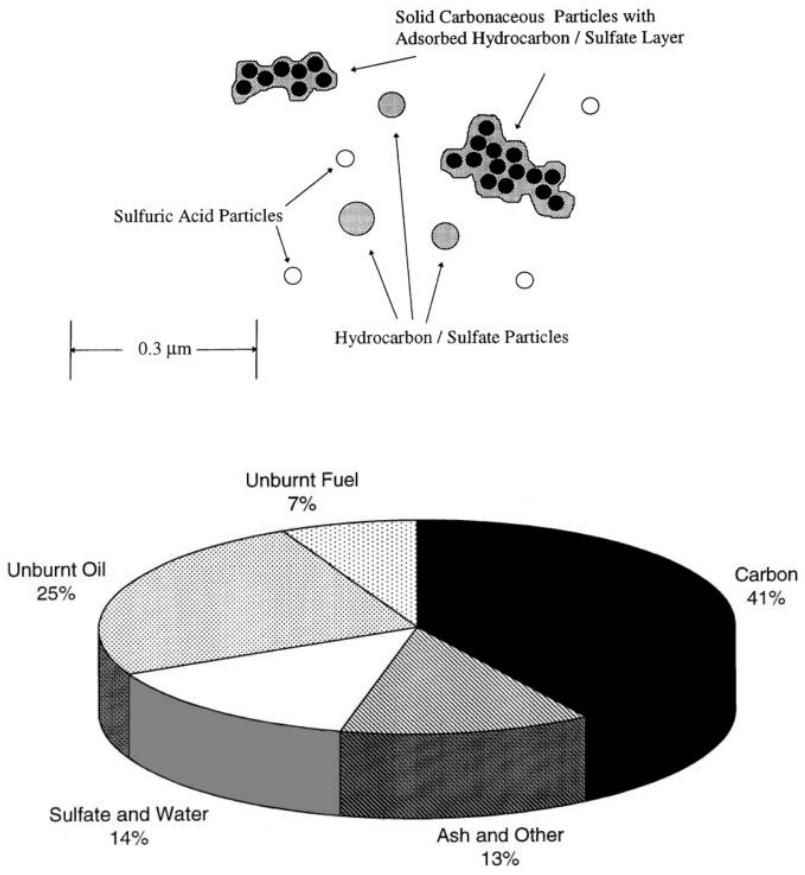

Figure 6: Typical heavy-duty diesel particle composition. (Kittelson, 1998)

In the Sakurai study, conducted at low to moderate loads showed that for the modes investigated, 90% of TOF content corresponded to hydrocarbons with volatility equivalent to C24-C32 alkanes, which are the major constituents in engine oil. Engine oil particulate contribution from cylinder wall oil film breakdown and evaporation is known to correlate strongly with in-cylinder temperatures. A study conducted using pure hydrogen as a fuel (Miller 2007) showed that as in-cylinder temperatures increased, TOF in PM also increased. In addition to unburned lubricant oil, recent studies have shown

that organic acids formed during combustion may contribute to PM mass (Arnold et al. 2012).

2.3.2 Sampling, Analysis, and Environmental Implications for Volatile PM

Accurate measurement of volatile PM mass can prove difficult (Kolodziej et al. 2013). For PM filter sampling, adsorption of gas-phase volatile material onto the filter media can cause positive filtration artifacts, while evaporation of semivolatile content from filtered PM can cause negative filtration artifacts (Liu et al. 2012). Higher levels of VOC in LTC exhaust may contribute to greater filtration artifacts. Other techniques such as integrating a particle size distribution measured with a scanning mobility particle sizer (SMPS) can be effective if the proper mass conversion technique is used. An advantage of such a technique is the lack of filter adsorption/evaporation artifacts.

The relationship between LTC combustion modes and greater HC concentrations is well known (Koci et al. 2013). HC species include both unburned fuel alkanes and polycyclic aromatic hydrocarbons (PAH) in addition to other compounds that contribute to PM formation upon dilution. Recent research has shown that increased HC in LTC emissions play a significant role in aerosol growth. Studies conducted using US-EPA 40 CFR Part 1065 dilution and sampling conditions have shown TOF greater than 88% for ultra-low sulfur diesel (ULSD) fuels, and even higher for biodiesel blends (Northrop 2010, Storey et al. 2008) .

Current government regulations for PM mass offer significant freedom with regards to the dilution ratio and temperature of sampling. According to EPA guideline 40 CFR, part 1065, any primary dilution ratio greater than 2:1 may be used, and any aging temperature from 42°C to 52°C may be used. For conventional engine conditions with high TOF, PM mass varies greatly as a function of dilution ratio and temperature due to gas to particle conversion processes, even with significant soot concentration (Shrivastava et al. 2006) leading to variable results when measuring PM mass. It stands to reason that varying dilution conditions will have an even larger effect on measured PM mass for LTC due to its higher TOF. The relationship between particulate formation and dilution conditions is very complex. Volatile material can be adsorbed onto EC particles, nucleate homogeneously, or condense onto EC particles. While low volatility compounds can be assumed to condense totally during dilution at ambient temperatures, semivolatile organic hydrocarbons (SVOC), and intermediate volatility organic hydrocarbons (IVOC) span a broad range of volatilities (Shrivastava et al. 2007; Presto et al. 2009) and may not convert to PM completely during the dilution process especially if EC is low and adsorption is the primary mechanism of TOF PM capture ((Lipsky & Robinson 2006)).

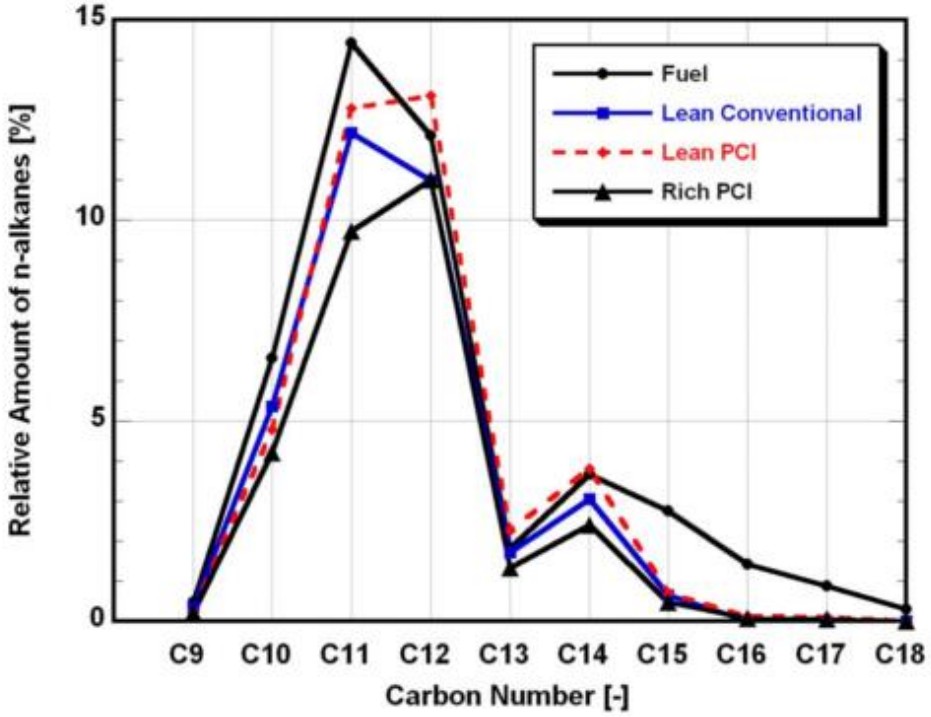

Figure 7. N-alkane distribution in fuel and DOC-out exhaust for conventional, Lean Premixed Compression Ignition, and Rich Premixed Compression Ignition. (Manbae Han, Assanis & Bohac 2008)

Compounds in diesel fuel and diesel exhaust span a large volatility range, with saturation pressures between 1.33x10e-5 and 1.33x10e-2 kPa at 25°C, and comprise a significant fraction of both diesel exhaust and fuel. The alkanes abundantly present in diesel fuel, dodecane (C12) through octadecane (C18) correspond to this pressure range (Figure 7. N-alkane distribution in fuel and DOC-out exhaust for conventional, Lean Premixed Compression Ignition, and Rich Premixed Compression Ignition. (Manbae Han, Assanis & Bohac 2008)While laboratory dilution systems cannot perfectly replicate atmospheric dilution and gas to particle conversion for such volatile materials, they offer

good control of temperature, humidity, and dilution ratio conditions for the study of particle conversion phenomena.

The dilution system used for particle measurement is critical for particulate emissions processing. Diluting exhaust gases with clean, dry, and temperature controlled air reduces particle concentrations and temperatures to levels manageable by particle sizing and counting instruments, and reduces water vapor concentrations to prevent condensation upon cooling. The dilution system also simulates the exhaust gas dilution upon discharge to the atmosphere for a vehicle for example. Laboratory exhaust gas dilution occurs in two stages. The primary dilution stage causes the most significant changes to particulate emissions. There are several types of dilution systems which have been well characterized and are commonly used for processing engine exhaust (Giechaskiel et al. 2008). A common method is constant volume sampling (CVS) dilution systems which are designed to dilute the entirety of the engine exhaust (Khalek et al. 2011). This type of system is quite expensive as it requires processing and conditioning of large quantities of air. Alternatively, a smaller portion of the exhaust flow can be sampled by diverting a small portion of the exhaust stream. This can be accomplished by using a rotating disk dilution system, which is capable of producing an extremely wide range of dilution ratios (Hueglin 1997), perforated tube dilutors (Ntziachristos et al. 2004) or vacuum ejector style dilution (Kittelson et al. 2006), which uses no moving parts, and is the dilution method used in this study.

The mechanisms involved in gas-particle partitioning are complex and varied. Low volatility species can undergo homogeneous nucleation, while higher volatility species undergo gas to particle conversion as a result of adsorption and absorption onto EC and lower volatility particulate matter (Kittelson 1998). Nucleation mode particles are generally thought to be incepted by heterogeneous nucleation of water and sulfuric acid (Khalek et al. 2000) and then grown by absorption of hydrocarbon species. Generally, growth of nucleation mode species in engine exhaust is subject to a size ceiling by the action of highly absorptive soot agglomerates accumulating precursor vapors. It has been suggested that engines with low EC emissions emit more nucleation mode particles (Bagley 1996), but LTC using ULSD fuel presents a unique particle growth scenario. Greatly reduced sulfur levels versus older diesel fuels will inhibit sulfuric acid and water hetero-molecular nucleation, but greatly reduced soot agglomerates will lessen HC precursor scavenging and may impact PM/gas partitioning (Seinfeld 1986; Khalek et al. 2000).

Primary Organic aerosols (POA) are emitted from both biological and anthropological sources. Diesel engines are a major anthropogenic source of POA. The effects POA from diesel exhaust pose a potential health and environmental risk. Partitioning theory (Shrivastava et al. 2006) shows that independent of temperature, POA emissions decrease when an aerosol is diluted isothermally by a much greater fraction than that of traditional laboratory dilution. Atmospheric dilution can be in excess of

10,000:1, over an order of magnitude greater than most laboratory dilution conditions. It has been shown that low laboratory dilution ratios of exhaust bias gas-particle partitioning towards the particle phase when compared to atmospheric conditions (Lipsky & Robinson 2006; Shrivastava et al. 2006). This is not to suggest that reducing POA by manipulating dilution conditions does not proportionally reduce PM exposure risk. Shrivastava et al. 2007 has shown that a large fraction of the material in concentrated plumes such as tailpipes evaporate as the plume dilutes to ambient conditions, with the vapors undergoing photo-oxidation to form lower volatility products that recondense (Hallquist et al. 2009). It is thought that more than half of primary particulate emissions undergo this process of evaporating and oxidizing to lower volatility products that form secondary organic aerosol (SOA) (Donahue et al. 2006). LTC PM may be more likely to undergo this process because of the larger TOF content.

The relationship between POA and secondary organic aerosols (SOA) is complex, not well understood, and has been the topic of extensive research recently. POA and SOA are the components that make up atmospheric organic aerosol (OA). OA may pose a potential human health hazard, and has an uncertain effects on climate change (Gentner et al. 2012). By definition, anthropogenic POA is formed immediately upon entry to the atmosphere, from tailpipes, chimneys, and other sources of emissions. SOA is formed by the process of oxidation of higher volatility gas phase organic compounds due to atmospheric photo-oxidation. There is still considerable debate as to whether POA or

SOA contributions dominate overall OA. Research tracing individual organic compounds with the goal of identification as POA or SOA has indicated that POA is the dominant source of OA, however more recent field measurements indicate the opposite ((Robinson et al. 2007). Recent smog-chamber experiments have shown that the evaporation of POA components during the process of diluting to ambient conditions, and the subsequent photo-oxidation of these vapors produces SOA in far greater quantities than traditional precursors. Furthermore, an extensive interdepartmental collaboration at Berkeley (Gentner et al. 2012), came to the conclusion that the majority of anthropogenic transportation sourced SOA is created from precursors emitted by diesel engines. This is despite the fact that gasoline engines comprise a far greater percentage of total fuels consumed in transportation both on and off road. These studies continue to improve the understanding of the total impact of diesel emissions. As this impact becomes better defined, aftertreatment systems can be implemented more effectively, with particular attention necessary for emissions from new technologies such as LTC.

Diesel aftertreatment is an effective method for reducing both gaseous and particulate emissions. DOC aftertreatment has been used since the 1990s to reduce HC and CO emissions, with conversion efficiencies greater than 90%. As ever-tightening regulations continue to drive lower emissions, aftertreatment will become even more necessary in supplementing advanced combustion controls to reduce emissions (Lucachick, Avenido, Watts, et al. 2014). Diesel Particulate Filters (DPF) have also been

used in conjunction with DOCs for removing soot particulate with 90-95% efficiency (Code & Walker, 2004). While DOC-DPF aftertreatment systems work very effectively for conventional combustion, recent research has shown that their performance suffers under LTC conditions (Patterson et al. 2006; Manbae Han, Assanis & Bohac 2008). The low LTC exhaust oxygen concentrations decrease oxidation rates, and competition for active catalyst sites is increased due to higher concentrations of CO and ethane. Light off temperatures for LTC conditions can be tens of degrees higher than conventional combustion modes, temperatures that may not be reached under certain light load LTC conditions (Manbae Han, Assanis & Bohac 2008). Under conditions of DOC light off failure, the exhaust composition would be especially unique, with particularly high HC content, and ultra-low soot emissions lowered even further by DPF activity. The growth of particles under these conditions has been largely unstudied, and the ostensible lack of nucleation sites suggests that OC normally found as TOF may instead partition as gas-phase, or find alternative PM conversion pathways.

3 Experimental Methods

3.1 Engine

The PPCI research was conducted on a GM A20DTH 2.0 liter turbo-diesel automotive engine equipped with full engine and fuel system control. This engine produces a peak 117.3 KW in stock condition, and is designed for use in small to midsize automotive applications. This modern engine is factory equipped with a variable

geometry turbocharger (VGT), variable swirl actuator (VSA), variable EGR control, and intake throttle control. The VGT system controls the exhaust pressure drop across the turbine to control both turbocharger boost pressure and exhaust manifold pressure. This control of exhaust manifold pressure is invaluable for controlling EGR rates, which vary from 20% to 60% for the operating modes included in the proposed research. The EGR system has been modified to utilize laboratory water as a cooling medium instead of engine block coolant, this enables the greater cooling capabilities necessary for running LTC. The stock Bosch common rail fuel injection system allows pressures as high as 1600 bar. High fuel injection pressures are necessary in promoting the in-cylinder mixing necessary for LTC operation. The research engine is equipped with an aftermarket water to air aftercooler, which gives enhanced control of intake air temperature. Engine specifications are listed below (Table 1. A20DTH Engine Technical Specifications)

Table 1. A20DTH Engine Technical Specifications

Number of cylinders	4
Displacement	1956 cc
Bore	83.0 mm
Stroke	90.4 mm
Bore distance	91.4 mm
Cylinder block height	239 mm
Conrod length	147 mm
Compression height	48.3 mm
Valve diameter I/E	30.5/ 27.9 mm
Engine height – crank center to top	485.1 mm
Engine length – RFB to front of Poly V belt	475 mm
Engine weight – Opel format, MT version	174.2 kg
Compression ratio	16.5
Output @ engine speed kW/rpm	117.3/4000
Torque @ engine speed Nm/rpm	259 / 1750
Idle Speed	850 rpm
No-load max. speed	5100 rpm
Exhaust Emission Standard	Euro V
Coolant Flow	151.4 L/min
Thermostat Opening Temp start/ fully open	88.3°C/95°C
Fuel System Maximum Pressure	160 Mpa

The engine control and data acquisition hardware and software are Drivven™ products made by National Instruments™ (NI). The stock engine wiring harness was modified with an adapter board to transition factory engine sensor and control signals to and from eight Drivven™ and NI modules/drivers. These modules/drivers interface with NI data acquisition modules mounted on a NI PXI-1050 combination chassis. These modules allow control of all factory engine actuators including the EGR valve, the VGT, the VSA, fuel rail pressure control valve (RPV), as well as injection duration, timing and

profile via LabVIEW/Drivven software on the host control computer. Control of these parameters was available on the host computer from the relative safety of the control room while the engine is operating.

Control of non-factory engine accessories was conducted externally of the Labview engine control. Aftercooler output air temperature control is made possible with an external laboratory PID-controlled water valve which meters water heated with a temperature controller and pumped through the aftercooler water circuit. The flow rate of the EGR cooling water is modified manually to achieve desired EGR cooler output temperature. The engine dynamometer is an eddy current style dynamometer with PID control for both load and speed.

Emissions characterization was accomplished using several instruments. The Fourier Transform infrared spectroscopy (FTIR) sampler is used to measure concentrations of a variety of gas-phase compounds including CO2, CO, H2O, and several hydrocarbons as defined in Fang et al. (2012). It is supplied with exhaust sample lines that are maintained at 191° C to prevent condensation of water and lower volatility organic species. Soot concentrations are measured with an AVL Microsoot analyzer, which uses the photoacoustic principle to measure black carbon concentrations. Dilution ratios are measured by monitoring carbon dioxide concentrations using a medical grade CO_2 meter and FTIR spectroscopy. PM sizing and counting is accomplished with a TSI

scanning mobility particle sizer (SMPS) and condensation particle counter (CPC) for exhaust that is conditioned in a dilution system.

Equation 1. Total Hydrocarbon Calculation

$$x_{HC} = x_{CH_4} + 2 \cdot x_{C_2H_2} + 2 \cdot x_{C_2H_4} + 2 \cdot x_{C_2H_6} + 3 \cdot x_{C_3H_6}$$
$$+5 \cdot x_{IC_5} + 5 \cdot x_{NC_5} + 7.5 \cdot AHC$$

Analysis of the volatility of the diluted and conditioned exhaust PM requires a TDMA system. TDMA experimentation was developed at the University of Minnesota and used in experiments by (Orsini et al. 1999; Liu et al. 1978; Rader et al. 1987). This technique involves operating two or more DMAs in series. In early testing, conductive heat-tape was used to apply elevated temperatures to the thermal conditioning tube as shown in Figure 8.

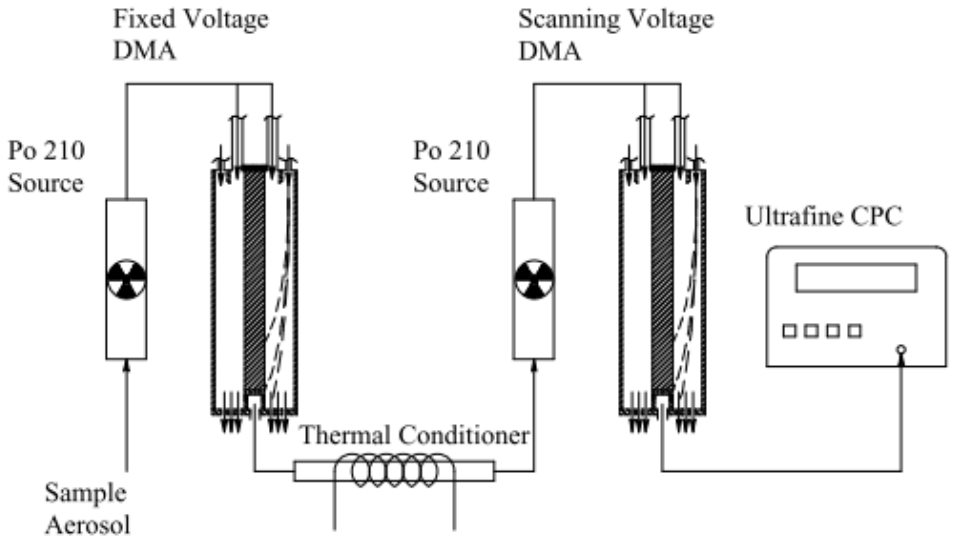

Figure 8. Conductive Tape TDMA Schematic

To better control conditioning temperature as compared to the Conductive Tape TDMA, an isothermal oil bath tandem differential mobility analyzer (ITDMA) was developed for TDMA studies. To simulate dilution under atmospheric conditions, a two-stage microdilution system was implemented based on a design by Abdul-Khalek, & Kittelson, (1998). During primary dilution, exhaust gases are cooled from temperatures as high as 300°C, to near room temperature by diluting at ratios in the range 5:1-20:1 within the primary ejector. During this process, rapid condensation and particle nucleation occurs due to the temperature change. Exhaust nanoparticle size distributions are extremely sensitive to dilution conditions (Khalek et al. 2000). The diluted mixture is then sent into the dilution tunnel, where the mixture ages. Within the dilution tunnel, particles continue to grow due to condensation, and coagulation. Finally, the mixture is further diluted at the secondary dilution stage ejector, which ranges from 5:1-20:1. The secondary dilution stage is intended to "freeze" the particle size distribution by diluting the mixture to the extent that coagulation and condensation are greatly slowed. After secondary dilution, the aerosol is sampled by an SMPS. The dilution temperature is controlled by cooling the dilution air in an ice bath, and then warming it to the desired temperature with a temperature controlled heater. The dilution ratio is controlled by ejector orifice size selection and regulated conditioning air pressure. The microdilution system and ITDMA are shown in Figure 9.

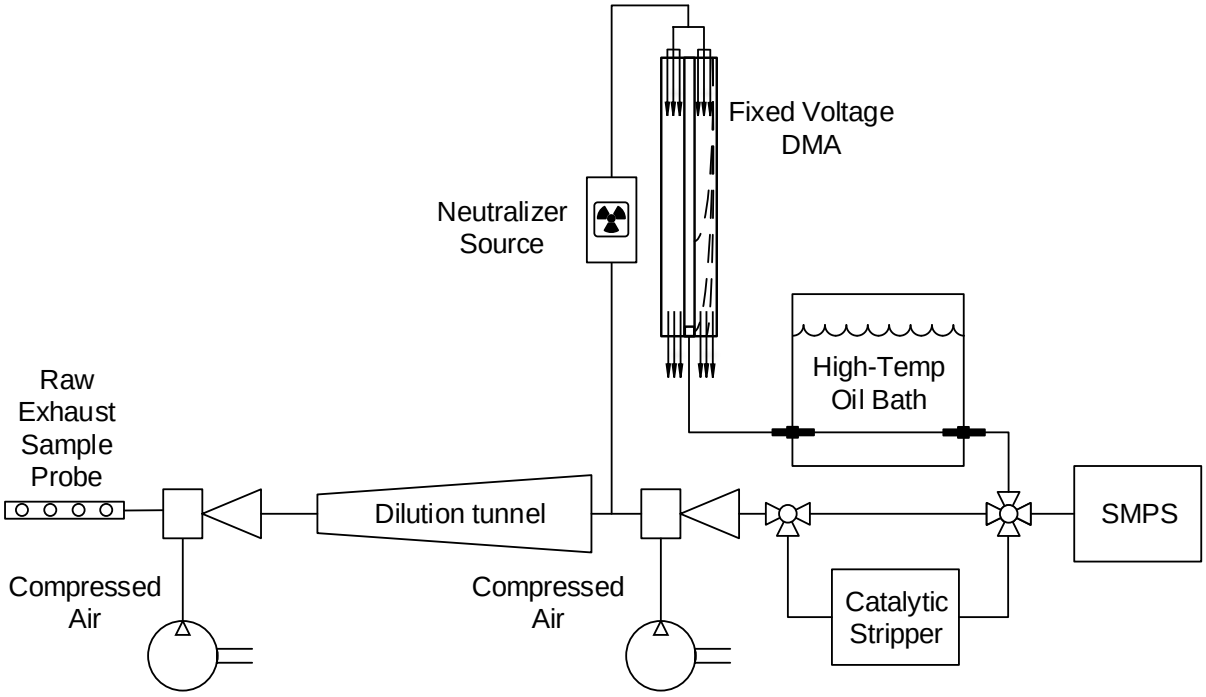

Figure 9. Oil Immersion Tandem Differential Mobility Analyzer with Microdilution System

In a TDMA study, the first DMA is used to select a monodisperse aerosol from a polydisperse mixture such as diesel exhaust. This monodisperse aerosol is heated under controlled conditions, which causes evaporation of volatile particulate content, and subsequently changes particle size for particles containing volatile content. The reduction in particle size is measured with a second DMA, and the volatility spectrum of the content can be determined by comparison with TDMA experiments conducted using pure substances. Further, TDMA analysis allows investigation of variability of particle volatility as a function of particle size.

Pressure signals from intake manifold, exhaust manifold, barometer, and engine air laminar flow element (LFE), as well as analog signals from a coriolis fuel flowmeter, CO_2 meter and dynamometer control unit are collected by a NI BNC-2095 module, and conditioned by a SCXI-1102 card within the PXI chassis. Thermocouple signals are sent to a NI TC-2095, and processed by an SCXI 1102 card in the PXI chassis.

ULSD fuel was used for the duration of the study. Two batches of #2 ULSD were consumed, with a difference in sulfur level of 1.6 ppm, and differences in density and LHV less than 1%. The test fuels were been analyzed for cetane number, sulfur content, density, and other properties as seen in Table 3. At 5 and 7 ppm, the research fuel's sulfur content was significantly lower than the 15 ppm ULSD standard demands.

Table 2: ULSD Properties

ULSD Fuel	Batch 1	Batch 2
Density (g/cc @ 15.56℃)	.8517	.8542
Kinematic Viscosity (mm^2/s)	2.399	2.705
Lower Heating Value (MJ/kg)	42.792	42.781
Cetane #	41.1	42.5
Carbon (Wt%)	86.99	86.84
Oxygen (Wt%)	<.05%	<.05%
Sulfur (ppm)	4.8	6.4
Hydrogen (Wt%)	13.01	13.16

3.2 Research Plan

This research study compared LTC modes to conventional combustion modes with equivalent speed and load. These LTC modes included PPCI and RCCI conducted as follows: 2 bar brake mean effective pressure (BMEP) at 1500 rpm, 4 bar BMEP at 2000 rpm For RCCI, a 1500 rpm 2.6 bar BMEP strategy, a 1500 rpm 4 bar BMEP strategy, and a 2600 rpm 5.6 bar strategy was chosen. These modes are light-duty to mid-duty modes with outputs ranging from 5 kW to 23.7 kW, power outputs suitable for operating a small vehicle in excess of 40 mph (Northrop, 2009). The 2 bar condition will use early low temperature combustion (ELTC), while the 4 bar conditions will be conducted using late low temperature combustion (LLTC). The comparison of equivalent LTC and conventional modes will allow a basis to compare LTC performance and emissions versus conventional combustion in fulfillment of the research objectives.

3.3 Research Objectives

The primary goals of this study are to better understand the volatility and formation of PM from LTC modes. LTC produces emissions that are not typical of conventional diesel combustion. In particular, PM from LTC is distinctly different and has thus far been poorly characterized in the literature. Better understanding of PM from LTC will improve technology development, help identify health risks, and improve testing procedures conducted to prove regulatory compliance. The results of this research conclusively tested the hypotheses that the PM from LTC can form without solid core

nucleation points, and that aftertreatment systems will further modify the formation mechanisms of PM from LTC. The specific proposed and successfully investigated three objectives of this study are as follows:

Investigate the formation of SVPM under a variety of dilution conditions for LTC operating modes and determine its volatility and composition. – The results shed light on the manner in which dilution conditions affect SVPM from LTC modes of combustion compared to conventional modes at similar engine speeds and loads and with conventional ultra-low sulfur diesel (ULSD) fuel. Full control of dilution temperature, dilution ratio, and mixture aging were implemented in handing the exhaust. Tandem differential mobility analyzer (TDMA) experimentation, a method previously developed for determining particle volatility (Sakurai, 2003) were used extensively to determine volatility properties as a function of particle size. A catalytic stripper (CS) was used to distinguish nonvolatile, solid species from gas and liquid-phase organic components. The results of the TDMA and CS give insight on the origin of SVPM, i.e. whether it condensed onto solid particles, or condensed onto nucleated organic species. Gas-phase emissions were analyzed with Fourier Transform Infrared Spectroscopy (FTIR) and other methods. Aerosol emissions were analyzed using a SMPS and Microsoot.

Characterize the effectiveness of modern aftertreatment systems in mitigating species that may form SVPM from LTC. While improvements in diesel engine design

such as cooled EGR, high pressure injection, and turbocharging enable cleaner combustion strategies such as LTC (Fino, 2007), aftertreatment of diesel exhaust is still necessary to reduce emissions, especially under higher loads where LTC is not possible. Aftertreatment systems modify engine-out exhaust with several mechanisms that have implications for particulate formation. Oxidation of semi-volatile HC in a DOC and removal of soot in a DPF greatly reduce particle concentrations. However, a study by Han et al. (2008) has shown that composition of LTC exhaust presents an environment in which DOC operation is quite variable. Because LTC particulate is comprised of such a large TOF due to increased OC emissions, the effect of DOC OC conversion on particulate formation is also an objective of the proposed research. DPFs are frequently used downstream of DOCs to remove particulate matter from the exhaust stream. For conventional combustion modes, the main goal of the DPF is the removal of EC particles. Despite the very low EC emissions inherent to LTC combustion, the effect of the DPF on particulate formation during dilution may significantly alter PM number distribution because of the removal of solid nucleation sites. This may potentially inhibit the conversion of gas phase species to the particle phase, and possibly encourage homogeneous nucleation for some species (Park et al. 2003, McMurry, P. H., Friedlander, S. K. 1979). The study of these DPF effects on particle formation was investigated for low load LTC.

Identify mechanisms for growth of SVPM under primary dilution in the exhaust plume. In this objective, aerosol models using volatility information gathered from the TDMA and GM/MS experimentation were created to simulate and understand the mechanisms of condensation and evaporation of LTC PM under atmospheric dilution. The composition and properties of LTC exhaust provides a unique aerosol modeling challenge due to large variation in volatility of species present in diesel engine exhaust. This challenge was met by the use of TDMA analysis of pure compounds in comparison of TMDA results from LTC exhaust particles to identify the volatility range present. Additionally, a model investigating the heterogeneous nucleation of sulfuric acid and water was created to identify the role of sulfuric acid and water clusters in the inception of LTC nucleation mode particles.

4 LTC PM Primary Dilution Behavior[1]

4.1 Summary

A known downside to LTC in diesel engines is increased hydrocarbon (HC) emissions. In this portion of the study, it is shown that semi-volatile species from LTC form the bulk of particulate matter (PM) upon dilution in the atmosphere. The nature of gas-to-particle conversion from high HC operating modes like LTC has not been well characterized. Here we explore engine-out PM and HC emissions from LTC and conventional diffusion combustion (CC) operation for two different engine load and speed modes using a modern light-duty diesel engine. An experimental method to investigate PM volatility was implemented. Raw exhaust was diluted under two dilution conditions. A tandem differential mobility analyzer (TDMA) was used to identify differences in volatility between particle sizes. The study revealed that LTC PM mass and number concentration showed a greater dependence on dilution conditions than PM from CC. There was also evidence of differences in particle volatility as a function of particle size for PM from LTC, with PM from CC having more consistent volatility characteristics. The results of this study show that significant semi-volatile PM emissions are present in LTC exhaust compared to CC operation though they are highly dependent on dilution conditions. This indicates that gas-to-particle conversion processes require

[1] The results presented in this chapter are based on the journal article Lucachick et al. (2013)

additional study to identify the clear impact of LTC implementation on real-world PM emissions.

4.2 Introduction

Species of concern for gas-to-particle conversion include low volatility fuel species and lubricating oil, as well as partially reacted higher molecular weight products of combustion like polycyclic aromatics. More recently, organic acids have also been identified as potential PM contributors. As shown in the results of this study, upon dilution, these species undergo gas-to-particle conversion by formation of new volatile nucleation mode particles, and also by accumulating on existing PM.

The volatile nature of PM from LTC makes characterization difficult, with prior studies seeing great variance in EC/OC ratio depending on measurement method.

4.3 Experimental

To simulate PM formation in atmospheric dilution conditions, controlled exhaust dilution was a necessity. To this end, a micro-dilution system combined with a catalytic stripper was used as shown in Figure 10. This two-stage dilution system uses vacuum ejectors to pull exhaust gas through an orifice at a dilution ratio of approximately 12:1. The exhaust was sampled at a port on the 2.5” diameter exhaust pipe at a location 8 feet downstream of the exhaust manifold to most closely replicate conditions on a vehicle tailpipe. The primary ejector was supplied with clean, temperature controlled CO_2 and H_2O-free compressed air which was cooled with a reservoir of dry ice. The temperature

of the compressed air supply was controlled such that the mixture of the compressed air and raw exhaust reach the target dilution temperature after adiabatic mixing. The resulting aerosol was aged in a dilution tunnel for approximately 1 second**.** The dilution ratio was monitored continually by measuring the CO_2 concentration within the aging tunnel using a medical grade CO2 instrument. A catalytic stripper effective at removing HC and sulfate material was used to remove volatile organic material and sulfates from the exhaust PM, leaving only solid PM material. The device consists of a heated oxidation catalyst through which the diluted sample passed. PM resulting from processing in the catalytic stripper has been shown to be primarily soot and ash (Abdul-Khalek, Imad S., Kittelson 1995).

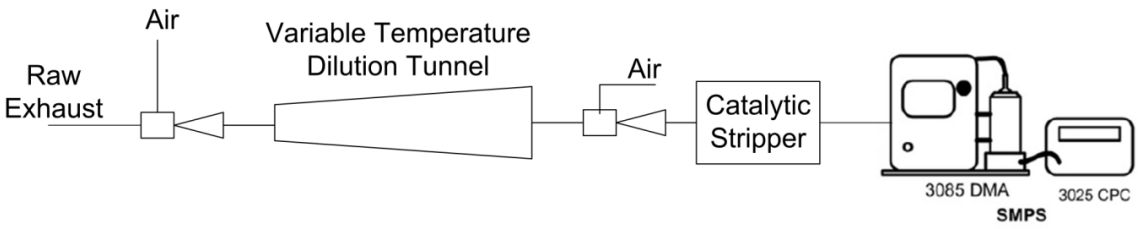

Figure 10. Dilution and sampling system

To identify differences in PM composition based on particle size, a tandem dynamic mobility analyzer (TDMA) system with thermal conditioning was used (Figure 8). This device allows selection of a near-monodisperse aerosol sample by selecting

particles of similar electro-mobility. After selecting the monodisperse PM, the thermal conditioning section processed the aerosol under controlled temperature conditions, causing a change in particle size due to evaporation of volatile PM species. The resulting change in particle size was measured using the SMPS. TDMA allowed characterization of PM volatility at specific particle sizes. TDMA is an effective technique for measuring size-dependent PM characteristics. If a monodisperse aerosol is thermally conditioned, and the result is a multi-modal particle distribution caused by different rates of shrinkage, then particles at that size are described as externally mixed (Sakurai, Park, et al. 2003). Sakurai discovered using TDMA with thermal conditioning that 70nm CDC PM was comprised of two particle types: “more volatile” and “less volatile”, as two distinct modes resulted from the original 70nm selection. By selecting multiple particle sizes for thermal conditioning, size dependent mixing characteristics of diesel PM can be investigated.Each of the four combustion modes in this study were run on separate days. Before beginning data acquisition, the engine was operated at the prescribed combustion condition for several hours to verify the steady operating conditions necessary for testing. Two LTC combustion strategies were implemented in this study. Early injection timing 1500 RPM LTC (ELTC) at 2 Bar BMEP, and late injection timing 1500 RPM LTC (LLTC) at 4 Bar BMEP similar to those described by Northrop et. al (2011) were tested alongside CC conditions at equivalent speeds and loads. The operating settings are defined in Table 3. Further details can be found in Lucachick et al. 2014.

Table 3. Engine Operating Parameters

Combustion Type	2 Bar Conventional	2 Bar ELTC	4 Bar Conventional	4 Bar LLTC
Load (N•M)	32.9	33.7	66.1	67.7
Speed (RPM)	1498	1498	1498	1498
Injection Pressure (Bar)	500	800	750	1200
Main Inj. Timing (DBTDC)	7	20	10	3
Main Inj. Duration (µs)	0.613	0.513	0.632	0.508
Pilot Inj. Timing (DBTDC)	19	N/A	21	N/A
Pilot Inj. Duration (µs)	0.21	N/A	0.1	N/A
EGR rate (%)	32.9	59.8	23.5	39
Intake Charge Temp (°C)	62.2	63.7	56.7	59.9
BSFC (g/kW•hr)	293.2	315.9	242.7	257.2
Air-Fuel ratio	41.50:1	23.44:1	27.31:1	18.11:1
Swirl Angle (deg.)	28.1	28.1	35.7	37.2

For each operating condition, primary dilution temperatures of 20 °C and 50 °C were used. The 20 °C dilution temperature is representative of dilution in a cool environment, while the 50 °C dilution temperature is in the range of dilution temperatures defined by EPA CFR part 1065 Engine Testing Procedures. Primary and secondary dilution ratios of 12:1 and 16.5:1, respectively, were used for all operating conditions. The secondary dilution ratio was verified before and after each test by flooding the

dilution tunnel with 1000 ppm NO/balance N_2 span gas, and measuring the NO concentration with the FTIR after secondary dilution. The secondary dilution ratio was shown to remain constant over the weeks of testing.

Full particle size distributions were sampled using the SMPS. Diluted exhaust PM was processed in the catalytic stripper and the resulting aerosol was sampled using the SMPS. For each operating mode and dilution temperature, 40 nm and 70 nm particles were selected by the TDMA for thermal conditioning. Each of the sizes were conditioned at two temperatures, 30 °C and 75 °C, and the resulting change in particle size is shown by subsequent scanning using SMPS. Raw exhaust was filtered at 191 °C and sampled with the FTIR. Periodically, flow to the FTIR was switched from exhaust gas to intake gas to measure CO_2 for EGR rate calculations.

4.4 Results and Discussion

4.4.1 NOx, Soot, CO, and HC Emissions

As compared to CC, LTC modes offer both advantages and disadvantages. The LTC modes used in the study have shown to produce greatly reduced emissions index of soot and NOx on a g/kg-fuel basis when compared to their equivalent CC modes (Figure 11). For 2 Bar BMEP modes, NOx and soot emissions are increased 15 and 34 fold, respectively, when comparing ELTC to equivalent CC. A similar, but less dramatic trend

is evident for the 4 Bar BMEP load, with NOx and soot increased 4 and 12 fold, respectively when comparing 4 Bar BMEP LLTC to equivalent CC.

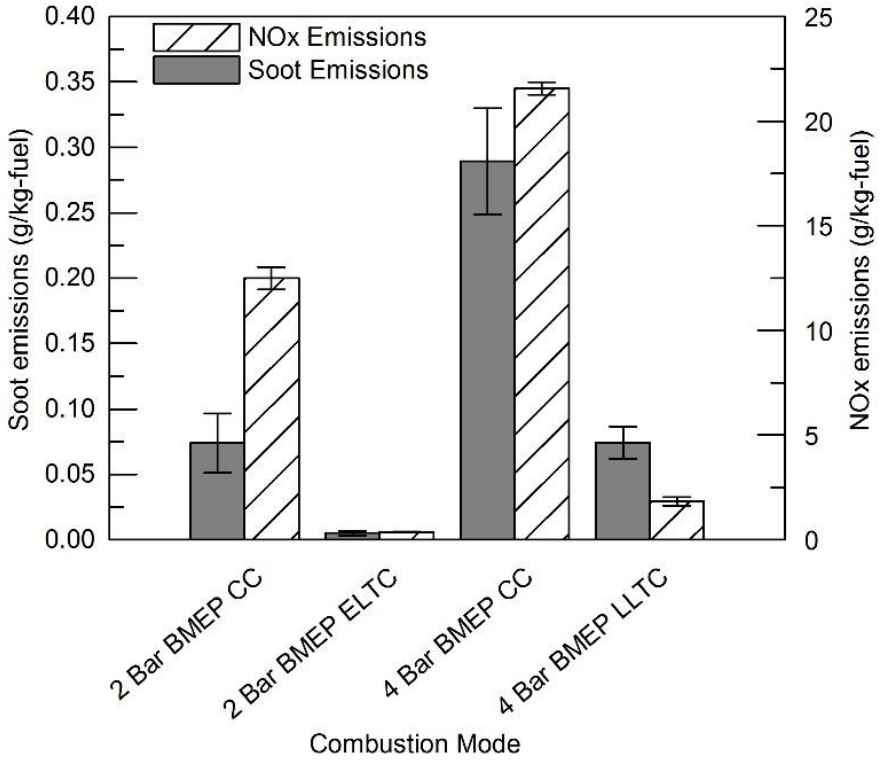

Figure 11. Soot and NOx Emissions by Combustion Mode

As expected, CO and HC emissions from the LTC modes increased when compared to CC. (Figure 12). These increased HC emissions are associated with the reduced combustion efficiency and compromised combustion phasing of LTC, with BSFC 7.7% higher for 2 Bar BMEP ELTC, and 6.0% higher for 4 Bar BMEP LLTC as compared to their equivalent CC modes.

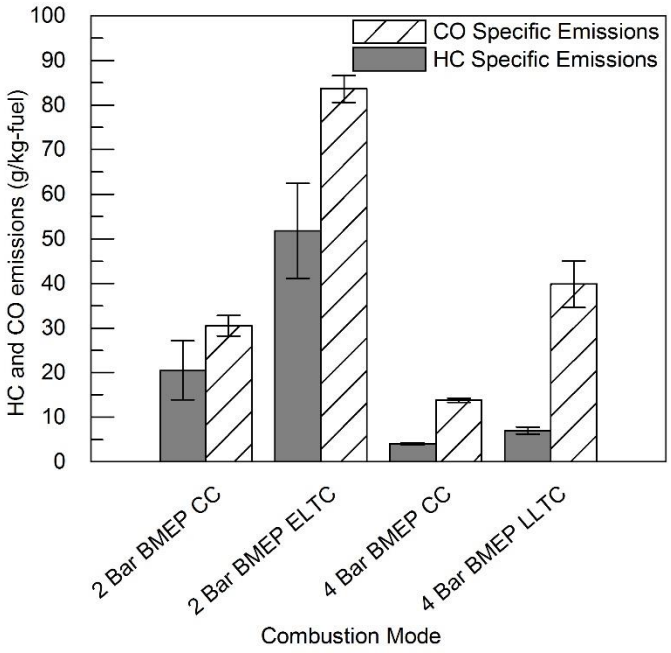

Figure 12. HC and CO Emissions by Combustion Mode

4.4.2 PM Mass and Number Concentrations

Volatile and solid fractions of the PM were measured for each combustion mode and for two primary dilution conditions as shown in Figure 13. The solid mass remained approximately constant for a given combustion mode as expected. Overall, measured PM mass concentrations for 2 Bar BMEP loads were significantly lower than those of 4 Bar BMEP modes as a result of greater solid mass for 4 Bar CC and higher volatile mass for the 4 Bar BMEP LLTC case. PM from 2 Bar CC is comprised of approximately 70% solid material regardless of dilution temperature. PM from 2 Bar ELTC is shown to be comprised of a greater portion of volatile material than PM from 2 Bar CC. The portion of volatile material varies from 82% when diluted at 50 °C to 92% when diluted at 20 °C,

a resulting increase of total PM mass by 32%. PM from 4 Bar BMEP CC is shown to be similar to PM from 2 Bar BMEP CC in that it is comprised of approximately 80% solid material, with little effect from dilution temperature. The volatile content of 4 Bar BMEP LLTC was extremely dependent on dilution temperatures. For 20 °C dilution, the volatile fraction of the PM was almost 80%, while for 50 °C dilution this fraction dropped to 31%, which is a solid fraction more similar to CC conditions. The increased dilution temperature resulted in an overall reduction in PM mass to 28% of the concentration at 20 °C dilution. Solid material is shown to comprise only a small fraction of PM from both LTC modes, and is the bulk of PM mass for both CC modes. Overall, PM mass concentration for LTC combustion shows a greater sensitivity to dilution temperature than PM from CC.

For LTC, PM number concentrations are even more sensitive to dilution conditions than PM mass concentrations as can be seen in Figure 14. PM number concentrations for 50 °C are within 25-60 million particles per cubic centimeter for all combustion modes. For 20 °C dilution conditions, PM number concentration increases by a factor of 15 for 2 Bar ELTC, and a factor of 23 for 4 Bar LLTC. For both 2 Bar and 4 Bar CC, number concentrations increase by less than 25% as compared to 50 °C dilution.

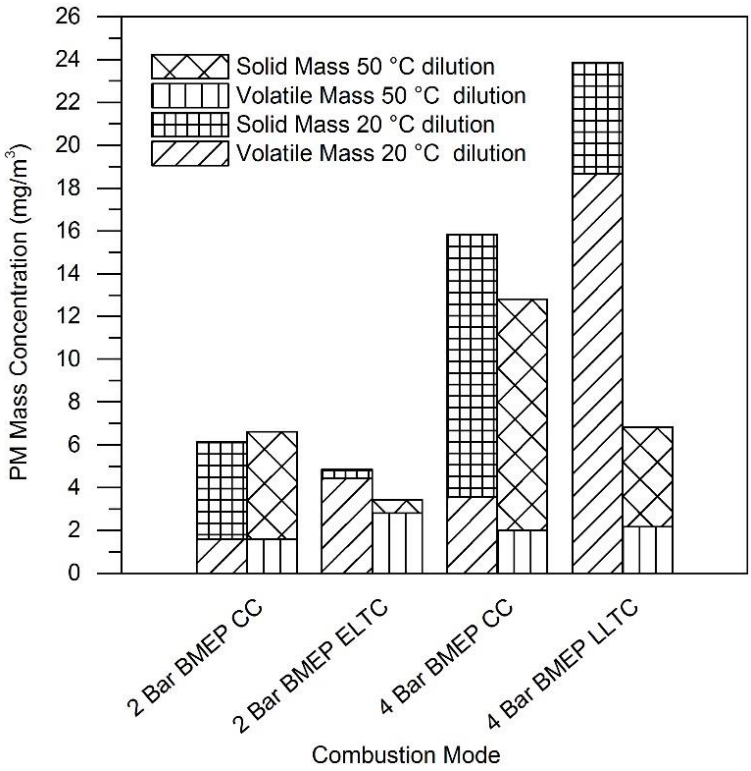

Figure 13. Volatile and Solid PM mass concentrations by combustion mode for 20℃ and 50 ℃ Primary Dilution Temperature

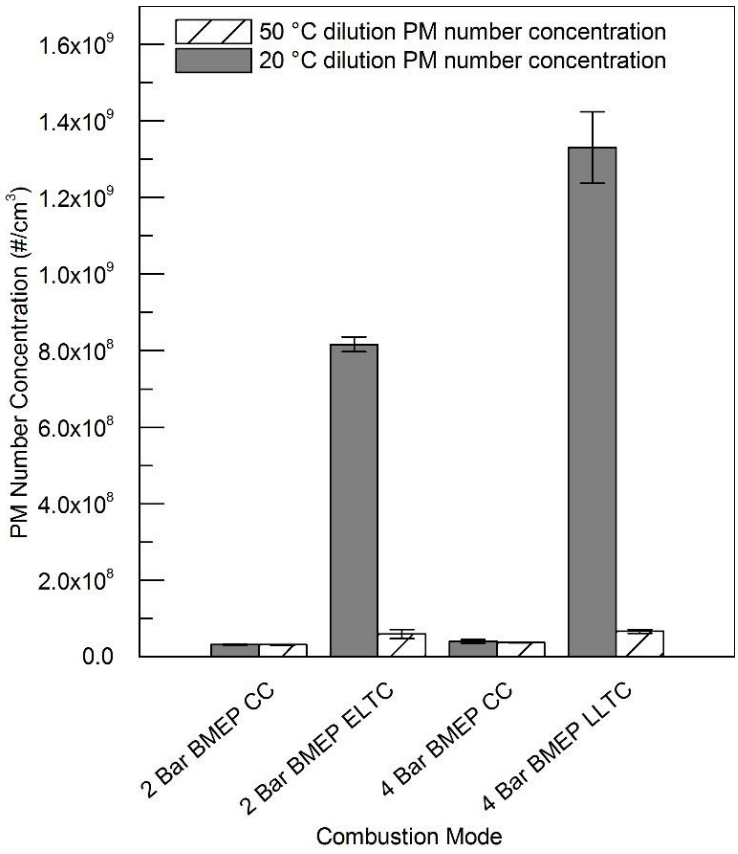

Figure 14. PM umber concentrations by combustion mode and dilution temperature

The sensitivity to dilution conditions highlights the unique volatility characteristics of PM from LTC, and the challenges inherent to measuring it. In this study, the differences in PM exhibited by a 30 °C difference in dilution temperature are easily discernible. EPA CFR part 1065 requires sampling temperatures within the range 47 ±5 °C: a 10 °C temperature spread. The results of this study suggest that for LTC PM mass, sampling at opposite ends of the EPA dilution temperature range may result in differences in PM mass and number concentration when sampling the same emissions, especially for PM from LLTC.

PM size distribution plots are shown in Figure 15. For 2 Bar BMEP CC, the 20 °C dilution condition appears to produce a very slightly larger concentration of nucleation mode particle than the 50 °C dilution condition. A similar trend is evident for 4 Bar BMEP CC. For LTC modes, there was a much greater dependence on dilution temperature. Decreasing dilution temperatures from 50 °C to 20 °C resulted in the creation of a nucleation mode, with an associated increase in mass and number concentration, further illustrating the primarily semi-volatile nature of LTC PM. The large nucleation mode is consistent with prior studies which showed that low soot emissions result in higher concentrations of nucleation mode PM. For both LTC modes, a two orders of magnitude increase in nucleation PM number concentration suggests that semi-volatile material is nucleating homogeneously, or nucleating on a very large nanoparticle mode comprised of particles smaller than 7.6 nm, and outside the measurement range of the instrument.

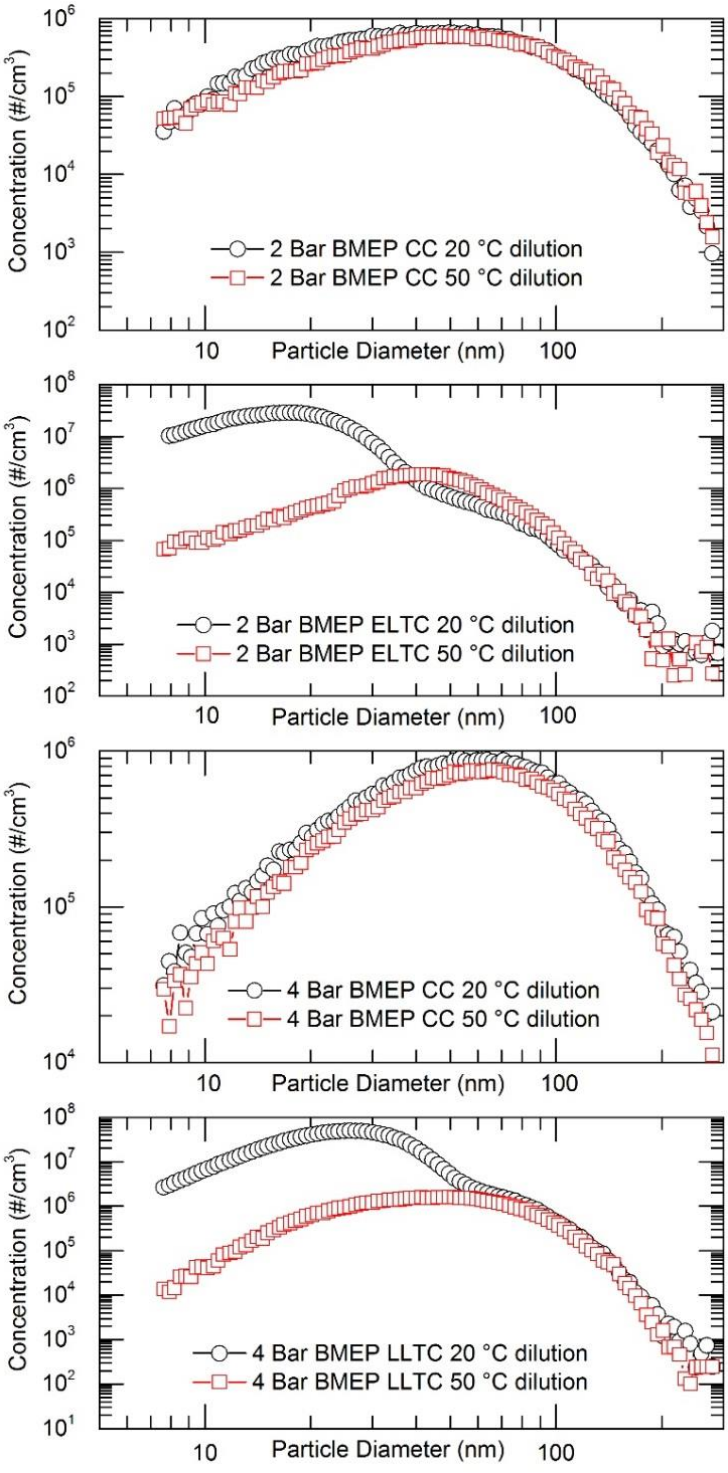

Figure 15. Total PM number concentrations by combustion mode and dilution temperature

4.4.3 Particle Volatility

Exhaust PM volatility for 20 °C dilution conditions was examined by thermal conditioning of monodisperse exhaust aerosols using the TDMA method outlined previously. Nominal 40 nm and 70 nm monodisperse aerosols were selected by the first DMA, their size distribution after conditioning at a slightly greater than ambient 30 °C (cool conditioning) was measured and compared to their size distribution after conditioning at 75 °C (hot conditioning). The reduction in particle size and number concentration due to conditioning is a matter of the conditioning temperature and the PM volatility. For each dataset, several secondary peaks are shown where larger particles with multiple charges traversed through the DMA alongside the desired particle size. These artifact particles are not addressed in this study. After conditioning, shrinkage and reduction in particle number is expected as the PM equilibrates at the conditioned temperature as can be seen in the figures.

4.4.3.1 2 Bar CDC TDMA

For the 2 Bar BMEP CC case, small changes in particle size and concentration resulted from thermal conditioning (Figure 16). There were subtle differences between particles selected at 40 nm and conditioned at 30 °C and 75 °C. Increasing conditioning temperature to 75 °C has no effect on the mode particle diameter, however, the concentration of particles at the mode diameter is reduced slightly, and the resulting average diameter decreases. This suggests that a most of the particles are mostly solid, and change very little in diameter, but a portion of the particles are of mixed volatility

and decrease in diameter at greater and more differing rates. Particles selected at 70nm are of a more uniform composition, and with less mixing of particles of differing volatilities. Mode particle diameter decreased by 2.5 nm, however there was little broadening of the particle distribution due to low and consistent rates of shrinkage.

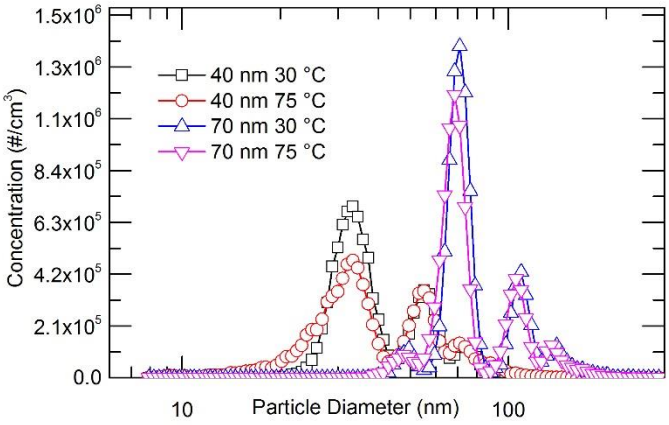

Figure 16. TDMA thermal conditioning effects on 40nm and 70nm particles from 2 Bar BMEP CC (20 °C dilution).

4.4.3.2 2 Bar ELTC PM TDMA

Results from TDMA experimentation expose slight differences in volatility characteristics between ELTC particles selected at 40nm and 70nm (Figure 17). For particles selected at 70nm, conditioning at 75 °C broadened the formerly narrow distribution, and the mode particle diameter shrank by 2nm, although particle concentration at the mode diameter was reduced by 65%, and a large fraction of the particles experienced much greater than 2 nm of shrinkage. In fact, an inspection of the distribution after thermal conditioning shows that the group of particles that shrunk by

greater than 20 nm comprise approximately 1/2 of the total number of particles in the distribution. However, the modest reduction in mode diameter suggests that a portion of the particles in this size range are mostly solid and shrink very little, consistent with accumulation mode primarily-soot particles and primarily-volatile in an externally mixed aerosol. Particles selected at 40nm appear less externally mixed, with a reduction in mode diameter of 17.6 nm due to conditioning at 75 °C. Virtually none of the particles selected at this diameter remained at the selected diameter, suggesting that there are very few solid particles at this size point. However, unlike particles selected at 70 nm, fewer than half of the particle number shrunk by more than 20 nm. This indicates overall lower volatility for the primarily-volatile particles at this size range as compared to particles selected at 70 nm, especially considering the enhanced Kelvin-effect for the smaller particles. Overall, for both particle sizes, the broadening of the particle distribution resulting from thermal conditioning suggests that particles span a mixed range of volatilities.

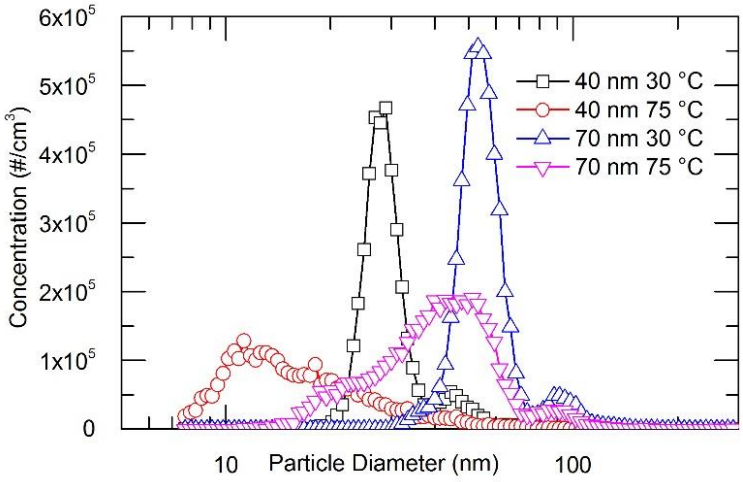

Figure 17. TDMA thermal conditioning effects on 40nm and 70nm particles from 2 Bar BMEP ELTC (20 °C dilution).

4.4.3.3 4 Bar CC PM TDMA

Results from TDMA experiments show that PM from this combustion mode exhibit less variation in composition as a function of particle size than the other modes tested in this study (Figure 18). PM selected at both 40nm and 70nm exhibited no reduction in mode diameter between conditioning at 30°C versus 75°C. There was a 14% reduction in concentration at the mode diameter for each case. Visually, the plots for 30 °C and 75 °C thermal conditioning look almost identical. This is evidence of PM consisting mostly of a solid core with a small fraction of volatile material; a trend that is common for both particle sizes examined for this combustion mode.

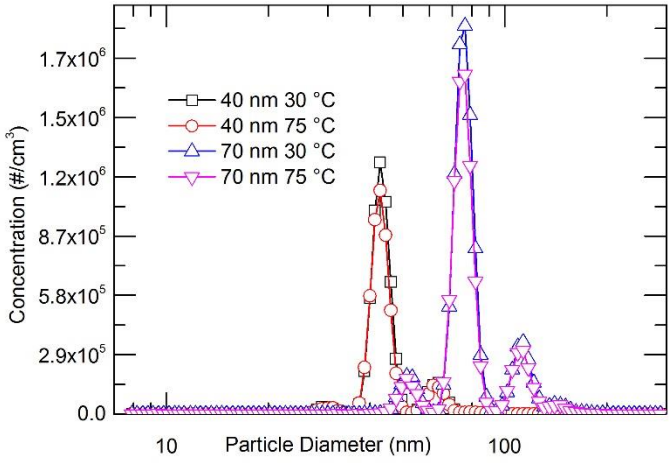

Figure 18. TDMA thermal conditioning effects on 40nm and 70nm particles from 4 Bar BMEP CC (20 °C dilution).

4.4.3.4 4 Bar LLTC PM TDMA

4 Bar LLTC TDMA conditioning results displayed characteristics seen in both 2 Bar ELTC and 2 Bar CC cases (Figure 19). Aerosol selected at 70nm showed very little change in diameter between conditioning at 30 °C and 75 °C. For particles selected at 40nm, there were great changes in particle diameter and concentration due to processing at 30 °C versus 75 °C**.** There was no definable shift in mode diameter, only a small amount of particles remaining at the upper diameter range of the near-monodisperse selected particles. This indicates that particles at this range are extremely volatile as they did not merely shrink, they entirely disappeared within the detection limits of the SMPS. The difference in volatility between 40 nm selected particles for ELTC versus LLTC indicates that either the PM forming volatile material in LLTC is of overall lower volatility than that of the PM forming volatile material in ELTC, or the 6 fold higher soot

concentration in LLTC resulted in the lowest volatility material absorbing and condensing onto soot in a manner preferential to condensing on nucleation-mode particles, which were relegated to growth by the remaining higher volatility material.

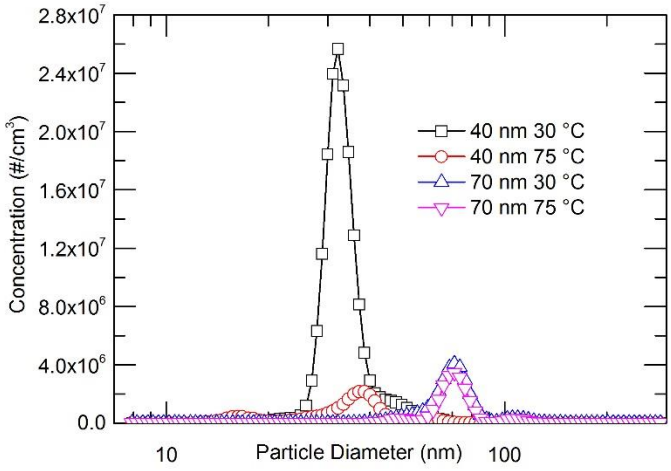

Figure 19. TDMA thermal conditioning effects on 40nm and 70nm particles from 4 Bar BMEP LLTC (20 C dilution).

4.5 Conclusion - Effects of Primary Dilution

While modern aftertreatment systems for diesel engines are effective at both catalyzing volatile material and filtering solid material, their efficacy in removing enough semi-volatile species to meet current and future PM regulations is still in question. If future regulations are imposed that consider both solid and semi-volatile PM, understanding the composition and formation of volatile PM from modes such as LTC becomes critical.

The results from this study indicate that PM from LTC is much more sensitive to dilution conditions than PM from CC because of higher concentrations of PM-forming organic material. PM mass concentrations from a 2 Bar BMEP early injection LTC mode increased by 30% due to low dilution temperatures, while PM mass from 4 Bar BMEP LLTC case more than tripled. The effect on number concentration was even more significant, with number concentrations increasing by an order of magnitude for both LTC conditions. Prior research has shown that the conditions in LTC exhaust inhibit removal of volatile material that may form LTC PM. The results of this study have shown that many fewer particles form in warm dilution conditions than cold dilution conditions; therefore fewer yet are likely to be present in the exhaust passing through a diesel particulate filter.

This work also shows that TDMA analysis techniques provide a valuable real-time method for examining PM volatility. While speciation methods are eminently valuable for characterizing PM from new combustion modes, the drawbacks of filter sampling are compounded by the volatility of PM from LTC. The flexibility for examination of particle volatility characteristics by particle size with TDMA techniques is a quality that is not attainable for off-site methods such as filters with post-GC/MS.

5 Effects of Tier IV Aftertreatment on LTC PM[2]

5.1 Summary

LTC results in increased hydrocarbon emissions as compared to conventional diesel combustion (CDC). Previous work has shown that exhaust conditions resulting from LTC inhibit oxidation of HC within a diesel oxidation catalyst (DOC). Further, these elevated HC emissions result in engine-out particulate matter (PM) that primarily consists of semi-volatile organic material. The current work shows that a DOC incompletely oxidizes this PM forming material. These results investigated the effectiveness of both a DOC and a diesel particulate filter (DPF) in reducing particle emissions for LTC. In this work, engine-out, DOC-out, and DPF-out exhaust were sampled using a micro-dilution system. Particle distributions were determined with a scanning mobility particle sizer (SMPS) and engine exhaust particle sizer (EEPS). A catalytic stripper (CS) was used to differentiate volatile and solid material in the PM. A Fourier Transform Infrared (FTIR) analyzer was used for light HC speciation. Soot concentrations were determined using a photo-acoustic sensor (Microsoot).

A recent study on DOC performance for LTC exhaust has shown that the high HC and CO levels deactivate a DOC and result in reduced conversion of these species. Further, the sub 200 °C exhaust temperatures present for low load LTC may be

[2] The results presented in this chapter are based on the journal article Lucachick et al. (2015)

insufficient for catalyst activation (Manbae Han, Assanis, Jacobs, et al. 2008). This can result in unacceptable PM emissions downstream of the DOC (Northrop, William F., Assanis, Dennis N., Bohac 2011) due to gas to particle conversion in the primary exhaust plume. Further, the low volatility species which tend to form PM in LTC are of higher molecular weight than most hydrocarbon emissions, and face a greater diffusion barrier to reaching a DOC surface and oxidizing (Author: Johnson 1994). This phenomenon is also supported by the work of Bohac et al. (2013) which showed that DOC HC conversion efficiency decreases with increasing carbon number, raising additional concerns that low volatility HC may escape the aftertreatment system and form particles upon dilution in the atmosphere.

DPFs are known to be highly effective for removal of PM from CDC (Code & Walker , 2004) in diesel engines, with efficiencies greater than 90% over a large range of particle size. Further, their removal efficiency for sub 100 nm particles increases with increasing DPF loading, as the accumulating soot cake provides an additional filtration mechanism (Swanson et al. 2013). Because PM from LTC is comprised of only a fraction of the soot of CDC, there is concern that temporal improvements in DPF efficiency due to the soot-cake layer may not occur for LTC as it does for CDC.

The objective of this study is the determination of the effects of aftertreatment on semi-volatile PM emitted from a low-load LTC combustion mode in a light-duty diesel

engine. It is known that the conditions present in LTC exhaust are detrimental to HC conversion in aftertreatment, however, the impact of this effect on DPF-out PM formed upon dilution in atmosphere demands further attention. Characterizing these effects is important for the development and application of engine mapping, and regeneration strategies used while operating in combustion modes that emit volatile PM. These include modes such as LTC, idle, and active DPF regeneration modes using post-injection. The engine was fitted with a close-coupled factory DOC-DPF aftertreatment system modified for laboratory study.

5.2 Experimental

To simulate dilution in atmosphere, all particles in this study were diluted to 25 °C in the primary dilution tunnel. The aftertreatment system was modified to allow sampling at several locations: downstream of the turbine, downstream of the DOC, and downstream of the DPF-out. Exhaust particles for both CDC and LTC were sampled downstream of the turbocharger. Though DPF removal efficiency for CDC particles is known to increase with soot loading (Swanson et al. 2013), the temporal removal efficiency effects for LTC particles is not known. Thus, LTC particles are sampled at DOC-out, and DPF-out locations in addition to downstream of the turbocharger. All particle distributions were measured using SMPS, after dilution with clean, dry, CO_2 free air. For all particle measurements, the CO_2 concentration after dilution was monitored to determine the dilution ratio. For DPF-out LTC particles, an engine exhaust particle sizer (EEPS) was utilized to observe transient phenomenon, and particle distributions were

measured at a rate of 1 Hz for the entirety of the test. A catalytic stripper (CS) was used to remove volatile organic material from sampled exhaust particles.

In a study of diesel particle mass and mobility, it was shown that for decreasing engine loads, particle effective density and fractal dimension increased (Park, Cao, et al. 2003). TEM images of these particles suggested that this is a result of high fuel and/or lubricating oil content. The study also showed that for a 10% load condition, effective density ranged from 1.2 g/cm^3 at 50 nm to .73 g/cm^3 at 120 nm. Particles at the 10% load point also exhibited a higher fractal dimension than particles from higher load operation, indicating a more compact particle. LTC particles are known to be comprised mostly of volatile organic material, suggesting that they would have similar density to unburned fuel and lubricating oil. Further, this composition high in volatile material would render them more likely to form similarly compact particles. For this study, to estimate mass, calculations assume spherical particles and specific gravity of 1. Prior to each test, a medium-load, post-injection assisted active DPF regeneration cycle was conducted to ensure that all soot and organic material was oxidized from the DPF. Post-injection duration was slowly ramped up until DOC-out temperatures reached 625 °C. The details of the regeneration cycle are shown in Table 4. This high temperature condition was held for ten minutes prior to switching to the experimental condition. The experimental combustion condition was allowed to stabilize for five minutes before data were

collected. Following the stabilization period, the engine was run uninterrupted at the setpoint for the duration of the test.

Table 4. Active Regeneration Parameters

Active Regeneration Parameters	
Load (N·M)	70.5
Rail Pressure (Bar)	800
RPM	1500
Pilot Inj. Timing/Duration	19 DBTDC / .21 ms
Main Inj. Timing/Duration	7 DBTDC / .59 ms
Post Inj. Timing/Duration	-80 DBTDC / .535 ms
DOC-out Temperature	625 °C

2 Bar ELTC with early injection and a low load CDC mode similar to those used in ref. (Lucachick, Avenido & Northrop 2014) were compared, with a focus on the effect of aftertreatment on the volatile particles from ELTC. The details of both modes are shown in Table 5.

Table 5. Engine Operating Parameters

Combustion Type	ELTC	CDC
Speed (RPM)	1498	1498
Load (N·m)	31.2	29.55
Injection Pressure (Bar)	840	500
Main Inj. Timing (DBTDC)	20	7
Main Inj. Duration (ms)	.515	.6
Pilot Inj. Timing (DBTDC)	NA	19
Pilot Inj. Duration (ms)	NA	.21
EGR rate(%)	60.8	35.2
Intake Manifold Pressure (kPa)	101.95	100.85
Intake Charge Temp (°C)	61.0	55.4
DOC Inlet Temp (°C)	191.06	197.51
BSFC (g/kW·hr)	327.2	309.8
Equivalence Ratio	.638	.336
Combustion Efficiency (%)	95.66	97.57

5.3 Results and Discussion

5.3.1 NOx, Soot, and HC Emissions

In agreement with prior results, the LTC condition exhibited significantly lower soot and NOx as compared to CDC as shown in Figure 20 Engine-out soot and NOx emissions increased 13 and 35 fold, respectively from ELTC to CDC. DPF-out soot emissions were not shown in the figure as total DPF-out soot concentrations were below the limit of detection of the Microsoot instrument for both modes. Aftertreatment conversion of NOx was negligible for both modes.

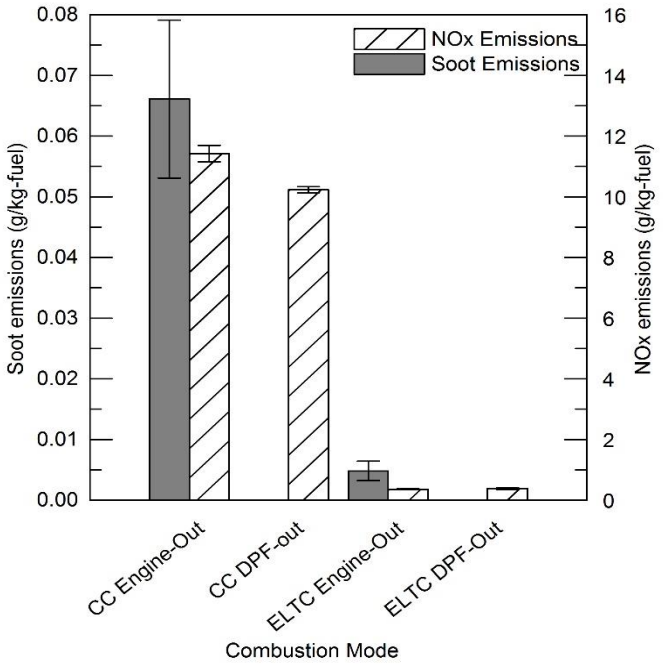

Figure 20. NOx and soot emissions by combustion mode and sampling location

Engine-out CO emissions were nearly three times higher for ELTC than (Figure 21). Nearly 100% CO conversion efficiency was achieved in the aftertreatment for CDC. CO Conversion efficiency for ELTC was poorer, at 50%. HC emissions for ELTC were only slightly higher than CDC, but this may be due to the limited number of gaseous hydrocarbons measurable with the FTIR. More than double the HC emissions were reported for ELTC as compared to CDC in a prior study utilizing a FID for HC measurement (Lucachick, Avenido & Northrop 2014). HC conversion efficiencies for CDC and ELTC averaged over the duration of the test were 77% and 55%, respectively.

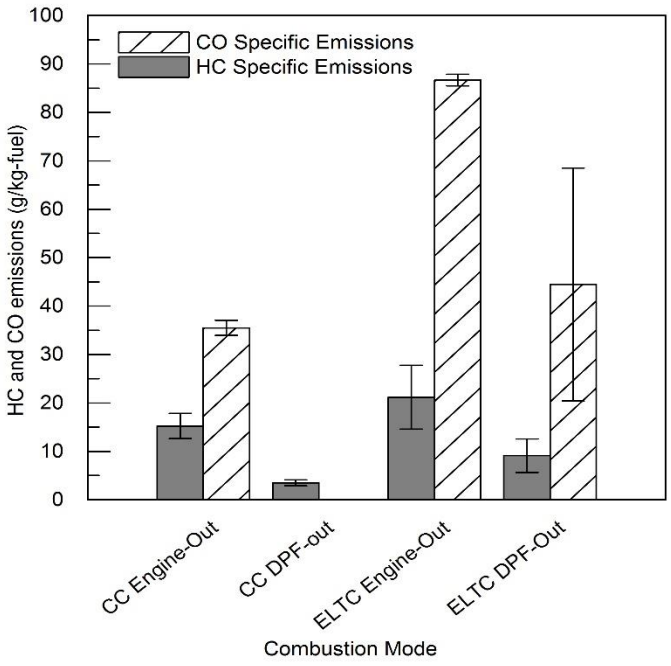

Figure 21. CO and HC emissions by combustion mode and sampling location

5.3.2 PM Mass and Number Distributions

Particle volatile and solid fractions for both combustion modes were estimated by integrating particle distributions taken from diluted exhaust and CS-processed diluted exhaust (Figure 22). Overall, total PM mass was very similar for both combustion modes; however, the particle compositions are quite different. Particles from CDC were found to be comprised almost entirely of solid material, and in mass concentrations very similar to soot measurements.

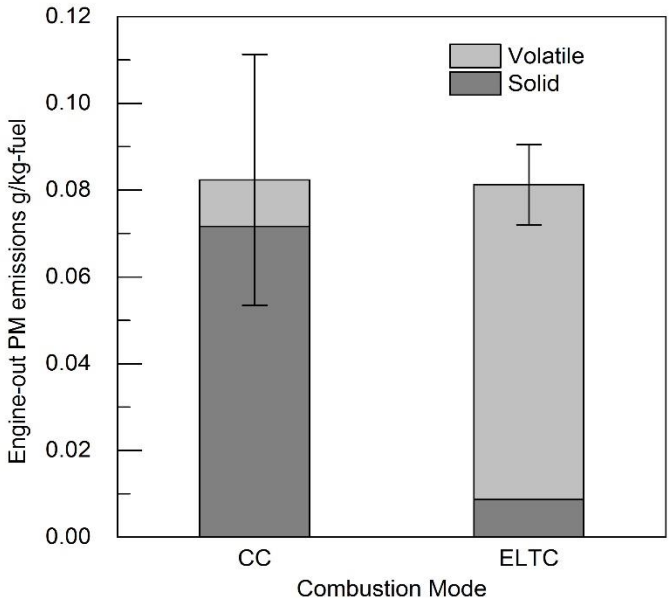

Figure 22. Engine-out particle volume and composition by combustion mode.

At the tested ELTC condition, the portion of the particle forming semi-volatile material that the DOC removed from the exhaust stream is evident in Figure 23 alongside engine-out particle distributions and CS-out particle distributions. The DOC scans were

taken at the 100 minute mark when apparent DOC conversion efficiency had reached its minimum. The DOC reduced total PM mass by 77% percent, while the CS removed 90% of PM mass. This is expected as the low space velocity and high temperature within the CS effectively convert all organic material.

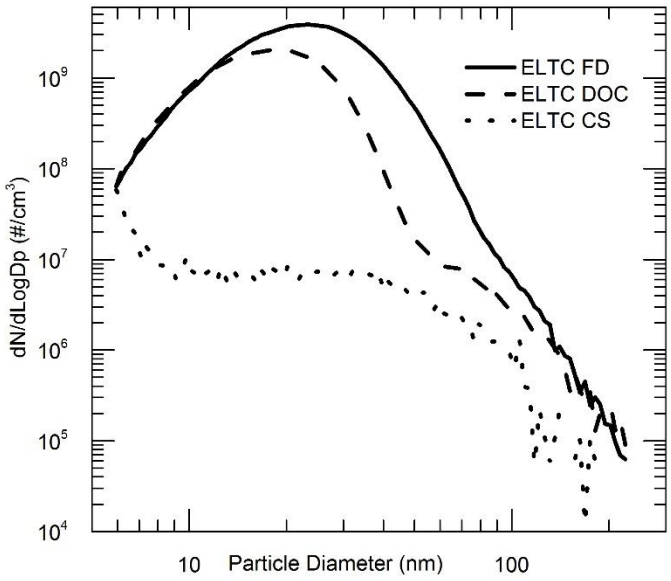

Figure 23. The effect of DOC and CS on ELTC engine-out particle distributions. FD represents full engine-out particle distributions

5.3.3 ELTC Aftertreatment Effects

ELTC aftertreatment-out particle emissions were highly transient in nature, and are explored in detail. The high-temperature active regeneration performed before the test left DOC-in temperatures at the beginning of the test 15 °C higher than the steady-state value of 190 °C (Figure 24). DOC temperatures and HC apparent conversion efficiency

(HCACE) are shown in Figure 24. The term HCACE is used because aftertreatment reductions in HC can be attributed to both oxidative conversion in the DOC and to a lesser extent the DPF, and absorptive storage in the DOC zeolite and DPF material. In this test, HCACE at the beginning of the test was 85%.The HCACE dropped to 40% within 75 minutes. It is not known whether conversion or storage is dominant in this test, however, HC storage can play a significant role. A study by (Knafl et al. 2007) using DOC catalysts with zeolite storage component on DOC idle light-down showed HCACE very gradually falling from 65% to 20% over a period of 50 minutes, despite the impossibility of conversion at the final observed 120 °C DOC temperature.

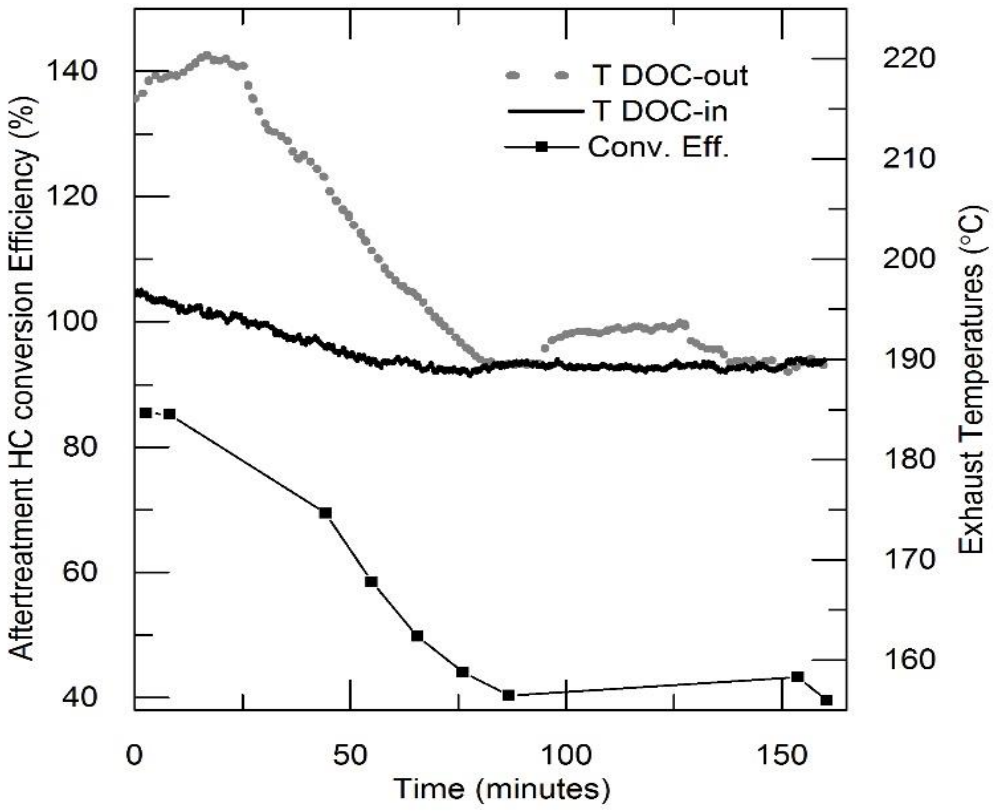

Figure 24. DOC-in and DOC-out temperatures with HC aparent conversion efficiency

A partially-active DOC is somewhat effective at reducing PM emissions (Figure 23), and a DPF offers additional benefit. In Figure 25, DPF-out particle mass as measured by EEPS is plotted along with DPF efficiency against time. DPF mass removal efficiency is constant at 99.8% until 65 minutes into the experiment, at which point it gradually falls to 92% at the 145 minute mark. This increase in PM emissions corresponds closely to falling HC conversion. This relationship is very sensitive, as PM removal efficiency is at 99.8% even at an HCACE value of 50%, but upon falling to 40%, PM emissions increase by two orders of magnitude. This extreme sensitivity can be attributed to volatile vapors existing at sub-saturated vapor concentrations at 50% HCACE, and supersaturated vapor concentrations at lower HCACE levels. The mechanisms responsible for the gradually diminishing HCACE levels are reduced HC conversion efficiency due to falling temperatures, catalyst deactivation, and reduced HC storage due to HC saturation of the absorptive DOC-DPF materials.

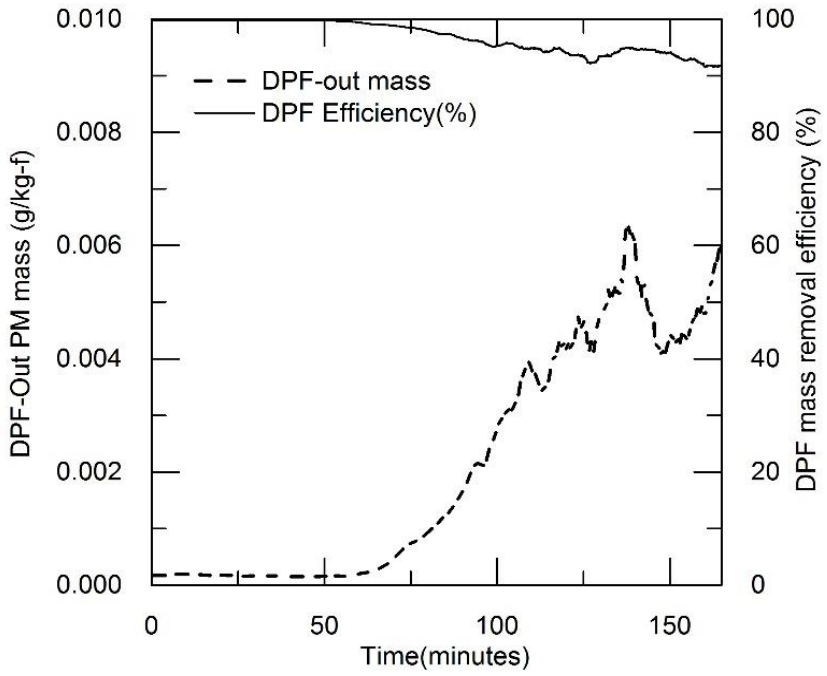

Figure 25. Transient DPF-out particle mass and HC emissions, and particle mass removal efficiency.

The implication of the observed DPF-out particle emissions trends is that material comprising these volatile particles exists in the gas phase and not in particle form while in the exhaust system. This is supported by a study by Lucachick et al. (Lucachick, Avenido & Northrop 2014) which showed that exposure to temperatures as low as 75 °C for ¼ second resulted in almost total particle mass evaporation for two sizes of ELTC particles Figure 26. Although low, the exhaust temperatures in this study are much higher than 75 °C and thus volatile material remains in gas phase. At low HCACE levels, this material has the potential to escape the aftertreatment system and form particles, as occurs in this study. Further, any hypotheses that the volatile material exists in the particle phase while in the exhaust system must be dismissed because that would result in

trapping by the DPF with the same filtration mechanisms that lead to the high efficiency soot trapping shown in this study and many others.

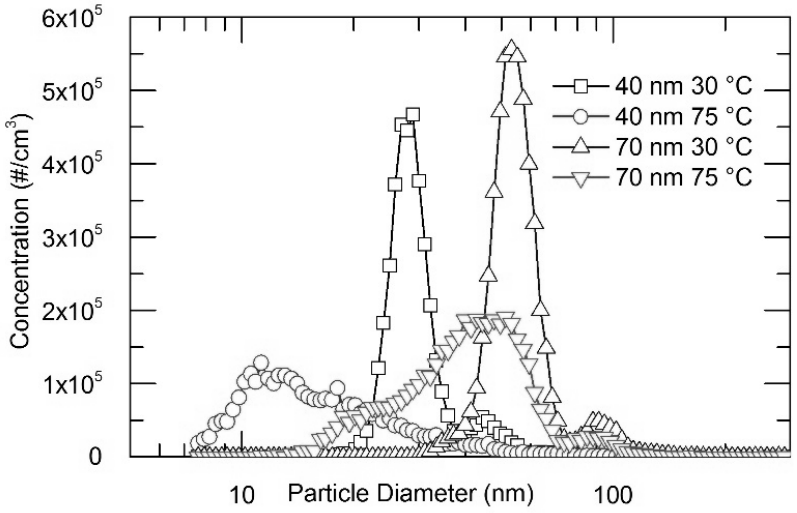

Figure 26. ELTC particle evaporation resulting from exposure to 75 °C for 1/4 second (adapted from (Lucachick, Avenido & Northrop 2014))

5.3.4 LTC Aftertreatment Conclusions

Previous work has shown that under atmospheric dilution, PM from LTC is comprised almost entirely of volatile material. This has raised concerns that DOC inactivity at low exhaust temperature and high CO levels may lead to volatile PM precursors that slip through a DPF in the gas phase and form PM upon initial dilution in the atmosphere. The results of this study illustrate the particle suppression characteristics of a modern diesel aftertreatment system for a low load LTC mode. A freshly regenerated

close-coupled DOC-DPF showed 99.8% efficiency in removing particle mass measured after dilution. This efficiency was maintained for over an hour at which time it began to fall in tandem with falling HCACE. Falling HCACE was attributable to both reduced conversion in the DOC-DPF as well as saturated HC storage capacity. This eventual deterioration of PM removal efficiency for LTC is in contrast to CDC where greater DPF loading generally results in greater PM removal efficiency.

The results presented here show that a modern aftertreatment system is effective in suppressing particle formation from low load LTC. The efficiency is especially good for approximately one hour following a regeneration cycle, but then deteriorates due to reduced HC conversion and limited HC storage capacity in the aftertreatment. However, even with HCACE levels as low as 40%, total aftertreatment PM mass removal efficiency exceeds 90%. The results presented here suggest that with intermittent regeneration, low load LTC modes can offer low DPF-out particle emissions when used in a modern engine equipped with aftertreatment. Further investigations are necessary to distinguish the individual effects of HC conversion and HC storage in mitigating PM emissions from volatile particle emitting combustion modes such as LTC.

6 Volatility Characterization of Nanoparticles from Single and Dual-Fuel LTC [3]

6.1 Summary

This section explores the volatility of particles produced from two diesel low temperature combustion (LTC) modes proposed for high-efficiency compression ignition engines; mechanisms of particulate formation and growth upon dilution in the near-tailpipe environment are explored. The number distribution of exhaust particles from low and mid-load dual-fuel reactivity controlled compression ignition (RCCI) and single-fuel premixed charge compression ignition (PPCI) modes were experimentally studied over a gradient of dilution temperature. Particle volatility of select particle diameters was investigated using evaporative tandem differential mobility analysis (ETDMA). Evaporation rates for exhaust particles were compared with ETDMA results for candidate pure n-alkanes to identify species with similar volatility characteristics. ETDMA results were used to define inputs to an aerosol condensation and evaporation model to support the finding that smaller particles in the distribution are comprised of lower volatility material than large particles under primary dilution conditions. Although our results show that saturation levels are high enough to drive condensation of alkanes onto existing particles under the dilution conditions investigated, they are not high enough to drive

[3] The results presented in this chapter are based on the journal article Lucachick et al. (2016)

homogeneous nucleation of these same compounds in the primary exhaust plume. Therefore, we conclude that observed particles from LTC operation must grow from low concentrations of highly non-volatile compounds present in the exhaust.

6.2 Introduction

The implementation of LTC in CI engines is known to emit greater unburned and partially burned hydrocarbon (HC) emissions compared to CDC. Jacobs (2007) showed double the HC emissions for PPCI versus CDC at the same engine speed and load. Prikhodko et al. (2010) showed an order of magnitude increase in HC for low load RCCI compared to equivalent speed and load CDC. These emissions contain a range of organic compounds with molecular weight ranging from methane to unburned fuel molecules and heavy polycyclic aromatic (PAH) compounds (Merritt et al. 2006). In-cylinder formation mechanisms and speciation of HCs from LTC have been thoroughly studied (Knafl et al. 2006), (Colban et al. 2007), (M Han et al. 2008). Although solid particle mass concentrations are very low for LTC, high concentrations of semi-volatile HC in LTC exhaust are known to form nanoparticles through nucleation and growth mechanisms upon primary dilution (Northrop et al. 2011). Further, we have shown in previous work that volatile material can slip through a close-coupled aftertreatment system composed of a diesel oxidation catalyst (DOC), and diesel particulate filter (DPF) and form particles under certain conditions (Lucachick et al. 2015). Although considerable research has characterized nanoparticles from CDC, very little has been done to specifically examine semi-volatile nanoparticles from LTC operation in CI engines.

Volatile material in LTC particulate arises from a multitude of sources. Unburned fuel is thought to heavily contribute to LTC-derived primary particles, but previous work has shown unburned fuel alkanes are not solely responsible for the increase in volatile particle emissions (Northrop et al. 2011). Other contributing species include low volatility components like methyl ester in biodiesel and polycyclic aromatic hydrocarbons (PAHs) present in diesel fuel and from combustion. The study by Merritt et al. (2006) on unregulated emissions from CDC and LTC showed orders of magnitude increases of particle forming PAH compounds for LTC modes in comparison to CDC modes. Other studies suggest that species beyond PAH and unburned fuel contribute to LTC particles. Sluder et al. (2004) deduced that in addition to unburned fuel species and PAH, additional semi-volatile species may include carboxylic acids and long-chain aldehydes. Another source of volatile particle forming material not exclusive to LTC is unburned lubricant oil, though prior work shows that the particle mass contribution from oil is small compared to the contribution from fuel (Franklin 2010).

Literature is extremely sparse regarding particle emissions from dual-fuel RCCI operation. In a study by Dempsey et al. (2014), a two-stage high temperature dilution process resulted in large reductions in particle mass and number concentration for increasing dilution ratio and increasingly high temperature dilution for several RCCI speed and load conditions compared to CDC operation. Additionally, the same authors

reported elevated HC emissions, implying the potential for semi-volatile particle growth at lower dilution temperature. In our previous work, we also found that RCCI combustion results in high concentrations of HC compounds that can slip through conventional DOC aftertreatment and form nucleation mode particles (Prikhodko et al. 2013)(Storey 2015). RCCI was shown to result in higher overall particle mass concentration then PPCI at tested dilution conditions though particles from both modes primarily consist of semi-volatile organics.

To date, accurate characterization of primary nanoparticles from LTC has been largely stymied by their high semi-volatile content. Here, we present a comprehensive overview of LTC nanoparticle volatility by experimentally comparing PPCI and RCCI operating modes using evaporative tandem differential mobility analysis (ETDMA). Volatility data is then used to elucidate the general composition of particles by comparing with single component evaporation data and a phenomenological condensation and evaporation model.

6.3 Experimental

6.3.1 Engines and Fuels

Table 6: Fuel Specifications

PPCI and RCCI	**Certification Gasoline**	**Certification Diesel**
Density (g/cc @ 15.56℃)	.734	.856
Lower Heating Value (MJ/kg)	43.003	42.654
Octane/Cetane	RON: 96.0	Cetane Index: 43.2
Carbon (Wt%)	86.47	87.07
Oxygen (Wt%)	<.01%	NA
Sulfur (ppm)	7	11
Hydrogen (Wt%)	13.28	12.93

6.3.2 Combustion Modes and Test Procedure

Several steady-state low to intermediate loads from 2 to 5.6 bar brake mean effective pressure (BMEP) were used in PPCI and RCCI combustion modes. For PPCI, a 1500 rpm 2 bar BMEP early injection strategy, and a 1500 rpm 4 bar BMEP late injection strategy was used. For RCCI, a 1500 rpm 2.6 bar BMEP strategy, a 1500 rpm 4 bar BMEP strategy, and a 2600 rpm 5.6 bar strategy was chosen (

Table 7). The gasoline fuel fraction for RCCI modes was 59.1%, 82.6%, and 87.1% by fuel energy fraction, respectively. These five modes represent operating conditions sufficient for propelling a mid-size passenger vehicle at low speed for the low-load cases and highway speed for the highest load case.

Table 7. Experimental Operating Parameters

	PPCI 2 bar	PPCI 4 bar	RCCI 2.6 bar	RCCI 4 bar	RCCI 5.6 bar
Intake T (°C)	63.7	59.9	34.5	50.1	35.0
Intake P (kPa, abs.)	103.0	110.0	95.8	101.3	132.1
Air-Fuel Ratio	23.4:1	18.11 :1	45.9:1	31.4:1	37.4:1
EGR %	63.7	59.9	33.0	0.0	0.0
Diesel Injection. Timing/ Duration (dbtdc/ms)	20/.513	3/.50 8	51	55	62
Diesel Rail Pressure (Bar)	800	1200	500	500	500
Gasoline Energy Fraction (%)	NA	NA	59.1	82.6	87.1

6.3.3 Gaseous Emissions Measurement and Analysis

Measurement of gaseous NOx, carbon monoxide (CO), and HC emissions was conducted using Fourier Transform Infrared (FTIR) analyzer for both RCCI and PPCI combustion. For RCCI combustion, a heated flame ionization detection (FID) instrument was used for measurement of total HC on a C_1 basis. For PPCI, total HC was estimated

using a weighted summation of the HC species measureable with the FTIR for representation on a C_1 basis.

6.3.4 Particle Emissions Measurement and Analysis

Soot mass emissions from the PPCI engine were measured using an AVL Microsoot photoacoustic analyzer and an AVL 415S Smoke Meter was used for the RCCI engine. These measurements are assumed to be comparable to soot mass concentration (Northrop 2011), though future studies are necessary to fully characterize the effect that LTC-produced soot will have on photoacoustic measurement as compared to CDC-produced soot.

Particle sizing and counting was conducted using a scanning mobility particle sizer (SMPS) comprising of a TSI 3080 electrostatic classifier and TSI 3025 condensation particle counter (CPC). A 3081 long column DMA was used along with a 3085 nano-dma for sub-10 nm particle measurements. To define initial conditions for the evaporation/condensation model, total particle mass emissions were estimated from SPMS results assuming particles are spherical with unity specific gravity. To simulate primary dilution in the atmosphere under controlled temperature and flow conditions, a two-stage dilution system was used. Primary dilution ratio was continually measured using a non-dispersive infrared CO_2 analyzer. Secondary dilution ratio was periodically measured before and after the experiments and found to be constant throughout the

experiments. Filtered, dry, CO_2-free, and temperature controlled air was used for primary and secondary dilution. A catalytic stripper (CS) was used to remove organic material from exhaust particles. An empirically derived, size-dependent loss correction factor was applied to the SMPS data to account for particle losses occurring in the CS.

Evaporative tandem differential mobility analysis (ETDMA) was used to explore particle volatility as a function of particle size. ETDMA employs a separate differential mobility analysis (DMA) column that selects a monodisperse particle distribution from the polydisperse aerosol. In this study, PPCI particles were selected using nominal DMA voltages of 80 and 340 to investigate "smaller" and "larger" nanoparticles particles at 18.9 nm and 40.2 nm, respectively. RCCI particles were selected using nominal DMA voltages of 40 and 200 to measure similarly sized smaller and larger nanoparticles at 13.3 nm and 30.4 nm, respectively. While it would be a more direct comparison to use the same sizes of smaller and larger particles for both studies, the sizes chosen were selected because they resulted in very tight monodisperse distributions, without confounding doubly charged particles. The monodisperse aerosol was then subjected to controlled elevated temperature conditions as it flowed through a tube submerged in an oil bath to maintain isothermal conditions. Changes in particle size due to evaporation were then measured by SMPS and analyzed as a function of evaporator residence time and temperature.

Measuring evaporation rates of pure compounds provides a valuable volatility benchmark from which to compare exhaust particles. An evaporative particle generator (EPG) was used to create heavy alkane particles as a baseline comparison for LTC exhaust particles. The resulting particles were processed with the ETDMA and the particle size reduction was measured using SMPS. A schematic of the EPG apparatus is shown in Figure 27.

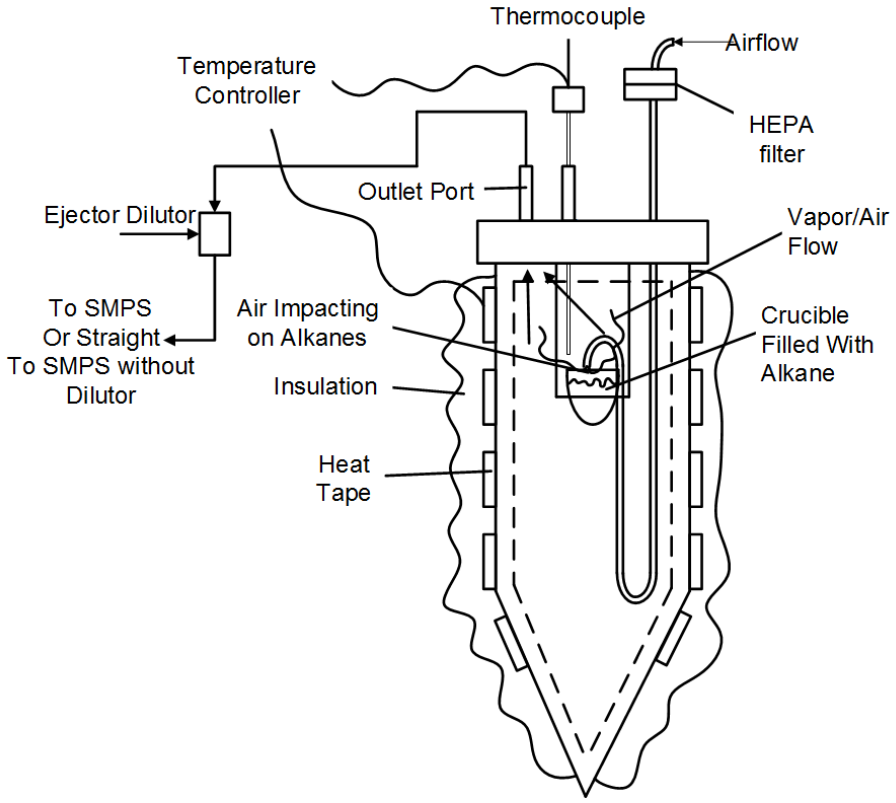

Figure 27. Schematic illustration of evaporative particle generator (EVP) used in single component ETDMA experiments

6.3.5 Results and Discussion

6.3.5.1 NOx, Soot, CO, and HC emissions

Emissions of NOx, consisting of NO and NO_2, and soot for the PPCI and RCCI modes tested in the experimental study are comparable to our previous work with the same engines at similar engine load conditions and are significantly lower than comparable CDC engine conditions (Lucachick et al. (2014a), Prikhodko et al. (2010), and Storey et al. (2008). Error bars represent the standard error of the mean of each dataset. Standard errors are not available for the RCCI data since only three samples were taken per condition using the AVL Smoke Meter. As shown in Figure 28a, RCCI NOx emissions were higher than PPCI at similar engine operating conditions. Soot mass emissions are similar for PPCI and RCCI modes, however 2 bar PPCI delivered the lowest fuel-specific soot emissions of all tested combustion modes and the 4 bar PPCI case had the highest soot mass concentration.

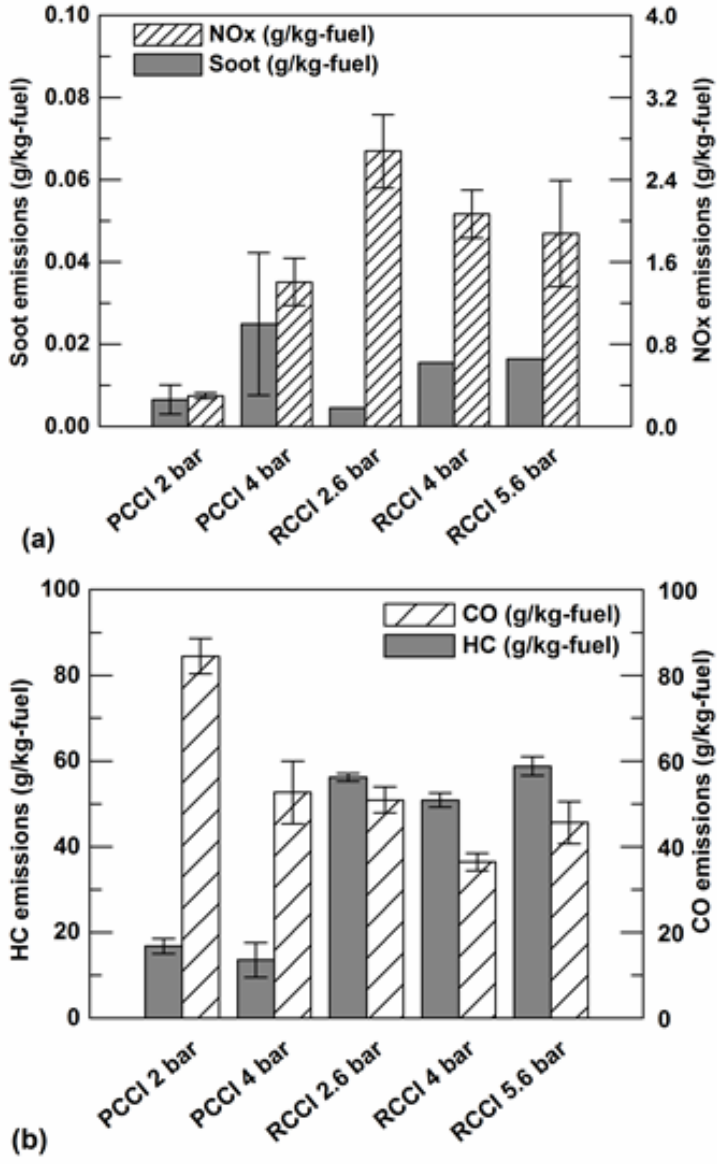

Figure 28. Fuel mass specific emissions by combustion mode: (a) NOx and soot, (b) HC and CO

HC and CO emissions were also in agreement with prior literature and are given in Figure 28b. CO emissions were similar for all modes, and several times higher than CDC from similar loads run in prior studies. The 2 bar PPCI operating point exhibited the

highest CO levels, with the highest EGR levels contributing to low combustion temperatures and the highest equivalence ratio of all the modes in the study. Gaseous HC emissions were found to be approximately three times higher for RCCI modes than for PPCI operation.

6.3.5.2 Dilution Sensitivity of LTC Particles

Previous studies have shown that a large soot accumulation mode serves as a sink for volatile vapors, thereby suppressing formation of nucleation mode particles (Bagley et al., 1996, Khalek et al., 2000). We showed the same phenomenon in previous work (Lucachick et al. 2014) where a large accumulation mode in CDC exhaust suppressed semi-volatile nucleation mode particle formation over a range of dilution temperature. Low soot levels also resulted in greater overall particle sensitivity to dilution conditions due to fewer solid sites for gas to particle conversion. This effect is extremely pronounced for LTC combustion modes which emit extremely low soot levels. Figure 4 shows that the RCCI and PPCI cases considered here exhibited high sensitivity to dilution temperature. Lower dilution temperatures can result in particle vapor precursor saturation ratios that increase by orders of magnitude, as will be discussed. Number concentration and geometric mean diameter (GMD) for all combustion modes are given in Table 1. The total particle number concentration increased by approximately one order of magnitude with decreasing dilution temperature while GMD decreased indicating a shift to nucleation mode particles.

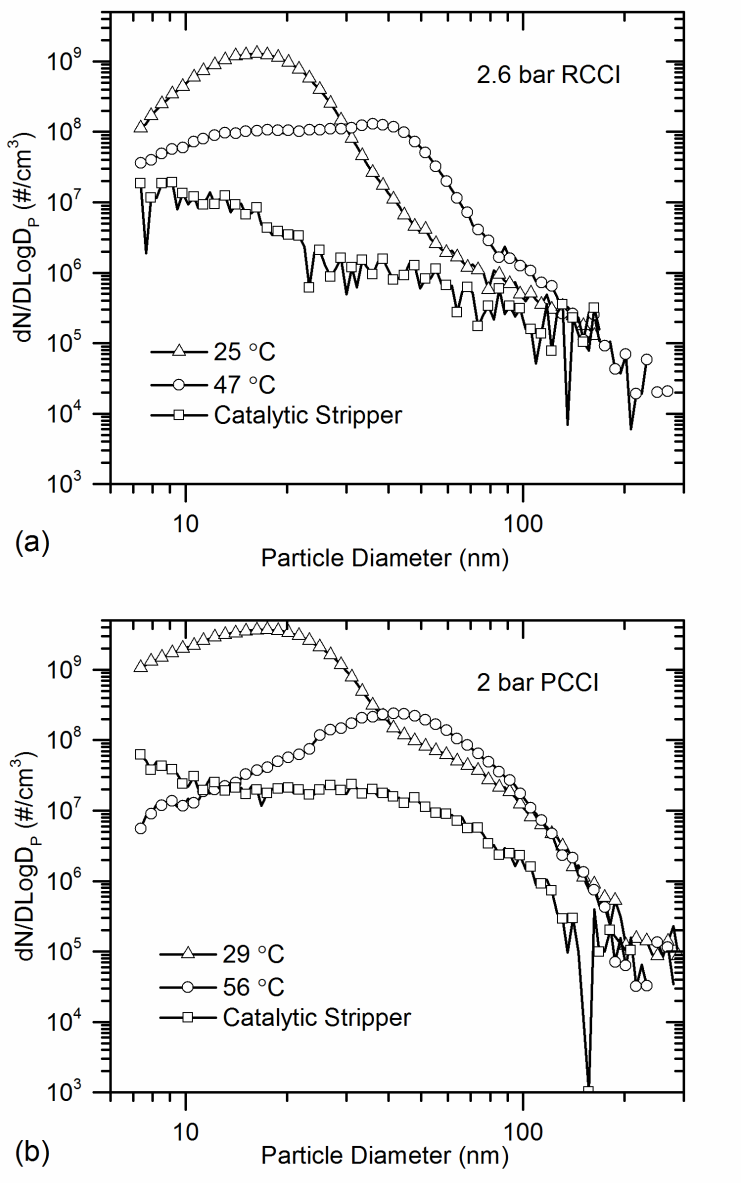

Figure 29. Total particle number distribution for two dilution temperatures and for solid particles resulting from catalytic stripper processing at engine operating conditions (a) 2.6 bar RCCI condition, (b) 2 bar PPCI condition

Table 8. Total particle number (TPN) concentration for warm dilution (47°C PPCI, 56°C RCCI), cool dilution (25°C PPCI, 29°C RCCI), and CS, and geometric mean diameter (GMD) for cool and warm dilution.

	TPN (10^7 #/cm^3)			GMD (nm)	
Condition	Cool	Warm	CS	Cool	Warm
PPCI 2 bar	60	10	1.4	16.0	37.4
PPCI 4 bar	150	7.5	4.1	24.4	43.2
RCCI 2.6 bar	60	10	.5	15.4	26.1
RCCI 4 bar	10	10	.24	17.7	25.7
RCCI 5.6 bar	20	20	.13	16.7	18.8

CS number concentration results show that semi-volatile particles contribute to the vast majority of total particle number, with CS number concentrations approximately two orders of magnitude lower than the number concentration for the cool dilution case for all combustion types, and approximately one order of magnitude lower than for the warm dilution case for all combustion types. One exception is seen in comparing warm dilution and CS number concentrations for 4 bar PPCI. The CS number concentration for the 4 bar PPCI point is approximately half that of warm dilution number concentration for the same mode. Although low, this combustion mode has the highest soot concentrations of any of the tested modes as confirmed in Figure 28. This soot exists in sufficient quantities to absorb the particle forming material and suppress the formation of large quantities of nucleation mode particles.

6.3.5.3 ETDMA Results

Size dependent particle volatility and external mixing characteristics were explored using ETDMA. Here, monodisperse particle distributions of different particle diameter were selected using DMA for RCCI and PPCI combustion modes. After DMA selection, particles not subjected to thermal conditioning were on average 5% smaller than predicted by classifier theory. The cause of this discrepancy is not fully understood, but the highly volatile nature of the particles may have resulted in particle shrinkage during and after traversing the classifier despite the lack of conditioning. Other experimental errors could have included aerosol or sheath flow control errors. To account for size selection error, particles were selected and measured directly by SMPS to identify the initial particle size before thermal conditioning.

Particles were selected using DMA voltages of 40 and 200 volts (13.3 nm and 30.4 nm nominal selected diameters) for the RCCI experiments. Particle distributions from which the sizes were selected are shown in Figure 30. Dilution temperature was controlled to 36 °C. Figure 31 shows the effects of thermal conditioning on RCCI particles. As shown in Figure 31, a conditioning temperature of 105 °C produced similar reductions in particle diameter for all RCCI loads for particles selected at 13.3 nm, with an average diameter reduction of 8 nm. This represents an average reduction in particle volume of 94%. As shown in Figure 31, a conditioning temperature of 105 °C resulted in diameter reductions of similar magnitude, averaging 16.3 nm for all three loads. This

reduction in diameter reduces particle volume by an average of 94%. Similar to particles selected at 13.3 nm, at least 94% of the particle volume was completely volatile for 30.4 diameter particles.

The effects of thermal conditioning on PPCI exhaust particles are shown in Figure 31. PPCI exhaust particles were selected using DMA voltages of 80 and 340 volts (18.9 nm and 40.2 nm nominal selected diameters) with dilution temperature controlled to 27 °C. Particle size distributions from which mono-disperse distributions were selected and the nominal particle diameters are shown in Figure 30. For particles selected at 18.9 nm, conditioning to 110 °C for 4 bar PPCI and 125 °C for 2 bar PPCI resulted in particle diameters reduced by 8.3 nm and 9.16 nm, respectively. This represents a total volume reduction of 87% and 91%, respectively. For particles selected at 40.2 nm, conditioning to 110 °C for LLTC and 125 °C for ELTC resulted in particle diameters reduced by 16.5 nm, and 22.4 nm, respectively. This represents reductions in particle volume of 86% and 96%, respectively. Our previous work has shown that the solid fraction of PPCI particles is greater than RCCI (Prikhodko et al. 2013). However, in the experiments conducted here soot mass concentrations for RCCI and PPCI (Figure 28) are comparable and ETDMA results indicate similar volatility profile for the two combustion modes. Figure 29 indicates that PPCI particles exhibit a more pronounced accumulation mode than RCCI after CS processing, providing some evidence of solid carbon agglomerates for the PPCI case that do not exist for RCCI. Regardless, the fractional volume reductions for

PPCI particles are similar to RCCI particles, indicating that the majority is comprised of volatile material.

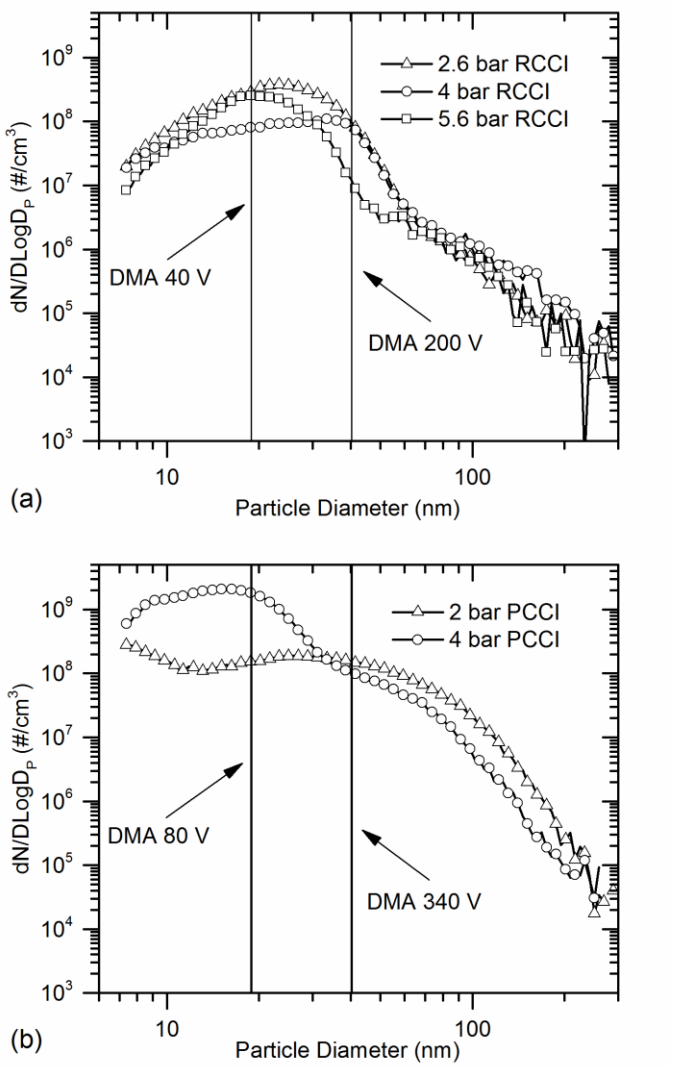

Figure 30. Particle number distributions at selected engine operating conditions showing selected DMA cut size voltages used in ETDMA analyses: (a) RCCI 36 °C dilution temperature, (b) PPCI Particle distributions 27 °C dilution temperature.

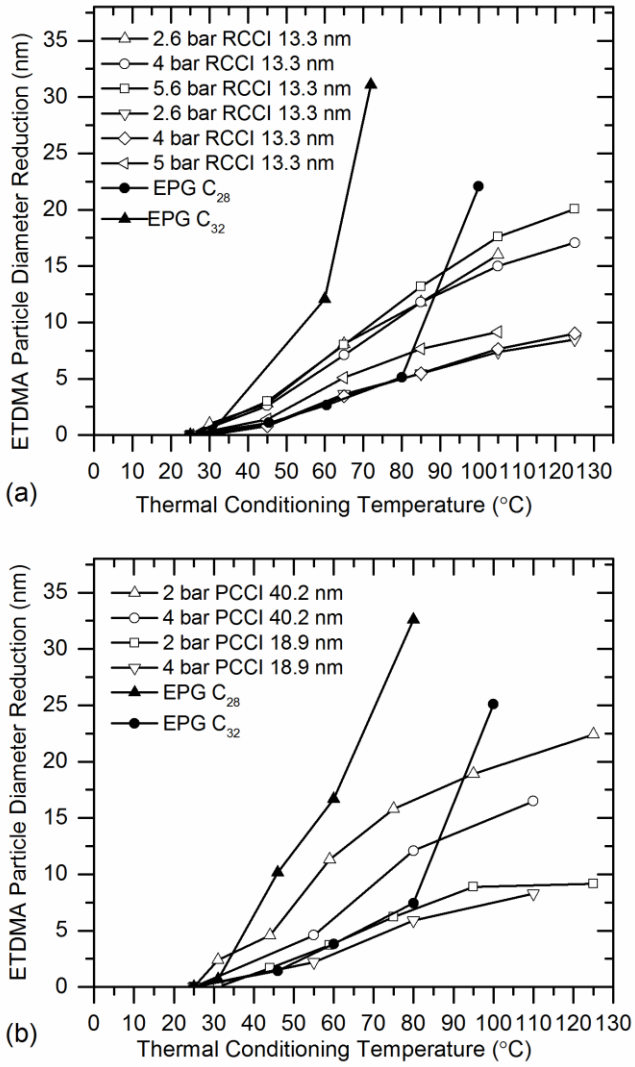

Figure 31. Reduction of particle diameter as a function of ETDMA thermal conditioning temperature for engine-produced particles compared to pure C32 and C28 alkanes of similar particle diameter: (a) RCCI 13.3 and 30.4 nm particles (b) PPCI 18.9 nm and 40.2 nm particles

The ETDMA results in Figure 31 show that for both RCCI and PPCI, larger particles experience greater reductions in diameter compared to smaller particles at a given conditioning temperature. If smaller particles had exactly the same composition as

larger particles, they would experience greater reductions in diameter at a given conditioning temperature due to evaporation enhanced by the Kelvin effect. The opposite is true in our results, providing evidence that the smaller particles are comprised of overall lower volatility material. It is unlikely that the smaller particles cannot be reduced further in size because they possess a solid core, because the catalytic stripper results show that the vast majority of particles in this size range are completely volatile with no solid core. This phenomenon is distinctly different than the trend common to CDC particles consisting of a volatile nucleation mode and a sooty, nonvolatile accumulation mode (Sakurai, Park, et al. 2003). Our finding of decreasing volatility with decreasing particle diameter is consistent with observations made by Shiraiwa et al. 2013 on secondary organic aerosols produced in an environmental chamber using dodecane and ammonia sulfate seed particles where higher volatility material preferentially partitioned to larger particle sizes. It is likely that the same phenomenon occurs with LTC-generated particles in the primary exhaust plume.

Exhaust particle diameter reduction of selected 30.4 nm and 40.2 nm particles are compared to particle diameter reduction of pure C_{28} and C_{32} particles of the same size (Figure 30) generated with the EPG apparatus. This range of alkanes spans the center of a response curve for gas-chromatograph testing of engine oil in Sakurai, Tobias, et al. 2003). Additionally, pure alkanes are a good surrogate for volatile exhaust particles because they are inert, nontoxic, prevalent in diesel exhaust particles, and are a primary

component of petroleum diesel fuel and lubricant oil (Chickos & Hanshaw 2004b). Alkanes were created in the EPG and size selected using DMA voltages of 200 and 340. At low to moderate conditioning temperature, RCCI and PPCI particles evaporated less than C_{32} particles, but more than C_{28} particles indicating that their overall volatility fell in between the two pure alkanes. For high conditioning temperatures, exhaust particles experienced less evaporation than both pure alkane types, illustrating that residual low volatility components remained in the engine-produced aerosols. Evaporation resistance at high conditioning temperature highlights the wide range of volatilities of compounds comprising LTC particles and further substantiates our finding of low volatility compounds contained within the exhaust particles.

Estimated saturation ratios of candidate alkanes were also calculated to explore particle growth under a variety of dilution temperatures. Total particle volume assuming spherical particles comprised of C_{28} and C_{32} alkanes were used to estimate pre-dilution particle-forming vapor concentrations in the experimental data. Saturation ratios as a function of temperature were estimated using the 2.6 bar RCCI particle volume data after primary dilution using relations developed by Chickos & Hanshaw 2004 for alkane saturation pressure and are shown in Figure 7. The calculation used the conservative assumption that the entirety of the precursor vapors transitioned to particle phase, making the entire precursor volume concentration measurable using SMPS. Saturation ratios are two orders of magnitude greater for C_{28} than C_{32} for all temperatures, and are more than

an order of magnitude larger than unity for both compounds for all temperatures investigated. This implies that volatility of oil and fuel alkanes in this volatility range is sufficiently low to promote condensation on existing particles under the observed dilution conditions. Critical saturation ratios (S_{crit}) required to homogeneously nucleate these alkanes were calculated using classical nucleation theory and equations found in Rusyniak et al. (2001); further details regarding nucleation calculations are found in the Appendix. S_{crit} values for both compounds were orders of magnitude higher than the measured saturation ratios S. This suggests that despite large saturation ratios, these compounds are unlikely to form particles via homogeneous nucleation. Therefore, it can be concluded that although these compounds will condense onto existing particles, it is very unlikely that they would homogeneously nucleate on their own. Thus, other condensation nuclei formed from sulfuric acid or other ultra-low volatility material are responsible for nucleation sites of semi-volatile LTC particles.

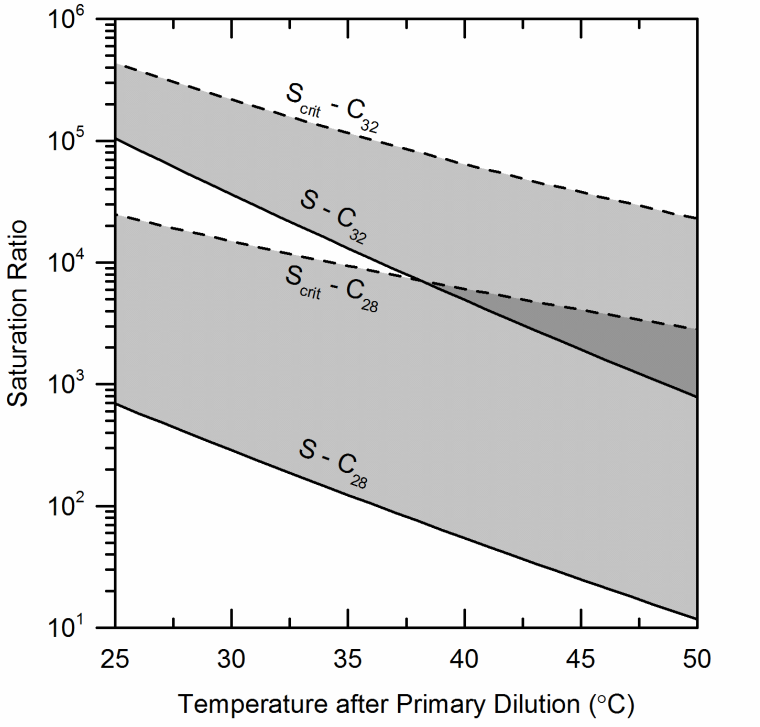

Figure 32. Calculated saturation ratio vs. dilution temperature estimated assuming total particle volume consists of solely C28 and C32 alkanes with total component mass concentrations from 2.6 bar RCCI condition used as an example.

6.3.5.4 Evaporation/Condensation Model Results

To validate the observation that smaller particles from LTC possess lower volatility than larger particles, a phenomenological aerosol evaporation and condensation model was used to study the gas to particle partitioning process under transient dilution conditions. This model used multicomponent evaporation/condensation theory from Vesala et al. 1997 to calculate the time-dependent evolution of particles made of three

components. Details regarding the evaporation/condensation model are found in the Appendix.

As shown in the comparison to pure alkanes in Figure 31, the ETDMA experiments show that the bulk of the initially evaporating LTC particle material spans a volatility range between C_{28} and C_{32} alkanes, with a portion of the particle having lower volatility and thus more resistance to evaporation at high thermal conditioning temperatures. Based on these results, three volatile material surrogates were chosen for examination using the evaporation model. An alkane between the two studied experimentally using the EPG and ETDMA (C_{30}) was chosen combined with one with higher volatility (C_{25}) and one with lower volatility (C_{35}). Using the same estimated vapor precursor concentrations used in the saturation ratio calculations from the 2.6 bar RCCI condition, the initial conditions assumed a Poisson-distributed particle distribution of initially incepted clusters with a mode diameter of 10 nm comprising a total volume equal to one third of the available vapor precursors. These clusters were given the initial condition of equal volume concentrations of C_{25}, C_{30}, and C_{35} alkanes. Particles were assumed to be homogeneously internally mixed during the evaporation/condensation process. The model simulated evaporation and condensation for 1 second, which approximates the time spent in the aging tunnel after primary dilution. Because the experimental results indicated that smaller particles were comprised of less-volatile material than larger particles, the composition history of smaller (D_P = 13.3 nm) and

larger (D_P = 30.4 nm) particles were modeled separately. The results of the analysis are shown in Figure 8. It can be seen that particle size has an impact on condensation and evaporation mechanisms, resulting in differences in final composition. 13.3 nm particles are comprised of only 29% C_{25} after one second's aging time, while 30.4 nm particles increase to 36% C_{25} after the same time period. Due to the Kelvin effect, initial condensation of C_{25} is inhibited for both 13.3 nm and 30.4 nm particles, but the effect is much more pronounced for the 13.3 nm particles, with initial C_{25} uptake occurring at only 60% the rate of the 30.4 nm particles. Additionally, growth due to C_{25} on the 30.4 nm particles actually exceeds growth due to C_{30} and C_{35} by 0.12 seconds into the aging process.

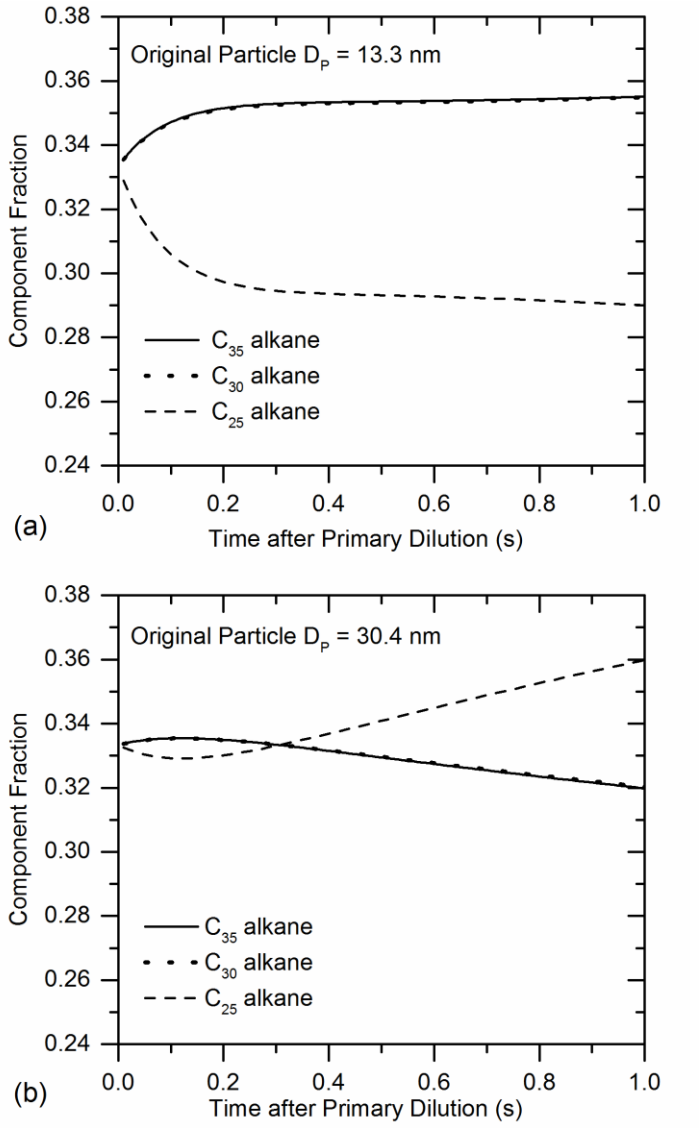

Figure 33. Simulated mass fraction history of three-component alkane particles for 2.6 bar RCCI engine condition: (a) 13.3 nm particles from 2.6 bar RCCI during primary dilution process. (b) 40.4 nm particles from 2.6 bar RCCI during primary dilution process.

The time derivative of particle diameter as contributed by C_{25}, C_{30}, and C_{35} is shown for 13.3 nm and 30.4 nm particles is shown in Figure 34. For both particle sizes, condensation dominates growth contributions from C_{30} and C_{35}, as low particle surface vapor pressure mitigates evaporation of these species, even for the smaller 13.3nm particles. This results in equivalent condensation rates for C_{30} and C_{35}. Since LTC particles would be comprised of far more than three individual components, real-world atmospheric evaporation over extended time periods would result in increasingly lower volatility for small particles. As suggested previously, this gives further evidence that the same mechanisms responsible for partitioning of volatile material to the particle phase over long time periods for secondary organic aerosols can act on primary LTC exhaust particles on a much shorter time scale.

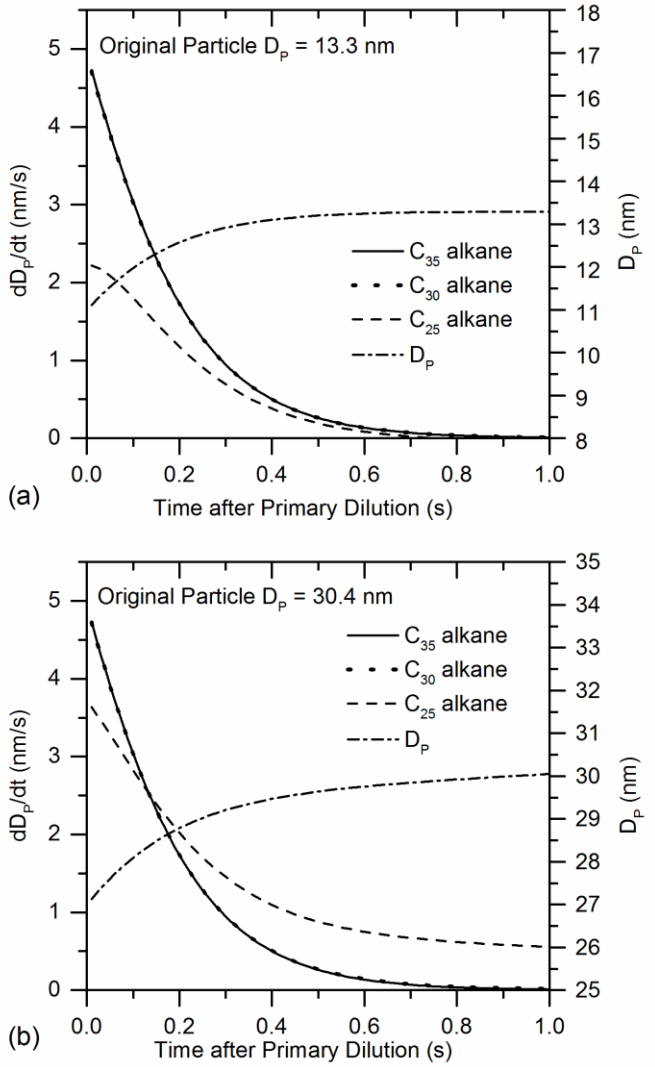

Figure 34. (a) Simulated particle growth and dD/dt contributions by component for three-component 13.3 nm particles from 2.6 bar RCCI. (b) Simulated particle growth and dD/dt contributions by component for three-component 30.4 nm particles from 2.6 bar RCCI.

6.3.6 Volatility Characterization of Nanoparticles from Single and Dual-Fuel LTC Conclusions

Results of this work show that volatile composition of particles generated by LTC in CI engines confers particle formation mechanics and mixing characteristics unlike known mechanisms for CDC particles. Both single-fuel PPCI and dual-fuel RCCI particle formation is highly dependent on dilution temperature, with particle number concentrations increasing by orders of magnitude for modest decreases in dilution temperature. Particles from CDC are much more insensitive to dilution temperatures due to a composition consisting primarily of soot.

In an additional contrast to CDC particles that generally exhibit a volatile nucleation mode and a sooty, nonvolatile accumulation mode, ETDMA results show that smaller LTC particles are comprised of material of lower volatility than larger LTC particles. Results also indicate that LTC particles are composed of a wide variety of volatile materials, with evaporation rates similar to pure C_{28} alkane at low temperatures, and greater than evaporation rates for pure C_{32} at higher temperatures. A phenomenological particle evaporation and condensation model using pure alkanes above, within, and below this range as surrogate volatile material shows that the Kelvin effect has a significant impact on particle composition during the aging process. The effect causes reduced condensation of more-volatile material that may condense in early,

high saturation ratio conditions, and relegates condensation of this more-volatile material to larger particles.

This study conclusively shows that the volatility range of LTC particles mostly falls within the range of alkanes similar to components in engine lubricating oil. The study of critical saturation ratios of alkanes similar in volatility to the material found in LTC particles shows that such material is not likely to homogeneously nucleate on its own, and that other extremely low volatility material is responsible for initiating nucleation of volatile LTC particles. The overall composition of LTC particles is still not fully known and these low volatility compounds could consist of a combination of sulfuric acid, heavy fuel species, lubricating oil components, PAH, and possibly oxygenated organic species such as dicarboxylic acids and aldehydes. Additional work should be performed to speciate LTC particles for quantification of the components responsible for their nucleation in the exhaust plume.

The primarily volatile nature of LTC particles poses additional concern for their removal using traditional engine aftertreatment solutions as prior studies have shown that LTC forming material can slip through a DOC-DPF aftertreatment system and form particles under certain conditions. The findings of this research are significant in that whereas the characteristics of CDC particles are known, LTC particles have not been extensively studied. Due to their differences in composition and physical properties,

regulatory rules and measurement methods designed for CDC particle emissions may not be appropriate for LTC particle emissions. More specifically, PM sample collection by filtration as required by some regulations will result in the collection of mass that likely doesn't represent the mass of primary aerosol emitted by the engine.

7 Analysis of Theoretical Nucleation Pathways

7.1 Introduction

The results of this study, and the results of prior studies by other researchers show conclusively that exhaust particle emissions from LTC are mostly volatile, and under most dilution conditions, particles without solid cores outnumber particles with solid cores by an order of magnitude or more. Classical nucleation theory indicates that oil and fuel alkanes of similar volatility to LTC particles does not exist in sufficient quantity to nucleate homogeneously, thus that material is condensing onto nucleation sites formed through one of two potential scenarios: ultra-low volatility organic material, or heterogeneously nucleated sulfuric acid and water particles. The potential for both cases is investigated classical nucleation theory as well as heterogeneous nucleation theory.

7.2 Nucleation Potential

7.2.1 Classical Nucleation Theory for Low Volatility Organic Material

In addition to alkanes from fuel and oil, other low volatility organic material has been found in CDC PM. Studies such as Merritt et al. 2006, and Storey et al. (2008) of unregulated exhaust emissions have determined that concentrations of compounds are nonvolatile enough to form particles in the primary exhaust plume. In classifying these compounds by saturation pressure, it is readily apparent that only the low-saturation pressure compounds are consistently present as PM in the literature. Further, it is

relatively easy to classify three classes of compounds in diesel exhaust with sufficiently low saturation pressures, one of which is alkanes discussed in the prior chapter. The nucleation potential of the remaining two classes are investigated in this chapter: polycyclic aromatic hydrocarbons (PAH), and dicarboxylic acids.

To investigate the nucleation potential of the organic compounds of interest, the procedure in Chapter 6 is used, with equations found in the Appendix in section *Homogeneous Nucleation Calculations,* where a vapor mass concentration is defined that is equivalent to the total measured particle mass for 2 Bar RCCI. This is of course a very conservative assumption because we have shown that a large portion of the particle mass is in a volatility range that is extremely unlikely to homogeneously nucleate. Further, as measured by GC/MS in previous studies, the very-low saturation pressure compounds of interest comprise an extremely small fraction of the total particle mass.

PAHs are common components of diesel exhaust PM, and can occur in greater concentrations in LTC than in CDC. In Figure 35 it is seen that for the 6 most commonly detected PAH compounds, only Benzapyrene would nucleate homogeneously, if it comprised approximately 20% of the measured particle mass, which is highly unlikely as this compound commonly exists only as an extremely small fraction of total particulate mass. In the study by Merritt et al. 2006, four types of PPCI combustion were investigated, and at most, Benzapyrene comprised .002% of the entire particulate mass

for a fuel-rich LTC case. Thus, it is extremely unlikely that any PAH could exist in quantities sufficient to nucleate homogeneously in the primary exhaust plume.

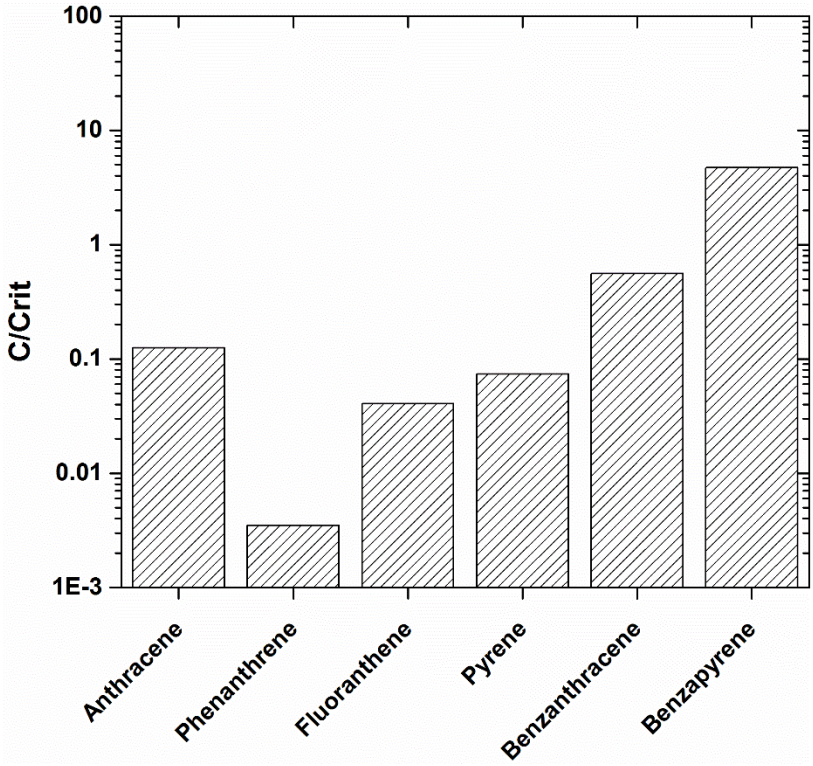

Figure 35. Ratio of Concentration to Critical Concentration for various PAH species, assuming particulate is comprised entirely of one species. Concentration taken from 2.6 Bar RCCI.

Several types of dicarboxylic acid have been found in small quantities in diesel exhaust PM (Kawamura et al. 1985), (Zervas et al. 2001). These compounds have saturation pressures similar to PAH and heavy alkanes, however, they have surface energies an order of magnitude greater than alkanes(McMurry & Tao 1989), (Queimada & Marrucho 2001), (Yudin & Hughes 1994). This makes the prospect of homogeneous

nucleation in concentrations similar to diesel exhaust impossible, despite their extremely low saturation pressure at atmospheric temperature. Thus, dicarboxylic acids are not responsible for the non-solid nucleation sites present in LTC exhaust as indicated by Figure 36. Further, this enhanced surface energy would be a huge barrier to growth of existing sub-10nm carboxylic acid particles, as the large surface energy greatly enhances evaporation due to the Kelvin effect.

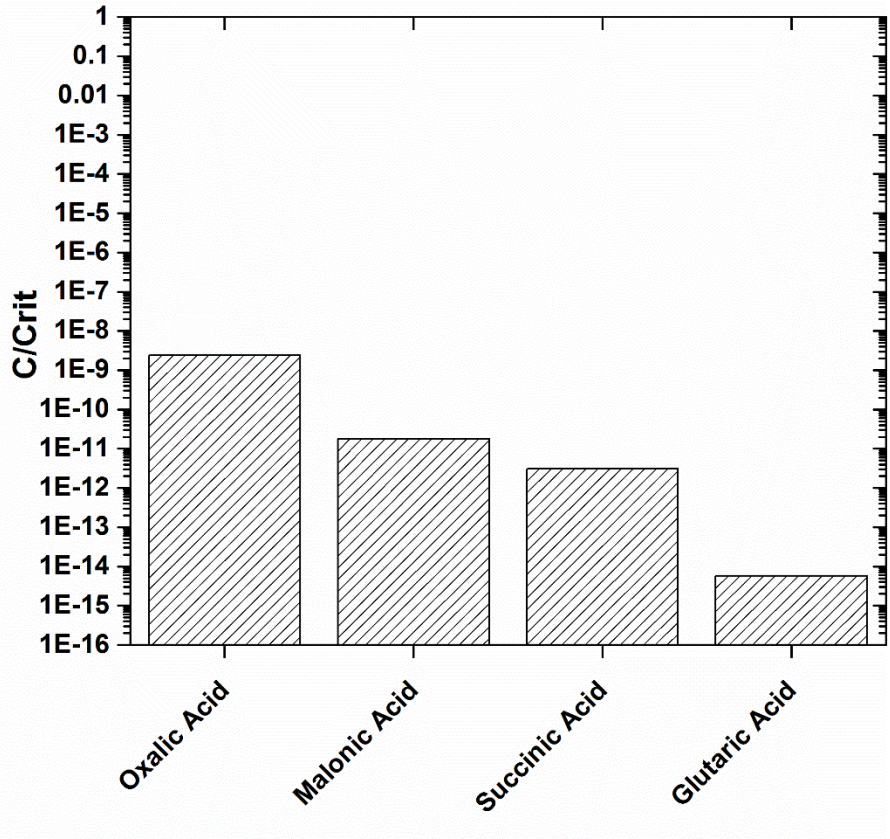

Figure 36. Ratio of Concentration to Critical Concentration for Carboxylic acid species, assuming particulate is comprised entirely of one species. Concentration taken from 2.6 Bar RCCI

7.2.2 Heterogeneous Nucleation Theory for Sulfuric Acid and Water

Despite the presence of carboxylic acids and elevated levels of PAH as compared to CDC, it is highly unlikely that these compounds are responsible for nucleation sites for particle growth in LTC. This leaves sulfuric acid as the remaining pathway to nucleation. Modern diesel must contain a maximum of 15 ppm sulfur to meet the classification for ULSD. The diesel fuel used through the course of this research contained no more than 7 ppm sulfur, and the gasoline used contained no more than 11 ppm sulfur as shown in Table 6 Despite the highly refined low sulfur fuels, heterogeneous nucleation theory shows that sulfuric acid exists in sufficient quantities in the exhaust plume for sulfuric acid/water particles to nucleate. In Figure 37, sulfuric acid/water heterogeneous particle formation is modeled using heterogeneous nucleation theory developed by Mirabel et al. (1974) with calculations outlined in the Appendix, in the section Sulfuric acid and water heterogeneous nucleation model

The independent parameters for sulfuric acid and water nucleation are temperature, water vapor concentration, and sulfuric acid vapor concentration. Temperature is controlled by the dilution system, and water vapor concentration is measured directly the FTIR. Sulfuric acid vapor concentration is difficult to measure directly, and was estimated in this study. Sulfur vapor contribution from fuel was easily determined by fuel consumption rate and fuel sulfur level. Sulfur vapor contribution from oil was estimated based on estimated oil consumption rate and estimated oil sulfur

content, the values of which are based on personal communications with Ricardo Hein (2014). Additionally, only a small fraction of sulfur vapor has converted to sulfuric acid at the point of dilution. An assumption of 4% conversion has been determined to be reasonable for diesel exhaust based on experiments and observations by Shi & Harrison (1999) and Baumgard & Johnson (1996). The equation for exhaust sulfuric acid concentration is shown in Equation 2. In this model, nucleated particle estimates are liberal because the model doesn't take into account scavenging of precursor vapors onto existing particles. Detailed calculations are found in the Appendix in section . Nucleation conditions for each combustion mode are shown in Table 9. 2 bar ELTC is compared to 2 bar CDC. Both 2 bar ELTC and 2 bar CDC operating conditions have extremely similar fuel consumption, efficiency, and brake power, but the exhaust composition of LTC is much more conducive to the process of heterogeneous nucleation of sulfuric acid and water. 2 bar ELTC uses EGR rates of 60%, while CDC uses EGR rates of 30%. Because heterogeneous nucleation rate are exponentially dependent on water vapor and sulfuric acid vapor concentration, heterogeneous nucleation theory predicts nucleated particles from ELTC to outnumber nucleated particles from CDC by five orders of magnitude. In practice, nucleation processes for CDC may be suppressed even further because of sulfuric acid absorption by accumulation-mode soot particles which are virtually non-existent for LTC.

Equation 2. Exhaust Sulfuric Acid Mass Concentration

$$[H_2SO_4] = \left(\frac{F}{A}\right)(Fuel\ Sulfur\ \%)(S\ to\ H_2SO_4\ \%)\left(\frac{M_{SO_4}}{M_{exhaust}}\right)\left(1-\frac{F}{A}\right)(\rho_{exhaust})$$

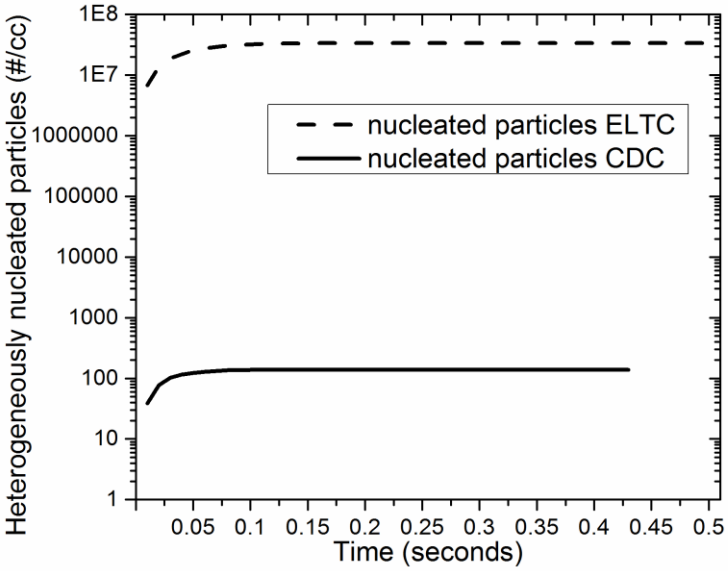

Figure 37. Simulated cumulative particles nucleated for 2 Bar ELTC and CDC after primary dilution

Table 9. Heterogeneous nucleation model initial conditions.

Parameter	2 Bar ELTC	2 Bar CDC
Diluted Temperature (°C)	25.0	25.0
Sulfuric Acid Vapor Pressure (Pa)	.000318	.000179
Water Vapor Pressure (Pa)	90583	58742
C/Ccrit	2.55	1.58

7.3 Potential Nucleation Pathways Conclusion

Despite the use of ULSD fuels and the increased PAH emissions from diesel LTC, modeling results presented here indicate that sulfur is still the main inception point of semi-volatile particles from diesel LTC. This is challenging from an emissions standpoint as it is impossible to capture sulfur in the exhaust stream as is done with soot particles in a DPF. Further, sulfur cannot be oxidized in a DOC like unburned hydrocarbons. However, the results from chapter 5 suggest that a modern aftertreatment system may have a transient effect on nucleation-mode sulfuric acid / water particles because of the potential for sulfur storage in the DOC zeolite and the DPF monolith.

8 Summary, Conclusions and Suggested Future Research

8.1 Summary of Research

Research on LTC modes continues to expand the envelope of internal combustion engine knowledge. Compared to conventional combustion, substantial reductions in NOx and soot emissions from these both single and dual fuel LTC modes have been proven in this study, with a small fuel economy penalty. Unfortunately, these combustion modes are not without their drawbacks. LTC modes cannot be achieved at the high power levels that CDC can achieve. This drawback is especially severe for single-fuel LTC, where the BMEP limit is approximately 30% that of the highest BMEP achievable by CDC. Additionally, LTC emits HC and CO in greater quantities than CDC. Further, these combustion modes emit PM that is unlike that of CDC PM which is primarily soot with

small amounts of organic compounds. Despite the reduced NOx and soot content, an aftertreatment system is still necessary to reduce elevated HC and remove PM.

In this work, an experimental study was undertaken to characterize the volatility and formation mechanics of PM from LTC modes, and to examine the effects of aftertreatment on low load LTC. In this comprehensive study, data is presented from two steady-state single fuel LTC modes, three steady-state dual-fuel LTC modes, and compared with baseline data from two steady-state CDC modes. Low sulfur fuels were used during the study, with ULSD #2 diesel with a maximum sulfur concentration of 7 ppm, and gasoline with a sulfur concentration of 7 ppm. These low sulfur fuels were used to minimize the effect of sulfur content on nucleation mode PM formation.

The single-fuel LTC modes were chosen to represent an early injection, low-load strategy, and a late injection, mid-load strategy. The early injection strategy allows greater premixing before combustion begins to occur, and is only applicable to low-load situations. The late injection strategy uses injection near TDC, with combustion delayed to beyond TDC to avoid the peak temperature and pressure conditions inherent to combustion centered at TDC. The conventional combustion modes used traditional pilot and main injection profiles combined with greatly reduced EGR rates to form a baseline of comparison for the LTC PM.

Prior literature on both LTC and CDC were used as a starting point to define the research goals of this study. The first goal was to investigate the formation of SVPM under a variety of dilution conditions for LTC operating modes and determine its volatility and composition. The second goal was to characterize the effectiveness of modern aftertreatment systems in mitigating species that may form SVPM from LTC modes. The third and final goal was to identify mechanisms for growth of SVPM under primary dilution in the exhaust plume.

To achieve the goals of this study, the single-fuel and dual fuel LTC modes were operated at steady state. Gaseous emissions were measured using an FTIR for all combustion modes, and for 2 Bar ELTC alone, total HC was measured using a FID. An AVL Microsoot was used to estimate soot emissions for single-fuel modes, and an AVL smokemeter was used to estimate soot emissions for dual fuel modes. An SMPS was used to measure particle distributions from particles processed in a microdilution system under controlled temperature and dilution ratio conditions. Evaporative TDMA was used to characterize particle volatility as a function of particle size, and to investigate internal and external mixing at different particle sizes.

For evaluating the performance of the aftertreatment system in mitigating PM emissions from LTC, high-speed particle measurement was necessary because of the transient nature of aftertreatment extinguishment and saturation. An EEPS was used at

high sampling rates to measure DPF-out particle emissions, while an SMPS was used periodically to measure particle distributions from engine-out and DOC-out locations.

To identify the mechanism behind the experimental results, a multicomponent evaporation model was developed. This model used Raoult's law and tabular physical chemistry data to model the mechanisms of growth of particles early in the dilution process. The results of the model identified the phenomenon responsible for the volatility characteristics of particles of different sizes. To characterize the formation of nucleation mode sulfuric acid particles, a heterogeneous nucleation model was developed to predict nucleation rates. This model predicts the rate of heterogeneous nucleation based on fuel sulfur concentration, fuel consumption, dilution temperature, dilution ratio, and fuel-air ratio.

8.2 Conclusions

The main conclusion of this work is that low temperature combustion particles are composed primarily of semi-volatile organic material as determined experimentally in this study. This has implications with regard to the unusual behavior of LTC exhaust as has been characterized in this work. As compared to conventional combustion, these semi-volatile particle precursor material exists in LTC exhaust in higher concentrations than in exhaust from conventional combustion due primarily to reduced combustion efficiency oil and fuel, and greater rates of formation of PAH and other classes of semi-

volatile material. Further, these concentrations are enhanced even further by the greatly elevated EGR rates.

A primary characteristic of LTC exhaust is the extreme sensitivity to dilution conditions. The results of this study showed that cool dilution, completely within the range possible from tailpipe to atmosphere, increased total particle number by orders of magnitude as compared to warmer dilution temperatures. This contrasted greatly with exhaust from CDC, where number concentration was largely insensitive to dilution temperature. Despite, the similar fuel consumption and equivalent power of these CDC modes, exhaust sulfur and water concentrations are also enhanced for LTC, greatly increasing heterogeneous nucleation rates of sulfuric acid and water. Additionally, the relative lack of accumulation mode particles, contrasts CDC exhaust, where ample accumulation mode particles absorb and condense large quantities of volatile material, suppressing nucleation particle formation. This lack of solid accumulation mode particles means that nucleated sulfuric acid and water particles can grow beyond the cluster size, as ample volatile material remains uncondensed due to the paucity of accumulation mode particles. This material readily condenses onto the nucleation clusters, forming nucleation mode particles in numbers much greater than that of conventional combustion exhaust.

The findings of the effects of aftertreatment on LTC PM were novel and unexpected. The results showed that a freshly regenerated Tier IV aftertreatment system was capable of reducing LTC number concentration by over 98% for approximately an hour of steady state ELTC combustion. After this point however, particle concentrations downstream of the DPF began to increase such that particle removal efficiency fell to approximately 90%. This reduction in aftertreatment efficiency occurred in conjunction with increasing DPF-out HC concentrations, and falling aftertreatment system temperatures. This gradual reduction in particle removal efficiency is in direct contrast with the results of similar studies of aftertreatment of CDC exhaust, where particle removal efficiency increases with soot loading on the DPF. Despite the eventual degradation in aftertreatment performance, the results are promising, as it suggests that with periodic regeneration, a Tier IV class aftertreatment system can effectively remove particles generated from low load LTC.

In comparing the volatility of LTC particles with pure alkane particles, it was found that particles from LTC were internally mixed, containing material of varying volatility. This volatility range was found to be centered near C28-C32 alkanes, but evidence of lower volatility material was also found. A study of saturation ratios of C28 and C32 alkanes in mass concentrations similar to total LTC particle mass concentrations shows that for the range of dilution temperatures normally achievable in the atmosphere, saturation ratios of much greater than unity occur. However, critical saturation ratios for

C28 and C32 are orders of magnitude greater than the concentration available, indicating that compounds in this range are extremely unlikely to contribute to homogeneous nucleation. The critical saturation ratios of a variety of other compounds suspected of initiating homogeneous nucleation were investigated, including PAH and organic acids. The results showed that despite their low vapor pressures, critical saturation ratios would not expected to be reached at the concentrations found in literature for any of the organic compounds investigated. This led to the application of sulfuric acid and water heterogeneous nucleation theory to investigate the potential of sulfuric acid and water as a source of particle nucleation for LTC. The results suggest that despite the use of ultra-low sulfur fuels, the high fuel-air ratios present in LTC make heterogeneous nucleation of sulfuric acid and water a significant source of nucleation mode particles due to the elevated sulfur and water concentrations as compared to CDC. Further, the lack of a sooty accumulation mode as a sulfur sink for LTC only serves to further enhance the formation of nucleation mode particles as compared to CDC combustion.

8.3 Suggested Future Research

Quite frequently research findings raise as many questions as they answer. Based on the results of this work, several recommendations for future work are outlined. As this study showed that particle formation for LTC is extremely sensitive to dilution conditions, comprehensive sweeps of temperature and dilution ratio should be made for the LTC modes tested in this study. These sweeps would require precise feedback control of both the dilution ratio, and the compressed air temperature to achieve adequate

throughput for this broad experiment set. This would likely require a complete redesign of the commonly used micro-dilution system. In this way, particle emissions for the entire range of realistic temperature and dilution ratios could be characterized.

In addition to the comprehensive dilution ratio temperature characterization, an additional high temperature, high dilution ratio primary dilution system should be developed. The primary goal of this high temperature, high dilution ratio system would be to investigate the growth of LTC particles under conditions when heterogeneous nucleation of sulfuric acid and water would not occur. Final dilution ratio and temperature would be similar to that used in this study by using a smaller, low temperature secondary dilution ratio. By carefully controlling the primary dilution ratio and temperature, conditions could be created where heterogeneous nucleation theory predicts no heterogeneous nucleation. This type of dilution would be attainable with current micro-dilution technology, as the results of this study and others have shown that heterogeneous nucleation rates diminish to zero rapidly with rising temperature and falling sulfur concentration. The presence of nucleation mode particles in this situation would suggest that unstudied nucleation pathways beyond sulfuric acid exist.

Finally, further study would include a more comprehensive characterization of the effects of aftertreatment on PM mitigation from LTC. This study should involve carefully controlling the aftertreatment system temperature to separate the effects of HC

conversion due to temperature drop from the effects HC and PM slip from zeolite/monolith saturation. Additionally, the more comprehensive characterization would require the investigation of not only low load LTC, but also mid-load, and high-load LTC.

In addition to the high primary dilution temperature study, a sulfur-free study should be conducted. This study should involve Fischer-Tropsch diesel fuel, or highly processed sulfur-free conventional diesel fuel. Additionally, sulfur-free lubricant oil should be used. Similarly to the results of the high temperature, high dilution ratio study, the presence of nucleation mode particles in a sulfur-free combustion study would suggest unstudied nucleation pathways beyond sulfuric acid heterogeneous nucleation.

Bibliography

Abdul-Khalek, Imad S., Kittelson, D.B., 1995. Real time measurement of volatile and solid exhaust particles using a catalytic stripper. *SAE technical paper*, No. 950236.

Abdul-Khalek, Imad S., Kittelson, D.B., Graskow, B. R., Wei, Q. Bear, F., 1998. Diesel exhaust particle size: measurement issues and trend. *SEA Technical Paper*, No. 980525.

Arnold, F. et al., 2012. First online measurements of sulfuric acid gas in modern heavy-duty diesel engine exhaust: implications for nanoparticle formation. *Environmental science & technology*, 46(20), pp.11227–34. Available at: http://www.ncbi.nlm.nih.gov/pubmed/23035617.

Author: Johnson, J.E. and D.B.K., 1994. physical factors affecting hydrocarbon oxidation in a diesel oxidation catalyst. *SAE technical Paper*, 941771(941771), p.941771.

Ayers, G.P., Gillett, R.W. & Gras, J.L., 1980. On the vapor pressure of sulfuric acid. *Geophysical Research Letters*, 7(6), p.433.

Bagley, S.T., 1996. Characterization of fuel and aftertreatment device effects on diesel emissions. *Research Report (Health Effects Institute)*, 76, pp.1–75.

Baumgard, K. & Johnson, J., 1996. The effect of fuel and engine design on diesel exhaust particle size distributions. *SAE technical paper*, 960131.

Birch, M.E. & Cary, R.A., 1996. Elemental Carbon-Based Method for Monitoring Occupational Exposures to Particulate Diesel Exhaust. *Aerosol Science and Technology*, 25(3), pp.221–241. Available at: http://www.tandfonline.com/doi/abs/10.1080/02786829608965393#.Va5QB0hOLDA.

Bohac, S. V et al., 2013. Speciated Hydrocarbon Emissions from an Automotive Diesel Engine and DOC Utilizing Conventional and PCI Combustion. , 2006(724).

Chickos, J. & Hanshaw, W., 2004a. Vapor Pressures and Vaporization Enthalpies of the n -Alkanes from C 21 to C 30 at T) 298 . 15 K by Correlation Gas Chromatography.

Chickos, J. & Hanshaw, W., 2004b. Vapor pressures and vaporization enthalpies of the n-alkanes from C31 to C38 at T= 298.15 K by correlation gas chromatography. , pp.2432–2440.

Chirico, R. et al., 2010. Impact of aftertreatment devices on primary emissions and secondary organic aerosol formation potential from in-use diesel vehicles: results from smog chamber experiments. *Atmospheric Chemistry and Physics*, 10(23), pp.11545–11563. Available at: http://www.atmos-chem-phys.net/10/11545/2010/ [Accessed February 28, 2013].

Code, T.U.S. & Walker, A.P., Controlling particulate emissions from diesel vehicles.

Colban, W.F., Miles, P.C. & Oh, S., 2007. On the cyclic variability and sources of unburned hydrocarbon emissions in low temperature diesel combustion systems. *SAE technical paper*.

Dec, J.E., 1997. A conceptual model of di diesel combustion based on laser-sheet imaging. *SAE technical Paper*, 970873.

Dempsey, A. et al., 2014. Particulate Matter Characterization of Reactivity Controlled Compression Ignition (RCCI) on a Light Duty Engine.

Donahue, N.M. et al., 2006. Coupled partitioning, dilution, and chemical aging of semivolatile organics. *Environmental science & technology*, 40(8), pp.2635–43. Available at: http://www.ncbi.nlm.nih.gov/pubmed/16683603.

EIA, 2012. Annual Energy Outlook 2012 with Projections to 2035. *Energy Policy*, 14, p.239.

Fang, W. et al., 2012. Dual-Fuel diesel engine combustion with hydrogen, gasoline. , (2012), pp.1–9.

Franklin, L., 2010. CONTROL STRATEGIES ON PARTICULATE EMISSIONS OF ETHANOL FUEL. , (December).

Gentner, D.R. et al., 2012. Elucidating secondary organic aerosol from diesel and gasoline vehicles through detailed characterization of organic carbon emissions.

Giauque, W.F. et al., 1960. The Thermodynamic Properties of Aqueous Sulfuric Acid Solutions and Hydrates from 15 to 300°K. *Journal of the American Chemical Society*, 82(1), pp.62–70. Available at: http://pubs.acs.org/cgi-bin/doilookup/?10.1021/ja01486a014.

Giechaskiel, B. et al., 2008. Particle measurement programme (PMP) light-duty inter-laboratory exercise: comparison of different particle number measurement systems. *Measurement Science and Technology*, 19(9), p.095401.

Hallquist, M. et al., 2009. and Physics The formation , properties and impact of secondary organic aerosol : current and emerging issues. , (November 2008), pp.5155–5236.

Han, M., Assanis, D.N., Jacobs, T.J., et al., 2008. Method and Detailed Analysis of Individual Hydrocarbon Species From Diesel Combustion Modes and Diesel Oxidation Catalyst. *Journal of Engineering for Gas Turbines and Power*, 130(4), p.042803. Available at: http://gasturbinespower.asmedigitalcollection.asme.org/article.aspx?articleid=1474413 [Accessed March 12, 2013].

Han, M., Assanis, D.N. & Bohac, S. V, 2008. Comparison of HC Species from Diesel Combustion Modes and Characterization fo a Heat-Up DOC Formulation. , 9(4), pp.405–413.

Han, M., Assanis, D.N. & Bohac, S. V., 2008. Sources of Hydrocarbon Emissions from

Low-Temperature Premixed Compression Ignition Combustion from a Common Rail Direct Injection Diesel Engine. *Combustion Science and Technology*, 181(3), pp.496–517. Available at: http://www.tandfonline.com/doi/abs/10.1080/00102200802530066 [Accessed February 4, 2014].

Heywood, J., 1988. *Internal Combustion Engine Fundamentals*, New York: McGraw-Hill.

Hueglin, C., 1997. an Accurate , Continuously Adjustable Dilution. , 8502(6), pp.1049–1055.

Inagaki, K. et al., 2006. Dual-Fuel PCI Combustion Controlled by In-Cylinder Stratification of Ignitability. *SAE Technical Paper 2006-01-0028*, 2006(724).

Jacobs, T.J., 2007. The attainment of premixed compression ignition low-temperature combustion in a compression ignition direct injection engine. *Proceedings of the Combustion Institute*, 31(2).

Jacobs, Timothy J., Bohac, Stanislaw., Assanis, Dennis., Szymkowics, P., 2005. Lean and rich premixed compression ignition combustion in a light-duty diesel engine. *SAE technical paper*, 2005-01-01.

Kalghatgi, G.T., Risberg, P. & Ångström, H., 2013. Advantages of Fuels with High Resistance to. , (724).

Kawamura, K., Ng, L.L. & Kaplan, I.R., 1985. Determination of organic acids (C1-C10) in the atmosphere, motor exhausts, and engine oils. , 19(11), pp.1082–1086.

Khalek, I. a. et al., 2011. Regulated and Unregulated Emissions from Highway Heavy-Duty Diesel Engines Complying with U.S. Environmental Protection Agency 2007 Emissions Standards. *Journal of the Air & Waste Management Association*, 61(4), pp.427–442. Available at: http://www.tandfonline.com/doi/abs/10.3155/1047-3289.61.4.427 [Accessed April 16, 2013].

Khalek, I.A., Kittelson, D.B. & Brear, F., 2000. Nanoparticle Growth During Dilution and Cooling of Diesel Exhaust : Experimental Investigation and Theoretical Assessment. , (724).

Kitamura, T. et al., 2002. Mechanism of smokeless diesel combustion with oxygenated fuels based on the dependence of the equivalence ratio and temperature on soot particle formation. *International Journal of Engine Research*, 4(4), pp.223–247.

Kittelson, D.B., 1998. Engines and Nanoparicles: A Review. , 29(5), pp.575–588.

Kittelson, D.B. et al., 2006. On-road evaluation of two Diesel exhaust aftertreatment devices. *Journal of Aerosol Science*, 37(9), pp.1140–1151. Available at: http://linkinghub.elsevier.com/retrieve/pii/S0021850205002235 [Accessed December 11, 2012].

Knafl, A. et al., 2006. Characterizing Light-Off Behavior and Species-Resolved

Conversion Efficiencies During In-Situ Diesel Oxidation Catalyst Degreening. , (724).

Knafl, A. et al., 2007. Comparison of Diesel Oxidation Catalyst Performance on an Engine and a Gas Flow Reactor. , 2007(724).

Koci, C.P. et al., 2013. Detailed Unburned Hydrocarbon Investigations in a Highly-Dilute Diesel Low Temperature Combustion Regime. , 2(1).

Kokjohn, S.L. et al., 2011. Fuel reactivity controlled compression ignition (RCCI): a pathway to controlled high-efficiency clean combustion. *International Journal of Engine Research*, 12(3), pp.209–226.

Kolodziej, C. et al., 2013. Comprehensive Characterization of Particulate Emissions from Advanced Diesel Combustion. , pp.1554–1566.

Kook, S., Bae, C., Miles, P. C., Choi, D., & Pickett, L.M., 2005. The influence of charge dilution and injection timing on low-temperature diesel combustion and emissions. *SAE technical Paper*, 2005-01-38.

Lipsky, E.M. & Robinson, A.L., 2006. Effects of dilution on fine particle mass and partitioning of semivolatile organics in diesel exhaust and wood smoke. *Environmental science & technology*, 40(1), pp.155–62. Available at: http://www.ncbi.nlm.nih.gov/pubmed/16433346.

Liu, B., Pui, D. & Whitby, K., 1978. The aerosol mobility chromatograph: a new detector for sulfuric acid aerosols. *Atmospheric …*. Available at: http://www.sciencedirect.com/science/article/pii/0004698178901920 [Accessed October 6, 2015].

Liu, Z. et al., 2012. Comparison of methods for online measurement of diesel particulate matter. *Environmental science & technology*, 46(11), pp.6127–33. Available at: http://www.ncbi.nlm.nih.gov/pubmed/22568856.

Lucachick, G., Avenido, A., Watts, W., et al., 2014. Efficacy of In-Cylinder Control of Particulate Emissions to Meet Current and Future Regulatory Standards. *SAE Technical Paper*, 1597.

Lucachick, G. et al., 2016. Volatility characterization of nanoparticles from single and dual-fuel low temperature combustion in compression ignition engines. *Aerosol Science and Technology*.

Lucachick, G. a, Kittelson, D. & Northrop, W., 2015. Effects of Aftertreatment on Semi-Volatile Particulate Matter Emissions from Low Temperature Combustion in a Light-Duty Diesel Engine. *SAE International Journal of Engines*, 8(2), pp.791–796.

Lucachick, G., Avenido, A. & Northrop, W., 2014. Exploration of Semi-Volatile Particulate Matter Emissions from Low Temperature Combustion in a Light-Duty Diesel Engine. *SAE Int. J. Engines*, 2014-01-13, pp.852–859.

Lucachick, G., Northrop, W. & Engineering, M., 2013. Semi-Volatile Particulate Matter

Emissions from Partially Premixed Low Temperature Combustion in Diesel Engines.

McClellan, R.O., Hesterberg, T.W. & Wall, J.C., 2012. Evaluation of carcinogenic hazard of diesel engine exhaust needs to consider revolutionary changes in diesel technology. *Regulatory toxicology and pharmacology : RTP*, 63(2), pp.225–58. Available at: http://www.ncbi.nlm.nih.gov/pubmed/22561182 [Accessed March 7, 2013].

McMurry, P.H. & Tao, Y., 1989. Vapor Pressures and Surface Free Energies of C14-C18 Monocarboxylic Acids and C5 and C6 Dicarboxylic acids. *Environmental Science and Technology*, 23(12), pp.1519–1523.

McMurry, P. H., Friedlander, S. K., 1979. New Particle Formation in the Presence of an Aerosol. *Atmospheric Environment*, 13(12), pp.1631–1651.

Merritt, P. et al., 2006. Unregulated Exhaust Emissions from Alternate Diesel Combustion Modes. , (724), pp.776–790.

Miller, A., 2007. Role of lubrication oil in particulate emissions from a hydrogen-powered internal combustion engine. *Environmental Science and Technology*, 41(19), pp.6828–6835.

Mirabel, P. et al., 1974. Binary homogeneous nucleation as a mechanism for the formation of aerosols. *Journal of Aerosol Science*, 5(1), pp.115–116.

Myhre, C.E.L., Nielsen, C.J. & Saastad, O.W., 1998. Density and Surface Tension of Aqueous H2SO4 at Low Temperature. *J. Chem. Eng. Data*, 43(4), pp.617–622. Available at: http://pubs.acs.org/doi/abs/10.1021/je980013g.

Northrop, W., 2010.). Particulate and Gas Phase Hydrocarbon Emissions From Partially Premixed Low Temperature Compression Ignition Combustion of Biodiesel. Dissertation.

Northrop, W.F., 2011. Comparison of filter smoke number and elemental carbon mass from partially premixed low temperature combustion in a direct-injection diesel engine. *Journal of engineering for gas turbines and power*, 133-10(102804).

Northrop, W.F. et al., 2011. Condensational Growth of Particulate Matter from Partially Premixed Low Temperature Combustion of Biodiesel in a Compression Ignition Engine. *Aerosol Science and Technology*, 45(1), pp.26–36.

Northrop, William F., Assanis, Dennis N., Bohac, S., 2011. Evaluation of diesel oxidation catalyst conversion of hydrocarbons and particulate matter from premixed low temperature combustion of biodiesel. *SAE technical paper*, No. 2011-0.

Ntziachristos, L. et al., 2004. Performance evaluation of a novel sampling and measurement system for exhaust particle characterization. *SAE 2004 World Congress and Exhibition*, 2004-01-14(724).

Orsini, D. a. et al., 1999. A New Volatility Tandem Differential Mobility Analyzer to

Measure the Volatile Sulfuric Acid Aerosol Fraction. *Journal of Atmospheric and Oceanic Technology*, 16(6), pp.760–772. Available at: http://journals.ametsoc.org/doi/abs/10.1175/1520-0426(1999)016<0760:ANVTDM>2.0.CO;2.

Park, K., Cao, F., et al., 2003. Relationship between particle mass and mobility for diesel exhaust particles. *Environmental science & technology*, 37(3), pp.577–83. Available at: http://www.ncbi.nlm.nih.gov/pubmed/12630475.

Park, K., Kittelson, D.B. & McMurry, P.H., 2003. A closure study of aerosol mass concentration measurements: comparison of values obtained with filters and by direct measurements of mass distributions. *Atmospheric Environment*, 37(9-10), pp.1223–1230. Available at: http://linkinghub.elsevier.com/retrieve/pii/S1352231002010166 [Accessed May 10, 2013].

Patterson, J., Hassan, M. & Clarke, A., 2006. Experimental study of DI diesel engine performance using three different biodiesel fuels. Available at: https://dspace.lboro.ac.uk/dspace-jspui/handle/2134/8410 [Accessed October 3, 2015].

Presto, A. a et al., 2009. Intermediate-volatility organic compounds: a potential source of ambient oxidized organic aerosol. *Environmental science & technology*, 43(13), pp.4744–9. Available at: http://www.ncbi.nlm.nih.gov/pubmed/19673260.

Prikhodko, V.Y. et al., 2013. Effectiveness of Diesel Oxidation Catalyst in Reducing HC and CO Emissions from Reactivity Controlled Compression Ignition. , pp.329–335. Available at: http://www.sae.org/technical/papers/2013-01-0515 [Accessed January 5, 2015].

Prikhodko, V.Y. et al., 2010. Emission Characteristics of a Diesel Engine Operating with In-Cylinder Gasoline and Diesel Fuel Blending. , 3(2), pp.946–955.

Queimada, A.J. & Marrucho, I.M., 2001. Surface tension of pure heavy n -alkanes: a corresponding states approach. , 4639, pp.1–10.

Rader, D.J., McMurry, P.H. & Smith, S., 1987. Evaporation Rates of Monodisperse Organic Aerosols in the 0.02- to 0.2-μm-Diameter Range. *Aerosol Science and Technology*, 6(3), pp.247–260. Available at: http://www.tandfonline.com/doi/abs/10.1080/02786828708959137 [Accessed June 13, 2014].

Reitz, R.D. & Duraisamy, G., 2015. Review of high efficiency and clean reactivity controlled compression ignition (RCCI) combustion in internal combustion engines. *Progress in Energy and Combustion Science*, 46, pp.12–71. Available at: http://dx.doi.org/10.1016/j.pecs.2014.05.003.

Robinson, A.L. et al., 2007. Rethinking organic aerosols: semivolatile emissions and photochemical aging. *Science (New York, N.Y.)*, 315(5816), pp.1259–62. Available

at: http://www.ncbi.nlm.nih.gov/pubmed/17332409 [Accessed February 28, 2013].

Rusyniak, M. et al., 2001. Vapor Phase Homogeneous Nucleation of Higher Alkanes : Dodecane , Hexadecane , and Nucleation Rate Measurements. *J. Phys. Chem. B*, 105, pp.11866–11872.

Sabatini, J., 2012. U.S. Diesel auto sales up 27% in 2011 while hybrid share sinks. Available at: < http://www.autoblog.com/2012/01/11/u-s-diesel-auto-sales-up-27-in-2011-while-hybrid-share-shrinks/>.

Sakurai, H., Tobias, H.J., et al., 2003. On-line measurements of diesel nanoparticle composition and volatility. *Atmospheric Environment*, 37(9-10), pp.1199–1210. Available at: http://linkinghub.elsevier.com/retrieve/pii/S1352231002010178 [Accessed April 5, 2013].

Sakurai, H., Park, K., et al., 2003. Size-Dependent Mixing Characteristics of Volatile and Nonvolatile Components in Diesel Exhaust Aerosols. , 37(24), pp.5487–5495.

Seinfeld, J., 1986. Atmospheric chemistry and physics of air pollution. *Willey Interscience, New York*. Available at: https://scholar.google.com/scholar?q=Atmospheric+Chemistry+and+Physics+of+Air+Pollution+%281986%29&btnG=&hl=en&as_sdt=0%2C24#0 [Accessed October 3, 2015].

Shi, J.P. & Harrison, R.M., 1999. Investigation of ultrafine particle formation during diesel exhaust dilution. *Environmental Science and Technology*, 33(21), pp.3730–3736.

Shiraiwa, M. et al., 2013. Size distribution dynamics reveal particle-phase chemistry in organic aerosol formation. *Proceedings of the National Academy of Sciences of the United States of America*, 110(29), pp.11746–50. Available at: http://www.pnas.org/cgi/content/long/110/29/11746.

Shrivastava, M.K. et al., 2006. Modeling semivolatile organic aerosol mass emissions from combustion systems. *Environmental science & technology*, 40(8), pp.2671–7. Available at: http://www.ncbi.nlm.nih.gov/pubmed/16683607.

Shrivastava, M.K. et al., 2007. Sources of organic aerosol: Positive matrix factorization of molecular marker data and comparison of results from different source apportionment models. *Atmospheric Environment*, 41(40), pp.9353–9369. Available at: http://linkinghub.elsevier.com/retrieve/pii/S135223100700787X [Accessed November 21, 2012].

Shuldiner, H., 2012. No TitleBosch Forecasts 10% Diesel Penetration in U.S. by 2015. Available at: , <http://wardsauto.com/vehicles-amp-technology/bosch-forecasts-10-diesel-penetration-us-2015> [Accessed January 1, 2013].

Sluder, C.S. et al., 2004. Exhaust Chemistry of Low-NO X , Low-PM Diesel Combustion. *SAE technical paper*, 2004-01-01.

Storey, J., 2015. The Contribution of Lubricant to the Formation of Particulate Matter with Reactivity Controlled Compression Ignition in Light-Duty Diesel Engines. *Emission Control Science and Technology*, 1.1, pp.64–79.

Storey, J.M.E. et al., 2008. Mobile Source Air Toxics (MSATs) from High Efficiency Clean Combustion : Catalytic Exhaust Treatment Effects. , 1(1).

Swanson, J. et al., 2013. Filtration Efficiency and Pressure Drop of Miniature Diesel Particulate Filters. *Aerosol Science and Technology*, 47(4), pp.452–461. Available at: http://www.tandfonline.com/doi/abs/10.1080/02786826.2012.763087 [Accessed October 22, 2014].

Vesala, T. et al., 1997. Models for condensational growth and evaporation of binary aerosol particles. *Journal of Aerosol Science*, 28(4), pp.565–598.

Yudin, M. & Hughes, B.D., 1994. Surface energy of solids 4/3 pg 16. *Physical Review B*, 49(8), pp.5638–5642.

Zervas, E., Montagne, X. & Lahaye, J., 2001. C1-C5 organic acid emissions from an SI engine: influence of fuel and air/fuel equivalence ratio. *Environmental science & technology*, 35(13), pp.2746–51. Available at: http://www.ncbi.nlm.nih.gov/pubmed/11452603.

Zheng, M., Reader, G.T. & Hawley, J.G., 2004. Diesel engine exhaust gas recirculation––a review on advanced and novel concepts. *Energy Conversion and Management*, 45(6), pp.883–900.

Appendix

Homogeneous Nucleation Calculations

$$J = Ke^{-W^*/kT}$$

Where J is the rate of homogeneous nucleation. K is a pre-exponential factor, W^* is the barrier height for nucleation, k is the Boltzmann constant, and T is temperature.

The pre-exponential factor K is calculated as follows:

$$K = (2\sigma M/\pi N_a)^{\frac{1}{2}}(P/kT)^2/\rho$$

Where σ is the surface tension, M is the molecular weight, N_A is Avogadro's number, P is the vapor pressure, and ρ is the density.

The barrier height W^* is defined as follows:

$$W^* = \frac{1}{2}n^*\Delta\mu$$

Where n^* is the number of molecules in the critical nucleation cluster.

The difference in chemical potential μ is defined as follows, under the assumption of ideal gas behavior.

$$\mu = kT\ln S$$

Where S is the saturation ratio $P/P_{sat.}$ where P_{sat} is temperature dependent and found in literature.

The Gibbs-Thompson relation is used to calculate n^* as follows:

$$n^* = \frac{32\pi\sigma^3 M^2}{3\Delta\mu^3\rho^2}$$

When the critical saturation ratio is reached, J=1.

Evaporation and Condensation Model

The mass fractions $Y_{i,j}$ of each component i for each particle diameter bin j are as follows:

$$Y_{i,j} = \frac{X_{i,j} MW_i}{MT_j}$$

Where $X_{i,j}$ is the mole fraction of each component i at each particle size bin j. MW_i is the molecular weight of each component , and MT_j is mixture molecular weight at each particle size bin j.

MT_j is defined as follows:

$$MT_j = \sum_{j,i=1}^{ni} X_{i,j}$$

Where ni is the number of components used. In this study three components were used.

$X_{i,j}$ is calculated as follows:

$$X_{i,j} = V_{i,j} \rho_i / MW_i b_j$$

Where $V_{i,j}$ is the volume fraction of each component i at each particle size bin j, ρ is the density of heavy alkanes, and b_j is the mole fraction basis at each particle size bin j.

b_j is calculated as follows:

$$b_j = \sum_{j,i=1}^{ni} V_{i,j}\rho_i/MW_i$$

Where $V_{i,j}$ is the volume fraction of each component i at each particle size bin j, and is initialized as equal volume fractions of each component at each particle size.

The vapor pressure $Psurf_{i,j}$ of each component i at the particle surface for a particle in size bin j is as follows:

$$Psurf_{i,j} = X_{i,j}Psat_i \exp\left[\frac{4\sigma MW_i}{\rho_i Dp_j RT}\right]$$

Where $Psat_i$ is the saturation pressure of each component i, σ is the alkane surface tension, and is assumed to be equal for all components, Dp_{ij} is the particle diameter at bin j, R is the ideal gas constant, and T is temperature.

The instantaneous rate of change of particle diameter $dDp/dt_{i,j}$ as contributed by the evaporation or condensation of each component i at each particle bin size j is defined as follows.

$$\frac{dDp}{dt}_{i,j} = 2\pi v_i(Pvap_i - Psurf_{i,j})/\left(\frac{2\pi MW_i}{N_a kT}\right)^2$$

Where ν_i is the volume per molecule of component I, $Pvap_i$ is the vapor pressure of each component i in the gas surrounding the particle. N_a is Avogadro's number.

The total particle instantaneous rate or change at each bin size j is represented by the sum of the the evaporation/condensation of each component and is as follows:

$$\frac{dDp}{dt}_{j} = \sum_{j,i=1}^{n} \frac{dDp}{dt}_{i,j}$$

The instantaneous rate of change of particle diameter $dVp/dt_{i,j}$ as contributed by the evaporation/condensation of each component i in one particle within size bin j is defined as follows:

$$\frac{dVp}{dt}_{i,j} = \frac{\pi}{2} \frac{dDp}{dt}_{i,j} Dp_j^2$$

The change in volume of each component i for one particle in particle size bin j for a very small time step Δt is as follows:

$$Vp(t + \Delta t)_{i,j} = Vp(t)_{i,j} + \frac{dVp}{dt}_{i,j} \Delta t$$

Where $Vp_{i,j}$ is the volume of each component i per particle at within size bin j.

The change in alkane vapor concentration Nv_i of each component i resulting from the evaporation/condensation of particles for a very small small timestep Δt is as follows:

$$Nv(t + \Delta t)_i = Nv(t)_i - \Delta t \sum_{j=1}^{nj} \sum_{i=1}^{ni} \frac{dVp}{dt}_{i,j} Np_j / v_i$$

Where Nv_i is the ambient vapor concentration of each component I, Np_j is the number concentration of particles in size bin j, and v_i is the molecular volume of a vapor molecule of component i.

To convert vapor concentration to vapor pressure the following relationship is used:

$$Pvap_i = \frac{Nv_i MW_{air} Patm}{N_a \rho_{air}}$$

Where MW_{air} is the molecular weight of air, Patm is the ambient air pressure, and ρ_{air} is the density of ambient air.

Sulfuric acid and water heterogeneous nucleation model

The equations used to calculate heterogeneous nucleation of sulfuric acid and water are adapted from the work of Baumgard & Johnson (1996) in a study on nanoparticles for CDC. The equations used by Baumgard & Johnson are derived and outlined by Mirabel et al. (1974). The rate of nucleation in particles per second, per unit volume is expressed by Mirabel et al. as follows:

$$J = C \exp\left[\frac{\Delta G^*}{kT}\right]$$

Where C is the frequency in which molecules collide onto a particle cluster passing through the energy barrier which clusters must surpass to grow into a stable size. ΔG^* is the free energy necessary to form a cluster having a composition and size that is in a state of unstable equilibrium with the surrounding gas phase material.

The equation for the free energy of formation of an arbitrarily sized cluster is as follows:

$$\Delta G = n_1 * (\mu_{1l} - \mu_{1g}) + n_2(\mu_{2l} - \mu_{2g}) + 4\pi r^2\gamma$$

Where n_1 and n_2 are the the number of molecules of water and sulfuric acid, respectively in the cluster. μ_{11} and μ_{22} are the chemical potentials of water and sulfuric acid, respectively, in a bulk mixture of the same composition as the cluster. μ_{1g} μ_{2g} are the chemical potentials of water and sulfuric acid, respectively, in the gas phase. R is the radius of the cluster, and γ is the surface tension of a bulk mixture of the same composition as the cluster.

By assuming the ideal gas law, the difference in chemical potential between a component in solution and one in gas form is defined for water and sulfuric acid, respectively, as follows:

$$\mu_{1l} - \mu_{1g} = -kT \ln \frac{P_1}{P_{1l}}$$

$$\mu_{2l} - \mu_{2g} = -kT \ln \frac{P_2}{P_{2l}}$$

Where P_1 and P_2 are the vapor pressures of water and sulfuric acid, respectively. P_{1l} and P_{2l} are the vapor pressures above the surface of a two-component mixture of sulfuric acid and water. Where chemical potential for assuming a perfect gas with respect to a reference state is as follows for the mixture of water and sulfuric acid, respectively.
By properly substituting the above equations with the original equation for the change in free energy, the change in free energy can be defined as follows:

$$\Delta G = -n_1 \left((\mu_{1l}^o - \mu_{1l}) + kTln\left(\frac{P_1}{P_{1sat}}\right)\right) + n_2 \left((\mu_{1l}^o - \mu_{1l}) + kTln\left(\frac{P_2}{P_{2sat}}\right)\right) + A\gamma$$

Where chemical potential is evaluated with respect to a reference state, and the chemical potential of water and sulfuric acid in solution are fitted to the following equations developed by Baumgard & Johnson (1996) based on tabular data prepared by Giauque et al. (1960).

$$\mu_{1l}^{o} - \mu_{1l} = 1.085 * 10^{-20} Exp\left(-.689\left(\frac{n_1}{n_2}\right)\right) + 10^{-21} Exp\left(-.067\left(\frac{n_1}{n_2}\right)\right)$$

$$\mu_{2l}^{o} - \mu_{2l} = 2.14 * 10^{-20} Exp\left(-2.99\left(\frac{n_2}{n_1}\right)\right) + 2.668 * 10^{-21} Exp\left(-.48\left(\frac{n_2}{n_1}\right)\right)$$

P_{1sat} and P_{2sat} are the saturation pressures of pure water and sulfuric acid, respectively. P_{1sat} is defined below along with P_{2sat} as determined by Ayers et al. (1980).

$$P_{1sat=} Exp(20.386 - (5132/T))$$

$$P_{2sat=} 10^{\left(8.28538 - \frac{2976.84}{T - 273.15 + 213.951}\right)}$$

A is the surface area of the cluster comprised of n1 and n2 molecules of water and sulfuric acid, respectively. The surface tension of bulk water and sulfuric acid mixture of the same composition as the growing cluster is defined as a seventh order polynomial which was developed using tabular data from Myhre et al. (1998).

$$\begin{aligned}\boldsymbol{\gamma} = {} & \mathbf{-37.7160922835076X^7 + 96.2702683653148X^6} \\ & \mathbf{- 95.2393577928433X^5 + 45.9542313307444X^4} \\ & \mathbf{- 10.9937025164687X^3 + 1.07810622932395X^2} \\ & \mathbf{- 0.02088588137011X + 0.07554611751020 5}\end{aligned}$$

In the above equations, X is the ratio of n_2 over the sum of n_2 and n_1.

By finding the partial derivative of the change in free energy with respect to the number of molecules of each component, and setting to zero, the maximum of the function (maximum is defined as ΔG^*) can be found. These equations are defined as follows:

$$\left(\frac{\partial \Delta G^*}{n_1}\right)_{n_2} = 0$$

$$\left(\frac{\partial \Delta G^*}{n_2}\right)_{n_1} = 0$$

In general form, the solution to these two equations, respectively, is as follows:

$$\left(\frac{\partial \Delta G}{n_1}\right)_{n_2} = \mu_{1l} - \mu_{1g} + \frac{2\gamma \bar{V}_1}{r^*} - \frac{3X^* V}{r^*}\frac{d\gamma}{dX}\bigg|_{x=x^*} = 0$$

$$\left(\frac{\partial \Delta G}{n_2}\right)_{n_1} = \mu_{2l} - \mu_{2g} + \frac{2\gamma \bar{V}_2}{r^*} - \frac{3V(1-X^*)}{r^*}\frac{d\gamma}{dX}\bigg|_{x=x^*} = 0$$

Where $\bar{V}_2$ and $\bar{V}_2$ are the partial molar volumes of V, where V is the solution molar volume defined as follows:

$$V = (1-x)\bar{V}_1 + x\bar{V}_2$$

The frequency factor C listed in the first equation, is defined as follows:

$$\boldsymbol{C = \frac{\beta_1 \beta_2}{\beta_1 \sin^2 \phi + \beta_2 \cos^2 \phi}[N_1 + N_2]\left(-\frac{P}{Q}\right)^{1/2}}$$

Where β_1 and β_2 represents the number of molecules of water and sulfuric acid, respectively, which impact the growing embryo per unit time, and is defined as follows:

$$\boldsymbol{\beta_1 = \frac{P_1}{(2\pi m_1 kT)^{1/2}}}$$

$$\boldsymbol{\beta_2 = \frac{P_2}{(2\pi m_2 kT)^{1/2}}}$$

Where P_1 and m_1 are the partial pressure and molecular mass of water, respectively, and P_2 and m_2 are the partial pressure and molecular mass of sulfuric acid. N_1 is the number density of water, N_2 is the number density of sulfuric acid.

ϕ is the angle formed by the original axis n_1 and the direction passing through the saddle point. The variables P and Q are functions of the second derivative of ΔG^* with respect to the new axis system defined by the direction passing through the saddle point. The variables P and Q are defined as follows:

$$\boldsymbol{P = \left(\frac{\partial^2 \Delta G}{\partial n_1^2}\right) cos^2\phi + 2\left(\frac{\partial^2 \Delta G}{\partial n_1 \partial n_2}\right) cos\phi sin\phi + \left(\frac{\partial^2 \Delta G}{\partial n_2^2}\right) sin^2\phi}$$

$$\boldsymbol{Q = \left(\frac{\partial^2 \Delta G}{\partial n_1^2}\right) sin^2\phi + 2\left(\frac{\partial^2 \Delta G}{\partial n_1 \partial n_2}\right) cos\phi sin\phi + \left(\frac{\partial^2 \Delta G}{\partial n_2^2}\right) cos^2\phi}$$

The angle of rotation ϕ is defined as follows:

$$\boldsymbol{tan2\phi = 2\left(\frac{\partial^2 \Delta G}{\partial n_1 \partial n_2}\right) / \left[\left(\frac{\partial^2 \Delta G}{\partial n_1^2}\right) - \left(\frac{\partial^2 \Delta G}{\partial n_2^2}\right)\right]}$$

This system of several simultaneous partial differential equations is solved numerically for the nucleation rate J.